IEEE Task Force on

Dynamic State and Parameter Estimation

Chair: Junbo Zhao, Mississippi State University, USA
Vice-Chair: Alireza Rouhani, Dominion Energy, USA
Secretary: Shahrokh Akhlaghi, Southwest Power Pool, USA

Members (Alphabetical Order):

- Abhinav Kumar Singh, University of Southampton, U.K.
- Abdul Saleem Mir, University of Southampton, U.K.
- Ahmad Taha, University of Texas at San Antonio, USA.
- Ali Abur, Northeastern University, USA.
- Antonio Gomez-Exposito, University of Seville, Spain.
- A. P. Sakis Meliopoulos, Georgia Institute of Technology, USA.
- Bikash Pal, Imperial College London, U.K.
- Innocent Kamwa, Laval University, Canada.
- Junjian Qi, Stevens Institute of Technology, USA.
- Lamine Mili, Virginia Polytechnic Institute and State University, USA.
- M. A. M. Ariff, Universiti Tun Hussein Onn Malaysia, Malaysia.
- Marcos Netto, National Renewable Energy Laboratory, USA.
- Mevludin Glavic, Independent Researcher, Bosnia and Herzegovina.
- Samson Shenglong Yu, Deakin University, Australia.
- Shaobu Wang, Pacific Northwest National Laboratory, USA.
- Tianshu Bi, North China Electric Power University, China
- Thierry Van Cutsem, University of Liège, Science, Belgium.
- Vladimir Terzija, Skolkovo Institute of Science and Technology, Russia.
- Yu Liu, ShanghaiTech University, China.
- Zhenyu Huang, Pacific Northwest National Laboratory, USA.

ACKNOWLEDGMENTS

The Task Force is truly grateful for the support of our sponsoring committee on Power System Operations, Planning and Economics Committee, and Bulk Power System Operations subcommittee.

The Task Force gratefully acknowledges the contributions of participants of our Task Force Meetings who contributed through their discussions in converging on this report.

KEYWORDS

Bad data, converter-based resources, Energy Management Systems, Dynamic state estimation, Forecasting-aided state estimation (FASE), Frequency stability, Kalman filter, Parameter estimation, Power system stability, Power system state estimation, Power system control, Power system protection, Power system operation, Power system modeling, Renewable energy, Robust estimation, State Estimation, Synchrophasor measurements, Sampled value measurements, Static state estimation (SSE), Tracking state estimation (TSE), Voltage stability.

CONTENTS

1. TF Objectives

This report of TF on dynamic state and parameter estimation aims to 1) review its motivations and definitions, demonstrate its values for enhanced power system modeling, monitoring, operation, control, and protection as well as power engineering education; 2) provide recommendations to vendors, national labs, utilities and ISOs on the use of dynamic state estimator for enhancement of the reliability, security, and resiliency of electric power systems.

2. TF Background and Achievements

The widespread deployment of phasor measurement units (PMUs) on power transmission grids has made possible the real-time monitoring and control of power system dynamics. However, these functions may not be reliably achieved without the development of a fast and robust dynamic state estimator (DSE). Indeed, the estimated synchronous machine state variables can be used by power system stabilizers, automatic voltage regulators, and under-frequency relays to enhance small signal stability and to initiate generation outages and load shedding during transient instabilities, etc. During the 2017 IEEE Power Engineering Society General Meeting held at Chicago, the Working Group on Power System Static and Dynamic State Estimation decided to form a new task force on “Power System Dynamic State and Parameter Estimation” to define its concepts, demonstrate its values for enhanced power system modeling, monitoring, operation, control, and protection as well as power engineering educations.

Thanks to the dedicated efforts by all TF members, this TF has made the following contributions:

- Three TF papers published in the IEEE Transactions on Power Systems:

-Y. Liu, A. K. Singh, J. B. Zhao, A. P. Meliopoulos, B. Pal, M. A. M. Ariff, T. Van Cutsem, M. Glavic, Z. Huang, I. Kamwa, L. Mili, A. Saleem Mir, A. Taha, V. Terzija, S. Yu, "Dynamic State Estimation for Power System Control and Protection," IEEE Trans. Power Systems, 2021.

-J. B. Zhao, M. Netto, Z. Huang, S. Yu, A. Exposito, S. Wang, I. Kamwa, S. Akhlaghi, L. Mili, V. Terzija, A. P. Sakis Meliopoulos, B. Pal, A. K. Singh, A. Abur, T. Bi, A. Rouhani, "Roles of Dynamic State Estimation in Power System Modeling, Monitoring and Operation," IEEE Trans. Power Systems, vol. 36, no. 3, pp. 2462-2472, 2021.

-J. B. Zhao, A. Exposito, M. Netto, L. Mili, A. Abur, V. Terzija, I. Kamwa, B. Pal, A. K. Singh, J. Qi, Z. Huang, A. P. Sakis Meliopoulos, "Power System Dynamic State Estimation: Motivations, Definitions, Methodologies and Future Work," IEEE Trans. Power Systems, vol. 34, no. 4, pp. 3188-3198, 2019. (**Highly Cited Paper according to Web of Science since March 2021**)

- Invited IEEE PES webinar sponsored by IEEE Transactions on Power Systems entitled “Dynamic State and Parameter Estimation for Power System

Monitoring, Modeling, Operation, Control, and Protection" on 11:00 AM-1:00 pm US ET/8:00 AM-10:00 AM US PT, 6th, Friday, November 2020.

- Tutorial at the 2019 IEEE PES General Meeting entitled "Dynamic State Estimation for Power System Dynamic Monitoring, Protection and Control: Motivations, Tools and Experiences" Sunday, August 4, 8:00 AM – 5:00 PM.
- Organized three panel sessions at IEEE PES General Meetings:
  - "Advanced Dynamic State Estimation for Next Generation of EMS: Structure, Algorithms and Experiences" at IEEE PES General Meeting, DC, 2021.
  -State Estimation for Power Electronics-Dominated Systems: Challenges and Solutions" at IEEE PES General Meeting, Canada, 2020.
  -"Dynamic State Estimation for Power System Monitoring, Protection and Control–Paving the Way for A More Resilient Grid" at IEEE PES General Meeting, Atlanta, 2019.

3. Power System Dynamic State Estimation: Motivations, Definitions, and Methodologies

In this Section, DSE is presented in a unified framework, which uses commonly accepted notations and formulations in power system dynamics and control literature to establish a firm baseline for future research and development efforts. The similarities and differences between DSE and other existing estimation methods, including forecasting-aided state estimation (FASE), tracking state estimation (TSE) and static state estimation (SSE), are clarified. Potential applications of DSE are identified and discussed to justify its significance for enhanced monitoring, protection, and control.

3.1 Motivations of DSE

Power systems are planned to be operated and controlled in a hierarchical manner [1]. The controls are particularly designed to deal with a variety of dynamic phenomena at multiple time scales [2]. For example, a synchronous generator's automatic voltage control is based on locally available measurements only. However, their voltage set points can be modified when the command from the centralized control center is received. Hence, there exists a hierarchical decentralized closed-loop control that responds to system variations and to set point changes. The centralized open-loop control is triggered by the operator after a decision-making process. Following this philosophy of design, most of the monitoring and control applications at the control center rely on the steady-state model of the system. However, in the real world, power systems never operate in a steady-state condition, as there are stochastic variations in demand and generation. The situation is further aggravated by the large-scale integration of distributed energy resources (DERs) on the generation side, and complex loads and new demand-response technologies on the demand side, such as electric vehicles and internet of things devices. Such a shift has given rise to larger uncertainties of the system's dynamic characteristics. Consequently, the steady-state assumption becomes questionable, and SSE methods are unable to capture these dynamics in an operational environment. As a result, SSE methods [3]-[6] used in today's energy management systems (EMS) should be reassessed and enhanced with new monitoring tools, such as DSE. DSE is capable of accurately capturing the dynamics of the system states and will play an important role in power system control and protection [7]-[11], especially with the increasing complexity resulting from the uncertainties by the new technologies being deployed in the generation and demand sides.

With the widespread deployment of PMUs and advanced communication infrastructure in power systems [12], [13], the development of a fast and robust DSE tool has become possible. The benefits of using DSE include but are not limited to:

- Improved oscillations monitoring: the estimated dynamic state variables can be used to carry out modal analysis [14], and the identified modes can then be utilized to adaptively tune power system stabilizers (PSS), thereby achieving better damping of inter-area modes of oscillation and improving system stability. Recall that the effectiveness of conventional PSS using local measurements may be limited by the observability of the modes in the signal. Using state estimates of entire regions as opposed to only local measurements will increase the stabilizer's response to inter-area modes if the generator has a significant influence on such modes. Note that there are several ways for monitoring the entire regions/systems via DSE, namely the hierarchical and distributed DSE and the centralized DSE using high-performance computing technique [15], [16], or reduced-order model of power system [17]. Hierarchical and distributed DSE methods are first implemented locally to monitor small areas, and their results are submitted to the control center for further processing. This is the widely used strategy in the current literature. The DSE based on high-performance computing for large-scale systems is in its infancy, and merits further research;
- Enhanced hierarchical decentralized control [18]-[20]: the availability of local and wide-area dynamic states obtained from DSE enables the design of effective local and wide-area controls; for instance, the estimated rotor speed and other states can be used as input signals to control excitation systems of synchronous machines [19], [20] or of FACTS devices [18] to damp out oscillations. The implementation can be in either fully decentralized or hierarchically decentralized manner;
- Improved dependability and reliability of protection systems [8], [21]-[23]: by testing the consistency between the PMU measurements and the dynamical model of the protection zone for which the parameters are identified by DSE, both internal and external faults can be effectively detected without any *a priori* protection relay settings, yielding more reliable protection systems compared with the traditional coordinated settings-based schemes; the dynamic states estimated online can be utilized to initiate effective generator out-of-step protections [11], [23] and transient stability monitoring based on the extended equal-area criterion or the energy function approach [23]; furthermore, fast state estimation is a prerequisite for the implementation of system integrity protection schemes that can prevent blackouts;
- Enhanced reliability of the system models utilized for dynamic security assessment (DSA) [24]: DSA requires the availability of accurate models of the generators and their associated controllers, of the composite loads, and the special protection schemes, to name a few. By developing DSE, both the static and dynamic models can be validated [25], and if incorrect parameter values are identified, they can be included as additional state variables in DSE for parameter estimation and calibration, yielding improved system models [26] and more reliable DSA;
- Other applications: improved synchrophasor data quality and cyber security leveraging the model information, such as filtering out measurement error that is modeled as Gaussian or non-Gaussian distribution [27], [28], detecting bad

and delayed measurements, or recovering missing data [29]; enhanced synchronous generators coherency identification and dynamic model reduction [30] using the estimated dynamic states and parameters; enhanced bus frequency and center of inertia estimation [31], [32] and detection of failures in controllers, such as excitation systems, PSS, etc., [33], [34].

3.2 Unified State Estimation Framework

This section develops a unified framework for various power system state estimation approaches, namely DSE, FASE, TSE, and SSE. Specifically, the system operating conditions and the associated mathematical models are first revisited. Then, the resulting state transition expressions are identified and subsequently customized for transient and quasi-steady-state operating conditions.

3.2.1 Quasi-Steady State versus Transient Operating Conditions

The states of a system are essential in any of two mutually exclusive operating conditions, quasi-steady and transient, see Fig. 1.

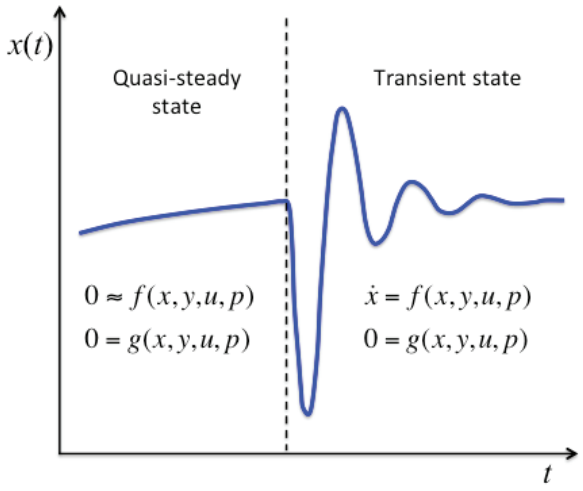

Fig. 1. Illustration of power system states

The tutorial example depicted in Fig. 2 is used to illustrate the models and concepts arising in the discussion. In this simple system, an aggregated load is served both by a local generator and an external grid represented by its Thevenin equivalent. Slow load evolutions can be analyzed by solving the system of algebraic equations (see below), while sudden changes, such as opening the CB, call for the solution of differential equations.

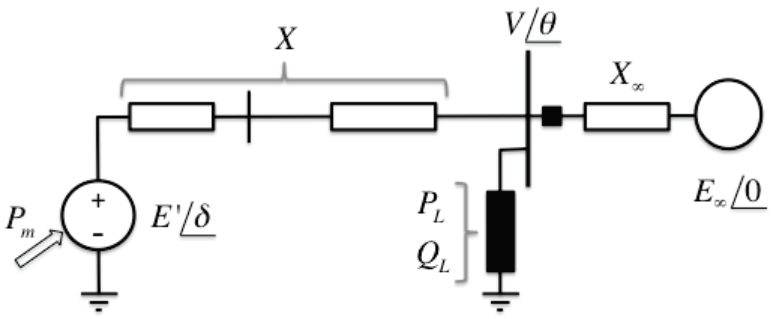

Fig. 2. Tutorial example

For this particular example, assuming a second-order classical dynamic model for the local generator, the system shown in Fig. 2 becomes:

Differential equations:

$$\frac{2H}{\omega_0}\dot{\omega} = P_m - \frac{E'V}{X}\sin(\delta-\theta)$$
$$\dot{\delta} = \omega - \omega_0$$

Algebraic equations:

$$P_L = \frac{E'V}{X}\sin(\delta-\theta) - \frac{E_\infty V}{X_\infty}\sin\theta$$
$$Q_L = \frac{V}{X}\left(E'\cos(\delta-\theta) - V\right) + \frac{V}{X_\infty}\left(E_\infty\cos\theta - V\right)$$

Input and state vectors:

$$x = [\delta, \omega]^T$$
$$y = [V, \theta]^T$$
$$u = [P_L, Q_L]^T$$
$$p = [X, X_\infty, P_m, H]^T$$

As far as the system parameters are concerned, they can be classified into the following categories:

- Well-defined (good enough accuracy) and constant parameters (e.g. network impedances, generator inertia constant, etc.). These define the coefficients of the model and do not have to explicitly appear in the functional dependence.
- Uncertain (constant or time-varying) parameters. These should be included in the state vector (***x*** or ***y***), to be estimated like any other regular variable (e.g., a line resistance changing with temperature).
- Time-varying parameters that evolve in accordance to a given control law or predefined action, leading to slow or fast dynamic phenomena (e.g., the tap setting of a transformer, the impedance of a shunt compensator, etc.). These should be included in the control vector (***u***).

For instance, in the tutorial example, the inertia constant H could be included in the state vector if one wishes to estimate a better value than that provided by the manufacturer, whereas the mechanical power P_m could be considered an input if the speed governor dynamics are not included in the model, or a state variable otherwise.

Transient operating condition: arises when a sudden disturbance takes place in the system. In this context, only electromechanical transients are considered and the associated governing equations are those customarily adopted for transient stability analysis, given by

$$\begin{aligned} &\dot{\boldsymbol{x}}(t) = \boldsymbol{f}(\boldsymbol{x}(t), \boldsymbol{y}(t), \boldsymbol{u}(t), \boldsymbol{p}), \quad \boldsymbol{0} = \boldsymbol{g}(\boldsymbol{x}(t), \boldsymbol{y}(t), \boldsymbol{u}(t), \boldsymbol{p}) \\ &\boldsymbol{x}_i^{min} \le \boldsymbol{x}_i \le \boldsymbol{x}_i^{max}, i \in \Xi \quad \boldsymbol{u}_i^{min} \le \boldsymbol{u}_i \le \boldsymbol{u}_i^{max}, j \in \Omega \\ &\boldsymbol{p}_i^{min} \le \boldsymbol{p}_i \le \boldsymbol{p}_i^{max}, l \in \Gamma \end{aligned} \tag{1}$$

where $\boldsymbol{x} \in R_n$ represents the system state vector, such as the internal states of a machine or a dynamic load, etc.; $\boldsymbol{y} \in \mathrm{R}m$ represents the algebraic state vector, such as voltage and current phasors; note that the algebraic equations include those that are associated with *the power flows and generators' stator*; $\boldsymbol{u}$ is the system input vector; $\boldsymbol{p}$ represents the model parameters; and $\boldsymbol{f}$ and $\boldsymbol{g}$ are nonlinear functions; due to physical limitations, controller design, some dynamic state variables, control inputs and model parameters are bounded by their upper and lower limits, which are represented by the sets Ξ, Ω, and Γ, respectively.

Quasi-steady state operating condition: refers to the situation in which the system operating point changes exclusively due to slow and smooth load/renewable generation changes. In this scenario, the generators and other controllers can almost instantly absorb these slow changes, yielding negligible changes of the dynamic states $\boldsymbol{x}(t)$, i.e., $\dot{\boldsymbol{x}}(t) \approx \boldsymbol{0}$. As a result, the system is mathematically characterized by:

$$\begin{aligned} \boldsymbol{0} &\approx \boldsymbol{f}(\boldsymbol{x}(t), \boldsymbol{y}(t), \boldsymbol{u}(t), \boldsymbol{p}), \\ \boldsymbol{0} &= \boldsymbol{g}(\boldsymbol{x}(t), \boldsymbol{y}(t), \boldsymbol{u}(t), \boldsymbol{p}), \end{aligned} \tag{2}$$

subject to equality and inequality constraints, where slowly varying voltage phasors, i.e., algebraic state variables, are of interest. Since system inputs are usually not perfectly known and the parameters are always inaccurate to a certain extent, state estimators capable of processing measurement snapshots are developed, including FASE, TSE, and SSE. It is worth emphasizing that, at the distribution level, individual loads may change abruptly enough for the distributed generators or local controllers to be subject to disturbances, requiring the dynamic model (1) to be resorted to.

In practice, the continuous-time models for both transient and quasi-steady-state operating conditions are transformed into their discrete-time state-space forms through some time discretization technique [36]. Then (1) can be written as

$$\boldsymbol{x}_k = \boldsymbol{f}(\boldsymbol{x}_{k-1}, \boldsymbol{y}_{k-1}, \boldsymbol{u}_k, \boldsymbol{p}) + \boldsymbol{w}_k, \tag{3}$$

$$\boldsymbol{0} = \boldsymbol{g}(\boldsymbol{x}_k, \boldsymbol{y}_k, \boldsymbol{u}_k, \boldsymbol{p}) + \boldsymbol{e}_k, \tag{4}$$

where $\boldsymbol{w}_k$ and $\boldsymbol{e}_k$ are error terms that include time discretization and model approximation errors. By treating the equality constraints (4) as pseudo-measurements and processing them together with the incoming measurements, a more general state space model for state estimation is

$$\boldsymbol{x}_k = \boldsymbol{f}(\boldsymbol{x}_{k-1}, \boldsymbol{y}_{k-1}, \boldsymbol{u}_k, \boldsymbol{p}) + \boldsymbol{w}_k, \tag{5}$$

$$\boldsymbol{z}_k = \boldsymbol{h}(\boldsymbol{x}_k, \boldsymbol{u}_k, \boldsymbol{p}) + \boldsymbol{v}_k, \tag{6}$$

subject to the constraints defined before, where $\boldsymbol{z}_k$ is the measurement vector, including pseudo-measurements, measured algebraic variables, real and reactive power injections, and flows, current phasors, etc.; $\boldsymbol{h}$ is the nonlinear measurement function; $\boldsymbol{v}_k$ is measurement error. The $\boldsymbol{w}_k$ and $\boldsymbol{v}_k$ are usually assumed to be normally distributed with zero mean and covariance matrices, $\boldsymbol{Q}_k$ and $\boldsymbol{R}_k$, respectively. Note that they are the superposition of different sources of noise/errors (e.g. from sensors, communication channels, or models) and may not follow a Gaussian distribution in practice.

To perform state estimation under the quasi-steady state operating condition, (2) is discretized as well, yielding a similar formula as (5) and (6) except for setting $\boldsymbol{x}_k \approx \boldsymbol{x}_{k-1}$. The use of conventional measurements from remote terminal units is sufficient. Conversely, when the system is operating under transient conditions, synchrophasor measurements may be the only source of information to carry out DSE. At the local level (e.g. generation station, substation, or FACTS device site), digital recorders or protection devices, also referred to as intelligent electronic devices, can provide the required synchronized information to execute DSE, possibly including key parameters of the monitored device.

Remark: for the existing DSEs, not all the equality and the inequality constraints are duly considered, for example, the inequality constraints of the states, control inputs, and model parameters. The latter may cause serious concerns, such as algorithm divergence, violation of physical laws, obtaining only sub-optimal solutions, to name a few. Thus, DSE methods that take into account all constraints are needed.

3.2.2 Dynamic State Estimation

To estimate the dynamic state vector or model parameters of the general discrete-time state-space model shown in (5)-(6), various nonlinear filters developed within the Kalman filter framework are used. It typically consists of two steps [35], namely a prediction step using (5), and a filtering/update step using (6). Specifically, given the state estimate at time step *k-1*, $\hat{\boldsymbol{x}}_{k-1|k-1}$, with its covariance matrix, $\boldsymbol{P}_{k-1|k-1}$, the predicted state vector is calculated from (5) directly or through a set of points drawn from the probability distribution of $\hat{\boldsymbol{x}}_{k-1|k-1}$, which is dependent on the assumed probability distributions of $\boldsymbol{w}_k$. As for the filtering step, the predictions are used together with the measurements at time step k to estimate the state vector and its covariance matrix. Depending on how the state statistics are propagated, different Kalman filters are available, such as extended Kalman filter (EKF), unscented Kalman filter (UKF), ensemble Kalman filter (EnKF), particle filter (PF) [36], to name a few.

The derived state-space equations (5)-(6) allow DSE to be applied rigorously to any power system, in any condition, provided the available computing power is sufficient for the size of the problem being addressed and the assumptions that all the equality and inequality constraints are appropriately enforced. The term 'dynamic', when applied to a quasi-steady state operating condition may be misleading, as the system dynamics are actually assumed to be absent/negligible and the state transitions are determined mainly by the smooth load evolution. In fact, under this scenario, we call the developed estimators either FASE or TSE.

Remarks: The state vector can be the enlarged one that contains $\boldsymbol{x}$ and $\boldsymbol{y}$ simultaneously, or the reduced one ($\boldsymbol{x}$ or $\boldsymbol{y}$), depending on whether algebraic or dynamic states are being estimated; the state vector $\boldsymbol{x}$ can be expanded to include uncertain parameters of

generators and associated controllers. On the other hand, except for the widely used recursive estimators that are based on the Kalman filter framework, other non-recursive estimators can also be adopted for the state and parameter estimation, such as the infinite impulse response filter, the finite impulse response filter [37], to name a few.

3.2.3 Forecasting-Aided State Estimation

The so-called FASE is a particular application of the DSE concept to quasi-steady-state conditions, in which the state-transition model (change in operating point) is driven only by slow enough stochastic changes in the power injections (demand and generation) and *the dynamics of* $\boldsymbol{x}_k$ *are sufficiently small to be neglected*. In addition, unlike the original DSE formulation, in the FASE approach, the state-transition model (5) is assumed to be linear, leading to

$$\begin{aligned} \boldsymbol{y}_k &= \boldsymbol{A}_k \boldsymbol{y}_{k-1} + \boldsymbol{\xi}_{k-1} + \boldsymbol{w}_k, \\ \boldsymbol{z}_k &= \boldsymbol{h}(\boldsymbol{y}_k, \boldsymbol{p}) + \boldsymbol{v}_k, \end{aligned} \tag{7}$$

where $\boldsymbol{y}_k$ *represents the algebraic state variables that specifically refer to the bus voltage magnitudes and angles*; furthermore, instead of resorting to the nonlinear state-transition models, the required transition matrix $\boldsymbol{A}_k$ and the trend vector $\boldsymbol{\xi}_{k-1}$, which is a function of $\boldsymbol{u}_k$, are identified from historical time series data. The widely used approaches for that are exponential smoothing regression or recursive least squares [38]-[43]. In other words, the current values are computed from a weighted average of the most recent past values, with an exponentially decreasing set of weights, disregarding any other information about the structure of the problem at hand.

When the input or the trend vector evolves smoothly, the FASE approach provides satisfactory results, generally better than the simpler TSE. However, potentially inaccurate results can be obtained in the presence of sudden changes caused by loads, DERs, system topology, to name a few, as the state transition coefficients take a while to adapt to the new situation [43]. There are some mitigation approaches proposed in the literature to address that, such as the normalized innovation vector-based statistical test, the skewness test [40], [41], etc. However, these tests are generally under the Gaussian assumption, which is difficult to hold for true in practice, yielding unreliable detection thresholds. Furthermore, the differentiation among different anomalies remains a grand challenge. Further research work along this line is required. One of the advantages frequently associated with FASE is that the predicted state provides useful information for security analysis and preventive control functions. However, the benefits of such a look-ahead or forecasting capability can be materialized in practice only if there is enough time for reaction, which may not be the case in transmission systems, featuring scanning rates of few seconds. The readers can refer to the two FASE review papers [44], [45] for more details.

3.2.4 Tracking State Estimation

With the assumption that the state transition matrix $\boldsymbol{A}_k$ is an identity matrix and the change in the state vector is very small, the FASE simplifies to TSE [46]-[50]. Formally, the TSE model is expressed as

$$\begin{aligned} \boldsymbol{y}_k &= \boldsymbol{y}_{k-1} + \boldsymbol{w}_k, \\ \boldsymbol{z}_k &= \boldsymbol{h}(\boldsymbol{y}_k, \boldsymbol{p}) + \boldsymbol{v}_k, \end{aligned} \tag{8}$$

where the change of state (random walk) $\boldsymbol{w}_k$ is assumed to be a white Gaussian noise with zero mean and known covariance matrix. One of the challenges in formulating TSE is the lack of an appropriate model to represent the dynamics of the system state. TSE assumes a quasi-steady-state condition where the system state remains unchanged other than an additive Gaussian noise $\boldsymbol{w}_k$. With the increasing penetration of DERs and flexible loads, the trend $\boldsymbol{\xi}_{k-1}$ is no longer negligible and the change of state cannot be simply replaced by a white Gaussian noise [38], [50]. This scenario is further aggravated in the presence of changes in network topology and parameters owing to line or transformer switching, or switching of capacitor banks or shunt reactors. As a result, it becomes a challenge to adopt TSE for practical applications.

3.2.5 Static State Estimation

The SSE arises from a further simplification of TSE, in which the state transition information is fully ignored and only the nonlinear measurement function is maintained. As a result, SSE has no memory of the states at the previous time steps [4]. It is worth pointing out that SSE may perform better than TSE or FASE in the presence of sudden changes. However, it cannot track system dynamics as compared to DSE. Furthermore, unlike DSE, it requires that the state vector be observable solely with the latest set of available measurements. In fact, adding pseudo-measurements through state or measurement forecasting to SSE is somewhat equivalent to performing a FASE [43], [45].

It is worth pointing out that a recent variation of SSE is the linear state estimation (LSE) [51]-[53], which uses voltage and current phasors from PMUs, leading to a linear measurement function:

$$\boldsymbol{z}_k = \boldsymbol{H}\boldsymbol{y}_k + \boldsymbol{v}_k, \tag{9}$$

where $\boldsymbol{H}$ is a constant matrix that consists of system transmission line parameters. LSE can track the online voltage magnitude and angle of each bus at the PMU reporting rate. However, it does not track the actual dynamics of the system, which are the dynamic states of machines, loads, etc.

3.3 Tools and Methods for Implementation of DSE

In what follows, we present a thorough yet not comprehensive review of the tools and methods for the implementation of DSE. The system observability concept is also discussed. After that, the focus is turned to DSE itself; the objective is to provide a summary of the different approaches, highlight their pros and cons, and discuss their implementation challenges.

3.3.1 Observability Analysis for DSE

Observability is defined as the ability to uniquely determine the states of the system from available measurements. For the SSE problem, observability analysis can be carried out by topological or numerical methods [6] and it results in a binary outcome. By contrast, for DSE, one may refer to strongly or weakly observable systems [54]-[56]. Furthermore, due to the nonlinearity and time-dependent nature of the problem, observability results are also time-dependent. The observability of a linear time-invariant dynamical system can be readily determined by whether or not its observability matrix has full rank. As for the nonlinear system in (5)-(6), one can

perform a linearization around a given operating point and assess its local observability. While this approach may be advantageous from a computational standpoint, it will occasionally lead to incorrect results under highly nonlinear operating conditions. We, therefore, advocate the use of methods that do not perform any linearization. To date, two methods have been proposed and they are described next.

1) Methods based on the Lie derivatives.

A nonlinear dynamical system is said to be observable at a state $\boldsymbol{x}_0$ if the nonlinear observability matrix obtained by using Lie derivatives at $\boldsymbol{x} = \boldsymbol{x}_0$ has a full rank [57].

This can be explained as follows: consider the nonlinear system given by (5)-(6), the Lie derivative of $\boldsymbol{h}$ with respect to $\boldsymbol{f}$ is defined as

$$L_f \boldsymbol{h} = \nabla \boldsymbol{h} \cdot \boldsymbol{f} \tag{10}$$

From the definition (10),

$$L_f^0 \boldsymbol{h} = \boldsymbol{h}, \qquad L_f^k \boldsymbol{h} = \frac{\partial L_f^{k-1} \boldsymbol{h}}{\partial \boldsymbol{x}} \cdot \boldsymbol{f} \tag{11}$$

Now, define $\boldsymbol{\Omega}$ as

$$\boldsymbol{\Omega} = \begin{bmatrix} L_f^0(\boldsymbol{h}_1) & \dots & L_f^0(\boldsymbol{h}_m) \\ L_f^1(\boldsymbol{h}_1) & \dots & L_f^0(\boldsymbol{h}_m) \\ \vdots & \dots & \vdots \\ L_f^{n-1}(\boldsymbol{h}_1) & \dots & L_f^{n-1}(\boldsymbol{h}_m) \end{bmatrix}, \tag{12}$$

and a gradient operator

$$\boldsymbol{O} = d\boldsymbol{\Omega} = \begin{bmatrix} dL_f^0(\boldsymbol{h}_1) & \dots & dL_f^0(\boldsymbol{h}_m) \\ dL_f^1(\boldsymbol{h}_1) & \dots & dL_f^0(\boldsymbol{h}_m) \\ \vdots & \dots & \vdots \\ dL_f^{n-1}(\boldsymbol{h}_1) & \dots & dL_f^{n-1}(\boldsymbol{h}_m) \end{bmatrix}. \tag{13}$$

The observability matrix $\boldsymbol{O}$ must have rank n for the system to be observable, and n is the dimension of the state vector $\boldsymbol{x}$.

In [58], this approach is used to determine the observability of several test systems in which the synchronous generators are represented by the classical model. Furthermore, the ratio between the smallest and the largest singular values of the observability matrix is used as a measure of the degree of observability. This work is further extended in [56], where the synchronous generators are represented by the two-axis model, including the model of the IEEE-Type1 excitation system. It is worth pointing out that the computation of the Lie derivative-based observability matrix can be cumbersome even for small-scale power systems. The automatic differentiation approach [58] can be used to reduce the burden of calculating the Lie derivatives of higher order.

2) Methods based on the empirical observability Gramian.

The empirical observability Gramian [59], [60] provides a way to analyze the state-output behavior of a nonlinear system. Different from analysis based on linearization, it is defined over an operating region of the original nonlinear dynamical system model and reflects the observability of the full nonlinear dynamics in the given domain. One important property is that the empirical observability Gramian for a system with

multiple outputs is the summation of the empirical Gramian computed for each of the outputs individually [54]. Therefore, the added observability after any sensor placement can be evaluated by calculating the empirical observability Gramian for each sensor. In [54] the observability of the system states is quantified by the determinant of the empirical observability Gramian. In [55], the level of unobservability of a nonlinear system is evaluated by the unobservability index approximated by the smallest eigenvalue of a Gramian matrix. In [61], different measures of the empirical observability Gramian, including the determinant, the trace, the minimum eigenvalue, and the condition number are compared. It is shown that when the observability is weak, the minimum eigenvalue and the condition number are better measures of observability. By contrast, when the observability is strong, the determinant is a better measure.

3.3.2 Implementations of DSE

From a Bayesian perspective, the DSE problem consists of recursively calculating some degree of belief in the state vector $\boldsymbol{x}_k$ at time k, given the data up to time k. Thus, it is required to calculate the conditional probability density function (pdf), $p(\boldsymbol{x}_k | \boldsymbol{z}_{1:k})$. The latter may be obtained recursively by the state prediction and updating steps. Suppose that $p(\boldsymbol{x}_{k-1} | \boldsymbol{z}_{1:k-1})$ at time k-1 is available, that is, state estimate at time step k-1, $\hat{\boldsymbol{x}}_{k-1|k-1}$, with its covariance matrix, $\boldsymbol{P}_{k-1|k-1}$ is given. Then, the prediction step involves applying (5) to obtain the *a priori* pdf of the state at time k via

$$p(\boldsymbol{x}_k \mid \boldsymbol{z}_{1:k-1}) = \int p(\boldsymbol{x}_k \mid \boldsymbol{x}_{k-1}) p(\boldsymbol{x}_{k-1} \mid \boldsymbol{z}_{1:k-1}) d\boldsymbol{x}_{k-1} \tag{14}$$

The probabilistic model of the state evolution $p(\boldsymbol{x}_k | \boldsymbol{x}_{k-1})$ is defined by the system equation given by (5) and the assumed probability distribution of $\boldsymbol{w}_k$. At the time instant k, when the measurements/observations $\boldsymbol{z}_k$ are available, the update step can be performed via Bayes' rule expressed as

$$p(\boldsymbol{x}_k | \boldsymbol{z}_{1:k}) = \frac{p(\boldsymbol{z}_k | \boldsymbol{x}_k) p(\boldsymbol{x}_k | \boldsymbol{z}_{1:k-1})}{p(\boldsymbol{z}_k | \boldsymbol{z}_{1:k-1})} \tag{15}$$

where the normalizing constant given by $p(\boldsymbol{z}_k | \boldsymbol{z}_{1:k-1}) = \int p(\boldsymbol{z}_k | \boldsymbol{x}_k) p(\boldsymbol{x}_k | \boldsymbol{z}_{1:k-1}) d\boldsymbol{x}_k$ depends on the likelihood function $p(\boldsymbol{z}_k | \boldsymbol{x}_k)$, which is defined by the observation model (6) and the assumed probability distribution of $\boldsymbol{v}_k$.

The recurrence relations (14) and (15) form the basis for the optimal Bayesian solution. However, this recursive propagation of the *a posteriori* density is only a conceptual solution in general; it cannot be determined analytically for the nonlinear dynamical system model [62]. It is in this sense that the EKF, UKF, EnKF, PF, and their variants only approximate the optimal Bayesian solution under the Gaussian noise assumption. In what follows, a thorough but not comprehensive review of these filters for power system DSE is presented.

1) Linearization-based Methods.

If the predicted state vector $\hat{\boldsymbol{x}}_{k|k-1}$ and its associated statistics $p(\boldsymbol{x}_k \,|\, \boldsymbol{z}_{1:k-1})$ are calculated from (5) directly through the Taylor series expansion, (14)-(15) will reduce to the EKF variants. Pioneering work along this line is done by [7] with the assumption that the instrumentation system at that time can measure power injections and frequency at generator buses accurately enough and at high enough sampling rates. With the advancement of PMU technologies, these assumptions can be alleviated. To this end, [63] proposed and investigated the benefits of adopting PMU data for real-time state estimation using EKF while [64], [65] leveraged data from relays, PMUs, FDRs to monitor and control system transients at the substation level. In [66], an EKF algorithm is proposed using the model decoupling technique to estimate the states and parameters of a classical generator model. Following their work, Ghahremani and Kamwa [67] proposed a modified EKF-based DSE to cope with cases where the field voltage is not accessible to metering due to brushless excitation systems. This work was later extended with the development of a decentralized DSE while relaxing the assumption of a known mechanical torque [68]. The linearization-based methods work well if the nonlinearity of the dynamical system is not strong, and the derivatives of nonlinear equations can be calculated. However, the system can be operated under stressed conditions, exhibiting strong nonlinearity. Furthermore, the derivatives can be challenging for complicated models and discrete switching events. To address these issues, derivative-free methods are preferred.

2) Derivative-Free-based Methods.

If $\hat{\boldsymbol{x}}_{k|k-1}$ and its associated statistics $p(\boldsymbol{x}_k \,|\, \boldsymbol{z}_{1:k-1})$ are calculated through a set of points drawn from the probability distribution of $\hat{\boldsymbol{x}}_{k-1|k-1}$, the resulted methods are derivative-free. The main ideas of these methods are to use either the deterministic sampling techniques such as the unscented transform and its variants or the Monte Carlo based sampling technique, to choose a set of sample points, which have the same mean and covariance as the *a priori* state statistics [62], [69], [70]. These points are then propagated through the non-linear functions $\boldsymbol{f}$ and $\boldsymbol{h}$, yielding an estimation of the *a posteriori* state statistics by using the Kalman filter structure, i.e., the mean and covariance estimates. Consequently, no difficult and complex calculation of Jacobian matrices is required. Depending on the types of the chosen points, different methods are proposed, including the UKF and its variants using sigma points, EnKF, PF, and their variants using ensembles or particles, which are Monte Carlo sampling techniques.

An UKF-based DSE using a fourth-order generator model is proposed in [71] to estimate the states of a single-machine infinite-bus power system. Along the same lines, a centralized UKF is developed in [72], [73] for a multi-machine system, while a decentralized strategy that does not require the transmission of local signals is advocated in [74], significantly increasing the computational efficiency. The decentralized UKF is further extended to estimate fourth-order generator model dynamic state variables, the unknown field voltage, and mechanical torque simultaneously [75]. It demonstrated improved performance about the approach proposed in [68]. In [76], the decentralized UKF is performed by incorporating internal angle in the dynamic model using local voltage and current phasors provided by PMUs and by decoupling the estimation process into two stages with continuous updating of measurement-noise variances. To further improve the estimation accuracy of the decentralized UKF, the measurement correlations of the PMUs are considered [77]. As

an alternative derivative-free method, EnKF uses Monte Carlo methods to estimate the error covariance matrix of the background error/noise, get an approximation to the filtered states, and produce an ensemble of initial conditions for the forecasting system. The latter is different from the UKF as sigma points need to be recalculated after the state filtering at each time instant. An EnKF method is firstly applied to track dynamic states of generators and their sensitivities to initial state errors, measurement noise, and unknown faults are investigated in [78]. That approach is further extended in [79] to consider time-correlated mechanical input power from DERs. While in [80], a maximum likelihood ensemble filter is proposed to estimate state variables by optimizing a nonlinear cost function and leveraging low-dimensional ensemble space to calculate Hessian preconditioning of the cost function. Different from the EnKF, PF uses the particles generated through Monte Carlo sampling to propagate and approximate the state statistics through nonlinear functions. An extended PF is proposed to estimate the fourth-order synchronous machine states using the iterative sampling and inflation of particle dispersion [81]. In [82], [83], the PF is applied to estimate synchronous machine states with detailed models.

3) Enhanced Numerical and Statistical Robustness.

The Kalman-type filters work well only under the validity of certain assumptions [35]. First, the system process and observation noise are assumed to have at each time instant zero means and known covariance matrices $\boldsymbol{Q}_k$ and $\boldsymbol{R}_k$, respectively. Secondly, they are assumed to follow a Gaussian distribution, at which the filter is optimal with minimum variances. Finally, the system model is assumed to be known with good accuracy. However, for most practical power systems, these assumptions do not hold. Indeed, $\boldsymbol{Q}_k$ and $\boldsymbol{R}_k$ are difficult to obtain in practice; the process and observation noise follow non-Gaussian distributions as demonstrated in [84]; the functions $\boldsymbol{f}$ and $\boldsymbol{h}$ are approximate; for instance, they may not account for all the nonlinearities of the system; some model parameter values may be unknown or incorrect, and the received measurements may be strongly biased due to impulsive communication noise, or cyberattacks [85].

In [36], it is shown that the performances of EKF, UKF, EnKF, and PF are greatly degraded in the presence of observation outliers due to their lack of robustness. To mitigate this issue, the normalized innovation vector-based test [74], [82] is usually used to detect observation outliers despite the vulnerability of this test to innovation outliers and non-Gaussian noise. In [86], a distributed two-stage robust UKF-based DSE using the least-absolute-value (LAV) estimator is presented to handle observation outliers in the PMU measurements. This approach has similar issues as the normalized innovation vector-based test. To this end, the generalized maximum-likelihood (GM) iterated EKF (GM-IEKF) [87]-[89] is proposed to deal with the observation and innovation outliers. However, its statistical efficiency is relatively low in the presence of non-Gaussian system processes and measurement noise. To address that, the robust GM-UKF [27], [28] is proposed that can achieve high statistical efficiency under a broad range of non-Gaussian noise while maintaining the robustness to observation and innovation outliers. A reformulation of the GM-UKF with multiple hypothesis testing [29] further enables it to handle three types of outliers. Note that the three types of gross errors or outliers include observation, innovation, and structural outliers [28]. They can be caused by either an unreliable dynamical model or real-time synchrophasor measurements with data quality issues. However, these GM-type DSE may yield biased

state estimates in the presence of large system uncertainties. To this end, the H-infinity EKF and UKF that rely on robust control theory are proposed [89], [90]. It is shown that the H-infinity filter can bound the system uncertainties but lacks robustness to outliers and non-Gaussian noise.

***Remark*:** Every approach has its domain of feasibility and beyond that, its performance is no longer guaranteed. Due to numerical issues, model errors, and cyber-attacks, to cite a few, the DSE may not converge. In this scenario, only the forecasted states from the dynamical system model are available. Since the system dynamic states cannot change immediately following a disturbance, the forecasted states are reasonably close to the true dynamic states given that the system dynamic model is accurate. Then, this type of information can still be useful for operation and control. If that is not the case, we may only use the state estimates at the previous time instant for further processing. This is similar to the traditional SSE. Future research about enhancing the robustness of DSE against divergence is required. DSE results should also be validated carefully to avoid converging to wrong state estimates. The data-driven methods or machine-learning-based tools can be taken as complementary to help that. This is another direction for research.

3.3.3 Parameter Estimation and Calibration using DSE

The application of the Kalman filter and its variants for the state and parameter estimation has been widely used in signal processing, communication, among others. Along this line, there are typically two ways for implementations [91]: i) joint estimation, that is, the unknown parameters are augmented with the system state variables for joint estimation. This joint state is estimated through a single Kalman filter recursion; ii) dual approach: it contains two parallel filters, one on the state and the other on the parameters; in other words, the parameters are treated as known within the state filter at any given time, k, while the states are treated as known in the parallel parameter filter. Note that these two approaches show little differences in the estimation results for most applications [91]. On the other hand, the observability analysis must be performed and the number of measurements should be sufficient to initiate parameter estimation. In the power system parameter estimation context, only joint estimation is used. For example, the transient reactance and inertia of the classical generator are augmented with state variables for joint estimation [93]. In [94], [95], [96], the UKF, the square-root UKF and constrained iterated UKF are used to estimate high-order generator model state and parameters simultaneously. The UKF is also used to estimate dynamic load parameters [97] and the frequency and fundamental power components [98]. Due to observability issues, not all unknown parameters can be estimated. Therefore, sensitivity analysis is carried out to narrow down the number of candidate parameters for calibration. This strategy is widely used in model validation and calibration, such as [26], [99], [100].

***Remark*:** The implementation of DSE for large-scale systems is challenging. To deal with that, the distributed or decentralized implementations proposed in the literature are encouraged. Another way of achieving that goal is through high-performance computing and parallel computing techniques [16], [101], which require further investigations. Furthermore, when augmenting the identified incorrect parameters into the state vector for calibration, local observability analysis should be carefully carried out to avoid multiple solutions as well as numerical issues.

3.3.4 Centralized vs. Decentralized DSE

There are two ways of DSE implementations, namely the centralized and decentralized ones. Centralized DSE assumes that the system is observable by PMUs and Kron reduction can be carried out to reduce the system to the generators' terminals. In addition, it requires accurate knowledge of each system component parameter as well as the real-time wide-area PMU measurements. By contrast, the decentralized DSE is implemented using only local PMU measurements. It assumes that the terminal bus of the interesting dynamic components is observed by PMU measurements and local observability of dynamic states is satisfied. If a generator terminal bus is not equipped with PMU, a PMU-based linear state estimator [51]-[53] for that local system should be performed first. Then, the estimated measurements at the interested terminal buses can be obtained and the decentralized DSE is executed. Note that the local phasor data concentrator (PDC) is in charge of communicating and processing the PMU measurements. Centralized DSE allows us to achieve global monitoring and control applications and has good robustness to data quality and security issues as the measurement redundancy is high. However, it has a large computational burden and strong assumptions about the accuracy of the whole dynamic system models. By contrast, decentralized DSE only needs local measurements at the terminal buses and the dynamic model of interested components, which is fast to execute and not impacted by the model inaccuracy of other system components. However, the local measurement redundancy is low, and therefore decentralized DSE has difficulties in dealing with PMU data quality and security issues. On the other hand, with a decentralized DSE, only local controls are implemented. If coordinated control is deployed between different local DSEs, additional communication bandwidth is required, making the comparison with the communication cost of the centralized DSE difficult to assess. Choosing between the two implementation schemes depends on the applications and the communication infrastructures being used. It should be noted that for both centralized and decentralized DSE-based applications, time tags of the estimated dynamic state variables are required when the communication network is involved [102].

3.4 Conclusions and Outlook

This section discusses the motivations, concepts and key tools, and methodologies that are used for dynamic state and parameter estimation. DSE is presented in a unified framework that uses commonly accepted notation and formulation in power system dynamics and control literature to establish a firm baseline for future research and development efforts.

Although significant research work has been done for DSE, there is still room for improvement. Here, several important aspects listed below are recommended for future work:

- **Enhancement of the accuracy and security of DSE**: the quality of the filtered/updated state vector relies heavily on the quality of the measurements and the predicted states. Therefore, to obtain reliable state estimates for dynamic systems, robust state prediction and state filtering with good efficiency is required. From the statistical robustness point of view, a robust DSE should be designed to be robust against several data quality issues, such as non-Gaussian measurement noise, bad data, cyberattacks, missing data, etc. From the

numerical robustness aspect, a robust DSE should be developed, such as robust square-root type filters or other alternatives that can converge under various operation conditions. Also, as the system is always subject to various uncertainties, a robust DSE should be designed that can bound the influence of these uncertainties. Furthermore, hybrid approaches that leverage the strengths of different theories are more likely to be used for complicated power systems. Finally, data-driven DSE based on artificial neural networks [103], [104] and operator theory [105] that do not rely on the power system model has been studied. Preliminary results indicate that these approaches can estimate the generators' rotor angle and/or rotor speed. More work along this line is needed to include the estimation of other dynamic state variables, and to validate them with real PMU data;

- **Observability Analysis**: the use of the smallest singular value of the observability matrix, be it the one obtained via Lie derivatives or other linear approximation approaches, for quantifying the degree of observability of a nonlinear dynamic system has not been formally proven. Although many simulation cases have strongly confirmed its validity, more work is needed to develop a computationally efficient and theoretically proven implementation of observability analysis. It is also worthwhile investigating the relationship between linearized (small-signal approximation) and Lie derivative-based observability matrices to define the region of validity for the computationally attractive small-signal approximation, in particular during system transients. Besides, both the accuracy and computational efficiency of the Lie derivatives-based approaches and the empirical observability Gramian based approaches should be carefully investigated and compared, both theoretically and numerically, for evaluating the observability of the dynamic states under specific system models and measurement configurations.
- **Dynamic Model Parameter Estimation and Anomaly Detection**: the current DSE-based parameter estimation techniques mainly focus on synchronous generators. They can be extended for model validation and calibration of various system components, such as inverter-based renewable generation units, dynamic loads, etc. It is worth pointing out that if there exist gross model parameter errors, parameter error detection and identification should be carried out first. Although this task is challenging for complicated models with many parameters, it is the key for parameter calibration to enhance the reliability and accuracy of system models. On the other hand, the DSE can be extended to detect the failures of various control devices by setting up appropriate criteria, including exciters, PSS, transformers, etc;
- **Dynamic Security Assessment**: it requires a robust and computationally efficient DSE to accurately and promptly initialize transient simulations. More work is needed to identify the major drawbacks and bottlenecks experienced by the industry in executing their current dynamic security assessment procedures and addressing them by robust DSE. These issues will motivate further research towards the development of DSE, which may be routinely executed along with SSE in future EMS;
- **Wide-Area System Integrity Protection Schemes (SIPS)**: enhanced system observability through internal angle and speed estimates will allow us to compute more accurate transient energy function and the latter may lead to several breakthroughs, such as faster out-of-step detection, more realistic

location of runaway generator and a minimal amount of generation/load to be shed to preserve system integrity without knowing the topology accurately;

- **DSE of Renewable and Other Asynchronous Distributed Sources**: wind, solar, and other DERs are playing an increasingly significant role in power generation. But, being asynchronous, intermittent, and without inertia, these sources are difficult to be controlled for global system stability. Developing DSE for these sources at their point of common coupling with the grid is a viable solution, from which we can accurately estimate the latent 'synthetic inertia in these sources, and use it for contributing to the rotor-angle stability of the system. Local DSE at each wind-turbine or photovoltaic panel, within a wind-farm or solar-park, can also be used for optimizing the performance of the whole farm or park;
- **DSE Computational Advancements**: DSE aims to estimate the system dynamic states in a very short time frame consistent with measurement cycles. For typical phasor measurements, the cycle is 30 milliseconds, which means all computation of one DSE step has to be finished within 30 milliseconds. This is a fundamentally high demand on the underlying computationally hardware and software technologies. High-performance computing would have to be considered in achieving such computational advancements [101];
- **Dynamic State Estimation of Active Distribution System and Microgrids**: the concepts, tools, and methodologies of DSE can be extended from the transmission system to the active distribution system and the microgrid. It is of interest to design robust controllers for the enhancement of microgrid stability in both grid-connected and island modes. This will promote a new energy management system for microgrid operation and control.

4. Roles of DSE in Power System Modeling, Monitoring, and Operation

4.1 Introduction

Dynamic state estimation (DSE) [106] is going to be very useful for time-critical monitoring, control, and protection of future electric power grids. This is largely due to the changes in generation mixes and load compositions, particularly the increasing penetration of intermittent, stochastic, and power electronics-interfaced non-synchronous renewable generation and distributed energy resources (DERs) [107]. In this context, where the system operating point changes more often and more rapidly, tracking the system dynamic state variables is of critical importance. Recall that dynamic state variables are the ones associated with the time derivatives in the set of differential-algebraic equations describing power system dynamics [108]. The dynamic state variables of the synchronous generators correspond to their electromagnetic and electromechanical processes, as well as their controllers [109]. As for the non-synchronous generations, the dynamic state variables are associated with the primary source of energy, e.g. solar photovoltaic arrays, batteries and wind turbines, as well as their controllers. Examples include the frequency at the point of common coupling between the power converter and the electric grid, the electric current in the converter, and the pitch angle of wind turbines. Furthermore, there exists an important challenge in the development and maintenance of accurate models for power electronics-

interfaced devices. DSE can be developed to validate the models and to estimate unknown or incorrect parameters.

Despite being initially mentioned in the 1970s [110], it was only in recent years that the power system community has picked up the momentum in DSE research. Part of the reason was the lack of appropriate metering infrastructure, like phasor measurement units (PMUs) and merging units (MUs) that are being widely deployed to capture the appropriate dynamics in power systems [12], [111]. Feasibility studies using PMU measurements for DSE are reported in [63], and subsequently, various Kalman filtering techniques, such as Extended Kalman Filter (EKF), Unscented Kalman Filter (UKF) [71], Ensemble Kalman Filter (EnKF), Particle Filter (PF) and their variants [36] have been applied to DSE. Data-driven DSE [105], observability analysis to guide measurement selection [56], and the enhancement of robustness against bad data and parameter errors are also developed in [86], [88], [112]. Readers may refer to [109] for a comprehensive summary of DSE algorithms.

Several online tasks can benefit from DSE but have not adequately deliberated the need for it. An example is the dynamic security assessment (DSA). Today's DSA tool assumes a steady-state initial condition [113], which would yield inaccurate results in the presence of fluctuations from DERs and loads; conversely, DSE could directly estimate the dynamic states and therefore provide more accurate initialization conditions for DSA [114]. Furthermore, for synchronous generators, numerous developed control schemes rely on power system stabilizers (PSS) to damp out oscillations. These control schemes use the rotor's speed as input. The direct use of measurements obtained from a meter installed on the shaft of the machine is not reliable; instead, the current practice is to use the compensated frequency [115], which is calculated using the voltage and current measured at the generators' terminal. However, the calculation of the compensated frequency is significantly affected under transient conditions [116], which leads to sub-optimal control response of the PSS. If DSE is deployed for frequency estimation, this issue can be effectively resolved. The rate of change of frequency (ROCOF) estimation can also be formulated in the state-space model for DSE [117]. Note that, in these examples, traditional static state estimation (SSE) could not provide reliable system dynamic states and quantities. Therefore, it is of critical importance to understand the role of DSE in power systems from various aspects. While SSE has been in energy management systems (EMS) for decades and its roles and implementation requirements are well established, the same does not apply for DSE. There is a large gap in understanding different roles of SSE and DSE and how DSE can be implemented in practice.

This section summarizes the efforts of addressing the aforementioned gaps and yields the following contributions:

- A comprehensive clarification of the roles of DSE from the power system modeling, monitoring, and operation perspectives are provided;
- Comparisons between SSE and DSE in practical implementations are thoroughly discussed, including measurement configurations, model requirements, software support, and potential applications based on the estimation results;
- Illustrative examples and summary frameworks have been presented to demonstrate the roles of DSE.

- The future applications are discussed to shed light on the transition from today's EMS to its next generation.

4.2 Comparisons with SSE and DSE

SSE has become a widely used tool in today's EMS, while DSE is a new tool for the industry and system operators. It is essential to clarify their implementation and functionality differences and, at the same time, enable a clear path transition from SSE-based EMS to the future DSE-based EMS with power electronics-dominated power systems.

4.2.1 Implementation Differences

SSE and DSE have different requirements concerning measurements, models, observability, execution rate, outputs, and applications. These differences are summarized in Table I. SSE mostly relies on SCADA measurements that are updated every 2-5s and some PMU measurements to gain more redundancy. But since SCADA measurements are not time-synchronized while those of PMUs are, effectively integrating those two sources of data needs to be taken care of. By contrast, for DSE, time-synchronized measurements with a reporting rate of 30 to 240 samples per second are used and they might come from PMUs and digital fault recorders (DFRs). Furthermore, there is a significant difference in the observability theory for SSE and DSE [54], [56]. For SSE, the topological- or numerical-based observability analysis typically determines whether the system is observable or not. If the system is unobservable, observable islands may be determined [6]. Furthermore, in the presence of ampere measurements, where multiple solutions may exist depending on the nature of the remaining measurements and the loading point, the observability analysis can also inform whether there are multiple solutions or not to the SSE problem. A network can be uniquely observable for heavily loaded cases, but "unobservable" (i.e., undefined Jacobian) when the ampere measurement value is nearly zero (unloaded line), which leads to a 0/0 indeterminate form. Thus, the answer depends on the line loading but is typically binary. By contrast, in DSE, one may refer to strongly or weakly or not observable systems. One way to quantify this is to compute the smallest singular value of the observability matrix from the Lie derivatives [56]. A higher (lower) value of the smallest singular value of the observability matrix indicates stronger (weaker) observability for a given measurement set. Furthermore, due to the nonlinear and time-dependent nature of the problem, observability results are time-varying. It is worth noting that under certain conditions, the system might be unobservable, but still detectable [118] for DSE. Detectability is a slightly weaker notion than observability. A system is detectable if all the unobservable states are stable. To enhance the observability of power system dynamic state estimation, some optimal PMU placement strategies [54], [119] have been developed. This work can be further investigated considering the robustness against data quality issues, model uncertainties, etc. Also, each prediction-correction step of the DSE must be numerically solved faster than the PMUs/DFRs/MUs scan rate, thereby posing some challenges on the computational power. To address this issue, decentralized/distributed DSE or parallel computing technique for centralized DSE is usually suggested [109]. Another important issue that merits attention is algorithm convergence. It has been shown for SSE that under heavy loading and topology error conditions, there may be convergence problems [120], [121]. Therefore, both numerical and statistical robustness need to be enhanced to deal

with that. The data quality issues, inappropriate initialization, and model errors/uncertainties may lead to convergence issues for DSE. Although several theoretical works have been carried out to prove the convergence of various types of nonlinear Kalman filters [122]-[124] under some assumptions, their applications to power systems under various conditions need thorough investigations. This is because some assumptions in the theoretical developments may not always hold. Thus, nonlinear Kalman filters without linearization are recommended for practical implementations, such as UKF, EnKF, PF, etc.

The outcomes of SSE and DSE are also different. SSE provides estimates of the bus voltage magnitudes and phase angles, which are the algebraic variables; on the other hand, DSE provides estimates of the dynamic state variables, such as those associated with generators/dynamic loads/DERs. There is also a joint DSE that estimates dynamic and algebraic variables simultaneously [109]. For some PMU observable networks, linear state estimation (LSE) that keeps up with the PMU refreshing rate is developed [51]. However, it does not track the actual system dynamics.

TABLE I
COMPARISON BETWEEN SSE AND DSE

	SSE	DSE
Measurements	From the SCADA (every ~ 2-10 sec.)	From PMU/DFR/MU (every 1/30 ~ 1/240 sec.)
Observability	Binary[1] (observable or not)	Time-varying (Strong/weak/not observable)
Update speed	1 snapshot (every ~ 2-10 sec.)	1 prediction + 1 filtering step of the Kalman filter (every < 1/30 sec.)
Models	Algebraic power flow equations	Differential-algebraic equations
Framework	Mostly centralized or distributed	Centralized& distributed/decentralized
Outputs	Algebraic variables (voltage magnitudes and angles)	Dynamic variables (machine/ dynamic load/ DERs dynamic variables)
Applications	Monitoring and control (operator in the loop)	Monitoring (operator in the loop), control and adaptive protection (operator out of the loop)

[1]Topological observability analysis provides a binary answer as the first byproduct, but it gives additional valuable information, such as which buses (islands) are observable or which pseudo-measurements should minimally be added to restore full observability. Numerical observability analysis, being based on the factorization of the Jacobian or Gain matrices, provides a "spectrum" or range of observability answers, depending on the condition number of the matrix being factorized. A network can be topologically observable but not algebraically (numerically) observable, owing to abnormal network parameters or measurement weights. In some cases, a network can be numerically observable for a certain combination of weights, but not for others. This is not exactly "binary".

When implementing SSE and DSE, the models used are different. In SSE, the generators and loads are simply modeled by power injections and, hence, the system

model used for SSE is represented using algebraic equations. While for DSE, the generators/dynamic loads/DERs, etc., and their controllers are represented by a set of DAEs. Note that it is not required to have PMUs installed at each generator terminal; if the generator terminal is observable via a local LSE, the DSE can be implemented.

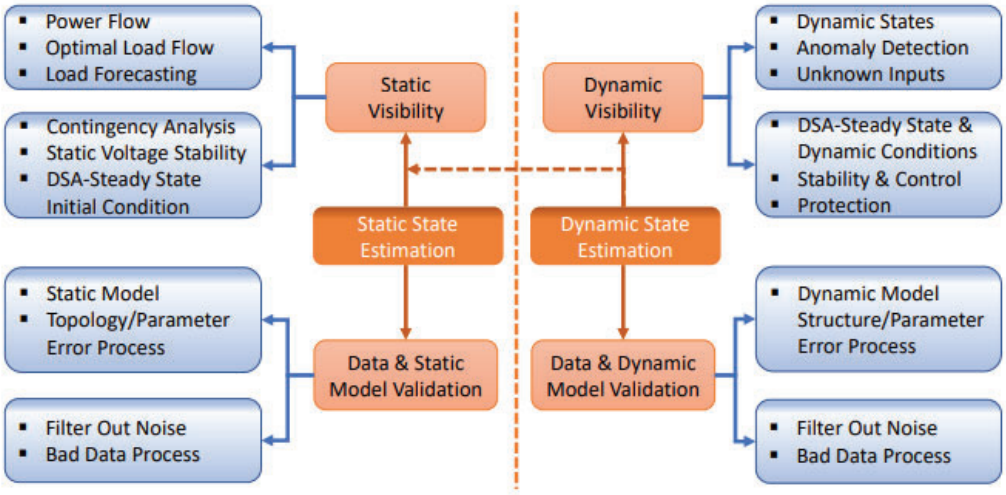

Fig. 3. Functional schematic comparisons between SSE and DSE.

4.2.2 Functional Differences

From the functionality perspective, both SSE and DSE have two essential roles, namely improving the targeted system visibility and validating the used data and models, which are summarized in Fig. 3. Since SSE is the snapshot-based static view of the system algebraic variables, its outputs allow the calculations of power injections and power flows across the systems. This provides the database for many applications in today's EMS, including system operations, such as power flow, optimal power flow, load forecasting, etc., as well as security assessment, i.e., static contingency and static voltage stability analysis. By contrast, DSE relies on fast sampled and time-synchronized measurements to track system dynamic changes, thus providing dynamic visibility, such as dynamic states, anomaly detection, unknown inputs estimation, etc. [33], [34], [125]. This dynamic information further allows other related applications, i.e., DSA [114], rotor angle stability assessment [125], adaptive power system protection [8], and so on. In terms of data and model validation for SSE, it relies on the measurement residual-based statistical test or robust estimation criteria for bad data processing and measurement model parameter error identifications. The bad data are caused by gross measurement errors or data transfer errors while model parameter errors can be due to transmission line parameters and topology inaccuracies. Since DSE relies on a set of DAEs, besides those parameter errors previously mentioned, there are also model errors in equations that govern the system dynamics, e.g., generator models and their related controllers. These errors are classified into two categories: innovation outliers, which are caused by parameter and/or input errors in the set of DAEs; and structural outliers, which are caused by a model structure that does not reflect well the system dynamics [28]. Note that the DSE outputs can be used to calculate the system algebraic variables as well. Therefore, the SSE functions can benefit from DSE. And

vice versa, the information provided by the SSE can be used to warm start the DSE process before an event occurs.

***Remark*:** with the increasing deployment of PMUs, many high voltage transmission systems are already observable with only PMU measurements, such as that of Dominion Energy, the 765/345/230 kV power grid in New York, and the 345 kV power grid in New England. As a result, the legacy nonlinear SSE algorithms can now be reformulated as the LSE [51]. As long as the computational power is sufficient, the LSE can be updated with the scan rate of PMUs but its results are also restricted to algebraic variables-based applications. Compared with the SCADA-based SSE, the LSE allows for faster real-time contingency analysis and voltage stability assessment, besides area angle limit monitoring. By comparing LSE with DSE, the LSE does not touch the dynamic equations and cannot provide the real-time picture of system dynamic states and the related controllers. For example, the rotor speed information is not available from LSE and thus many applications based on them cannot be done. The importance of dynamic states for power system monitoring, visibility, and operation will be highlighted later. In summary, the fundamental differences in terms of potential applications are that LSE only deals with algebraic variables while DSE provides both dynamic and algebraic variables of the system.

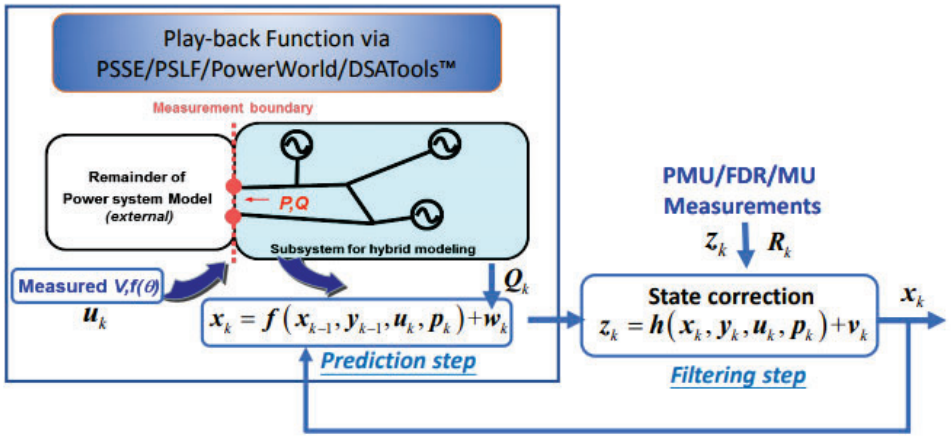

Fig. 4. Implementation of DSE using existing commercial tools.

4.2.3 Practical Implementation of DSE

Several vendors offer commercial software for SSE implementation while there is no commercial software for DSE. However, we can leverage the capabilities of existing commercial tools and enable the DSE implementation. The practical implementation of DSE is shown in Fig. 4, where the system is modeled by the following state-space model after time discretization of DAEs, and considering the available measurements:

$$\boldsymbol{x}_k = \boldsymbol{f}(\boldsymbol{x}_{k-1}, \boldsymbol{y}_{k-1}, \boldsymbol{u}_k, \boldsymbol{p}_k) + \boldsymbol{w}_k,\ \mathbb{E}\left[\boldsymbol{w}_k \boldsymbol{w}_k^\top\right] = \boldsymbol{Q}_k \tag{16}$$

$$\boldsymbol{z}_k = \boldsymbol{h}(\boldsymbol{x}_k, \boldsymbol{y}_k, \boldsymbol{u}_k, \boldsymbol{p}_k) + \boldsymbol{v}_k,\ \mathbb{E}\left[\boldsymbol{v}_k \boldsymbol{v}_k^\top\right] = \boldsymbol{R}_k \tag{17}$$

where $\boldsymbol{x}_k$ and $\boldsymbol{y}_k$ represent system dynamic and algebraic state vectors, respectively; $\boldsymbol{z}_k$ is the measurement vector from and/or DFRs and/or MUs; $\boldsymbol{u}_k$ is the system input

vector that drives the state transition; $\boldsymbol{p}_k$ denotes the system parameters; $\boldsymbol{f}$ and $\boldsymbol{h}$ are vector-valued nonlinear functions; $\boldsymbol{w}_k$ and $\boldsymbol{v}_k$ are the system process and measurement error vector, respectively, with covariance matrices $\boldsymbol{Q}_k$ and $\boldsymbol{R}_k$.

It is clear from Fig. 4 that the implementation of DSE has two main steps, namely the state prediction via (16) to obtain predicted state at time *k* and the state correction step that integrates the state prediction and measurements in (17) for filtering. It is interesting to note that the widely used commercial software, such as PSSE/ PSLF/ PowerWorld/ DSATools have the so-called event playback functions available. This playback function allows us to implement equation (16) automatically. The main idea of the play-back function is to take the measured voltage phasor as the input $\boldsymbol{u}_k$ of (16) and obtain the predicted state vector. Then, by resorting to the Kalman filter framework, the predicted state vector is integrated with the received measurement vector in (17) for the estimation of dynamic states. To fully leverage this playback function, it is suggested to use nonlinear Kalman filter techniques that do not require linearization, such as UKF, EnKF, PF, and their variants. Another useful implementation of DSE is to take unknown dynamic states or control inputs as additional state variables for joint estimation. This is because there may be a lack of accurate controller information or the control models may be of poor quality. Therefore, it can be concluded that only the filtering step needs to be coded along with the playback function for practical DSE implementation. In other words, no major changes are required, and only an additional module needs to be added to make the smooth transition of the play-back function for practical DSE implementation. It should be noted that we do not need to wait for an event to trigger the DSE. As long as the measured vector $\boldsymbol{u}_k$, typically the voltage magnitudes and angles/frequency, are fed into the playback function, the DSE can be implemented to continuously monitor the dynamic states. For a successful implementation of DSE, the observability analysis using Lie derivatives should be carried out first and the required measurements should be provided [56]. Besides the basic observability requirement, higher measurement redundancy would lead to better estimation accuracy and capability of handling bad data. Some works [54], [119] about PMU placement strategy for improving the observability of dynamic state estimation have been investigated.

4.3 DSE for Modeling, Monitoring, and Operation

Three major application areas that can potentially benefit from DSE have been identified and elaborated in this paper, namely: a) modeling, b) monitoring via the enhanced dynamic visibility, and c) operation. Each of them is discussed below.

4.3.1 Modeling

Following the 2003 Northeastern U.S. and Eastern Canada blackout, the North American Electric Reliability Corporation (NERC) has been developing standards for periodical model validation [25]. The model validations include synchronous generators and their related controllers, wind farms, solar farms, dynamic loads, etc. In this section, we first present the generator model validation and calibration framework, followed by other DSE-based applications from a modeling perspective.

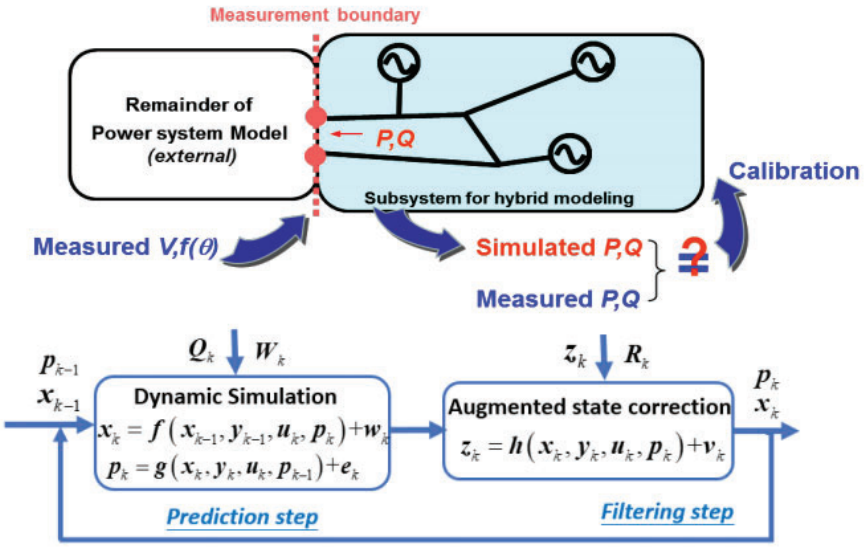

Fig. 5. DSE-enabled model validation and calibration.

1) Generator Model Validation and Parameter Calibration

In the existing commercial software, the "event playback" function is leveraged to validate dynamic models using PMU data. The key idea is to take the measured generator terminal voltage magnitude/phase angle or frequency as model inputs to obtain model outputs of real power P and reactive power Q. These responses are compared with the measured P and Q to validate the model accuracy [26], [100], [126]. When the model of the subsystem is accurate, the simulation responses should match statistically well the actual responses. By contrast, when significant mismatches are observed, the model is considered inadequate and parameter calibration is needed. This process can be found in the upper part of Fig. 5, where $\boldsymbol{e}_k$ is the parameter error with covariance matrix $\boldsymbol{W}_k$ and $\boldsymbol{g}$ is the parameter transition function. The differences between Figs. 2 and 3 include: 1) statistical test between the simulated responses and the measured response to validate the model and 2) augmenting suspicious parameters obtained from sensitivity analysis and engineering judgment with the system dynamic states for joint estimation. Note that the criterion for model validation is a byproduct of DSE, namely the innovation vector-based statistical test.

To calibrate the system models, both the system model structure and parameters need to be carefully investigated. Traditionally, they can be found from the manufacturer's databases. However, parameters might drift during operations due to a variety of factors, e.g., environmental changes, the aging process, and coupling effects. Taking generators offline for testing and parameter calibration is costly and affects the system's reliability. Therefore, online calibration has been an important application of DSE. Since not all parameters are identified using the present measurement sets, it is, therefore, critical to select appropriate candidate parameters before starting a parameter calibration procedure. The calibration typically includes four main steps [26], [100], namely 1) initial checks, 2) sensitivity analysis, 3) parameter estimation, and 4) parameter validation using other disturbances. The first step is to eliminate obvious errors in parameters that are not realistic, such as fractional values for the model flags

that should be integers, parameter values outside the normal ranges, swapped values for limiters, and incorrect statuses of controllers. The sensitivity analysis provides a guideline in determining parameter sensitivity for different disturbances and identifying the candidate parameters for calibration. The selected parameter vector $\boldsymbol{p}$ is augmented with the original state vector for joint estimation as shown in the lower part of Fig. 5. The joint DSE methods are based on, e.g., EKF, UKF, constrained UKF, and many other Kalman filter variants. After calibration, it is necessary to perform model validation using different events so that the identified parameters are not local optima. If the model deficiency for other events is detected, the calibration process should be repeated until there are no inconsistent responses between models and measurements.

The model validation process can be used to guide parameter estimation via DSE. There can be direct use of DSE to track parameter changes or identification of unknown machine parameters. For example, the UKF algorithms have been leveraged in [94], [127] to estimate the parameters of synchronous machines. The measurements may include voltages and current signals from the stator and the field winding or PMUs. A constrained UKF is further developed in [96] to narrow down the parameter search space and yield better parameter estimation results. DSE-based generator inertia, sub-transient reactance, and governor dead-band estimation approaches can be found in [93], [128].

2) Other Parameter Estimation Applications

Besides synchronous machine model validation and calibration, the targeted dynamic components can be dynamic loads, wind farms, and other power electronics-interfaced DERs [97], [127], [129], [130] as long as they are appropriately described by DAEs and their related local fast measurements are available. In [97], the first-order exponential dynamic load model is organized as the state-space model and a UKF is used to track the unknown parameters. Motivated by the parameter estimation of synchronous machines, the state-space model of DFIG is derived and the unknown parameters are augmented with its dynamic states for joint estimation via EnKF or UKF [127], [130]. It is worth noting that there are only a few works on DSE for parameter estimation of dynamic loads and solar/wind farms. As the DSE technologies for synchronous machines are becoming mature, extending them for dynamic components, especially the power electronics-based DERs and dynamic loads, is worth further investigation. The power system coherency identification would also benefit from the estimated dynamic states, especially the rotor angles and speeds [131], [132]. The identified coherency allows the development of model reduction for stability assessment and islanding control. Another potential application of DSE is the dynamic reduction of large power systems [133], where the equivalent model parameters can be estimated together with the machine dynamic states.

4.3.2 Monitoring

One of the key DSE applications is to provide enhanced dynamic visibility for power system monitoring. Part of the dynamic visibility of DSE has been shown in Fig. 3 but a more detailed summary includes seven key functions: i) dynamic state trajectory tracking, ii) oscillation monitoring, iii) bus frequency, ROCOF, and center of inertia (COI) frequency estimation, iv) data quality detection and correction, including cyberattacks, v) unknown control inputs identification, vi) anomaly detection and vii)

other applications that involve larger time constants than the electromechanical dynamics. The dynamic state trajectory tracking is a natural product of DSE as it provides the time series of the generator and its controller states in the presence of system disturbance. Among these, the generator rotor speed and angle have been widely used in power systems for oscillation detection [14]. For example, in the damping-torque-based forced oscillation source location, the rotor speed and angle are required [134]. The estimated machine rotor speeds also allow us to resort to the frequency divider for bus frequency estimation [31]. This interesting result reveals that if the system machine rotor speeds are available, all bus frequencies can be estimated. Since the number of machines is much smaller than the number of buses, it significantly reduces the requirement of PMU installations for bus frequency monitoring. The real-time COI frequency plays an important role in power system stability analysis and control. Via the DSE outputs, we can obtain the COI frequency at the same refreshing rate as the PMU measurements. This provides the online reference frequency for control [32]. Note that a widely used industry practice is to leverage generator terminal voltage and current measurements to calculate an approximated internal machine rotor speed. However, its accuracy is questionable as can be seen in the following example: a three-phase short-circuit occurs at Bus 16 of the IEEE 39-bus system on t=0.5s and the fault is cleared after one cycle by opening the transmission line connecting buses 16 and 17. The machines are modeled using the subtransient model with a DC1A exciter, PSS1A stabilizer, and IEEE-G3 governor. Fig. 6 shows the estimated generator 5 internal rotor speed by DSE, the numerical derivative with low pass filter, and numerical derivative with washout filter [135] of the derived generator angle from the terminal voltage and current measurements. As expected, the numerical derivative of the approximated rotor angle suffers from numerical errors at the moment the event happens; numerical derivative with washout filter can address that but at the cost of modifying the time-domain response. By contrast, the DSE can accurately track the rotor speed. On the other hand, ROCoF has been utilized as an important parameter for system protection, especially for the inverter-based generations. By treating it as a dynamic state instead of an algebraic variable, an accurate estimation of it can be achieved [117].

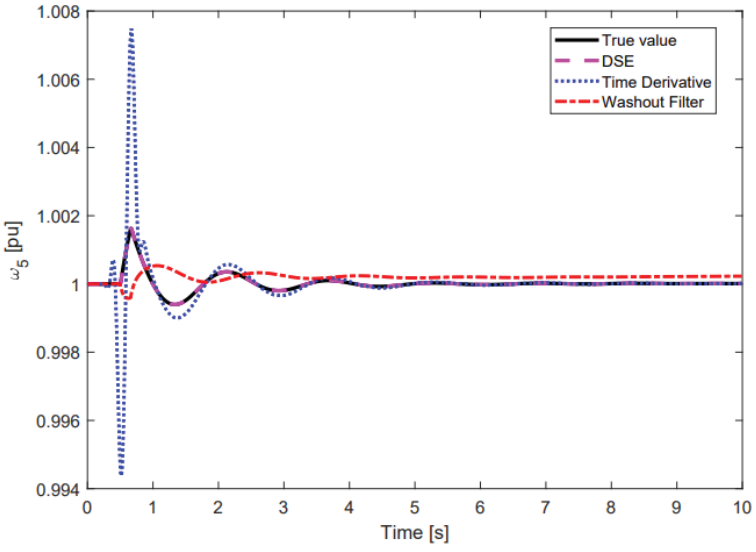

Fig. 6. Comparisons of different methods for internal generator frequency estimation.

The measurements are always subject to noise and even large errors caused by communications, instrument transformer saturation, cyber-attacks, etc. It is important that DSE naturally filters out the measurement noise and provides more accurate data for other applications. Since the field measurements typically follow non-Gaussian distributions [84], robust DSE developed based on the robust statistics theory is needed [136]. While for randomly occurred bad measurements, both normalized residual statistical tests and robust detection are developed. However, it is shown that the threshold for the traditional normalized residual statistical test is not analytical and depends on different systems characteristics [27]. Also, it does not provide reliable outputs in the presence of unknown measurement noise statistics. This is not the case for the robust estimation that automatically detects and suppresses bad data. For the cyber-attack scenario, robust DSE with high breakdown points or novel machine learning-aided DSE might offer a solution [137]. This is still an open area that requires further investigation.

Another important visibility is on the excitation system that could significantly affect the system's stability. Although PMU measurements might be used to calculate the excitation voltage in certain cases [138], this cannot be generalized to the modern brushless excitation systems. Furthermore, under stressed conditions, the excitation voltage is restricted by timer-based over-excitation limiters, which may dramatically affect the system stability margin [139]. The traditional DSA model typically does not capture if the state variables corresponding to exciter output are saturated or not. When saturation occurs, it is no longer a state variable and thus should be kept as an unknown input estimation. To achieve this goal, the excitation voltage is taken as the unknown variable for a two-stage estimation, where the estimation of input is done first and then substituted into the original model for DSE. Both EKF [67], [68], and UKF [75] considering unknown excitation voltage are used for that and the UKF has a better capability of handling the model nonlinearities and saturation effect. These two approaches require the local generator frequency to ensure the observability of unknown inputs. However, the local generator frequency is typically not measured directly by the PMUs. To deal with that, a correlation aided robust DSE for unknown input and state estimation is proposed in [140]. Compared with the previous works, no generator frequency measurement is required, and it has better robustness in dealing with bad data. It is worth noting that the unknown (i.e., not measured) mechanical torque of the turbine-governor system is also estimated using the approach in [140].

Besides the unknown control inputs, there are also anomalies, such as controller failures or malfunctions that can affect the system's stability. For example, if over-excitation occurs, a voltage security issue may arise. Furthermore, if the failure of the excitation system happens but without being detected, the accuracy of the differential-algebraic equations will be negatively impacted, leading to incorrect conclusions about system stability. It is very important to detect these failures timely to avoid the risk of exciter and voltage regulator damages. By relying on the estimated dynamic states and checking the consistency between the control model outputs and expected outputs, the over-excitation and abnormal mechanical power changes can be detected [141]. The multiple models-based DSE technique is also developed to detect excitation failures in [33]. Those techniques may be further extended to deal with the anomalies of other controllers, such as governors, and power system stabilizers.

Other DSE-based monitoring applications use DAEs but with much larger time constants as compared to electromechanical dynamics. This is the case, for instance, of the increasingly important real-time thermal rating of lines and cables, which is drastically changing the customary way in which static security assessment is performed. Indeed, the existing assets are reaching their conservative ampacity limits, typically defined on a seasonal basis, without due consideration to meteorological conditions (temperature, wind speed, etc.). The simultaneous, real-time estimation of the external parameters arising in the thermal models of lines and cables can help us improve the operation of underground cables [142], [143].

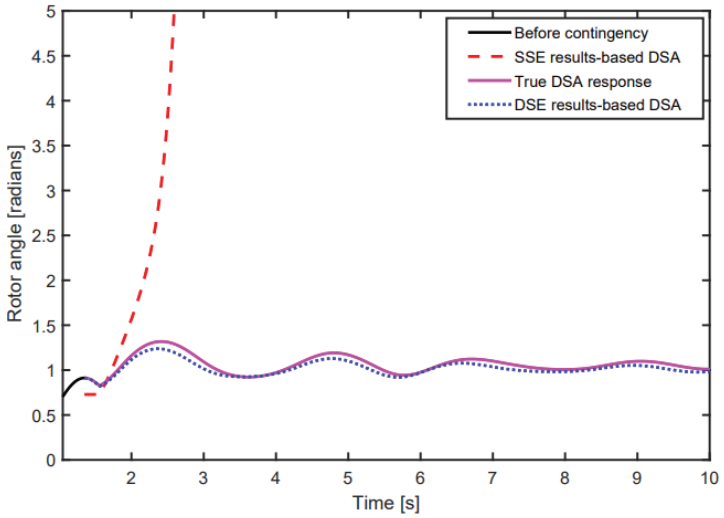

Fig. 7. Influence of initial conditions on DSA results.

4.3.3 Operation

SSE plays an important role in today's power system operations, especially the essential database for contingency analysis, static voltage stability, and optimal power flow. Compared with SSE, DSE outputs would also offer new benefits to today's EMS. Two main categories are elaborated here, namely DSA and dynamic stability assessment.

Model-based DSA relies on the initialization of dynamic models. The inaccurate initialization of variables might lead to different conclusions about whether the system is stable or not. In the legacy power systems, the operating point evolves slowly in time and the SSE results can be used to calculate the system's initial conditions that are required by DSA tools [113]. In other words, if the system is in equilibrium at 60Hz (or 50Hz), SSE is adequate for initializing the differential equations, which is how DSA is done in today's EMS. When the system is not at equilibrium or not at 60Hz (or 50Hz), SSE can’t be used to initialize the differential equations. Indeed, in future power systems with high penetration of DERs, the variables will change more often and more rapidly, rendering SSE too slow to provide DSA tools with an accurate picture of the system states. But it is during this period that DSA would be even more important for power system operation. One example is the 2003 Northeast blackout, where the system frequency deviated from 60Hz for hours and DSA would help to guide the operator's restorative actions. Model initialization for DSA is therefore the first important role of DSE. This is demonstrated through a simple numerical simulation carried out on the

IEEE 39-bus system. The system is assumed to be operated under the scenario, where the loads and DERs have large stochastic behaviors, yielding some oscillations of the synchronous generators. The operator would like to assess if the system can withstand a contingency. To this end, at t=1.3s, a three-phase short-circuit is applied at Bus 28 and cleared after 30ms by opening the transmission line connecting Buses 28 and 29. Two cases are considered: 1) the model is initialized by using the estimated bus voltage magnitudes and angles obtained from SSE at t=1.3s; 2) the model is initialized by using the dynamic states obtained from DSE at t=1.3s. DSA is then performed in both cases. The rotor angle of Generator 9 concerning that of Generator 10 is displayed in Fig. 7. It can be observed that the SSE-based DSA indicates that the system loses stability while the actual system remains stable. By contrast, the DSE-based DSA reflects true system behavior. The key insight is that in the SSE-based initialization, the derivatives of dynamic state variables are set to zeros based on the quasi-steady-state assumption, but the actual system already deviates from a steady-state due to the variations of relatively large loads and DERs. As a result, the calculated states using SSE-based DSA are not accurate. This is not the case for DSE-based DSA as their results contain non-zero derivatives and can be directly used for non-quasi-steady-state initialization.

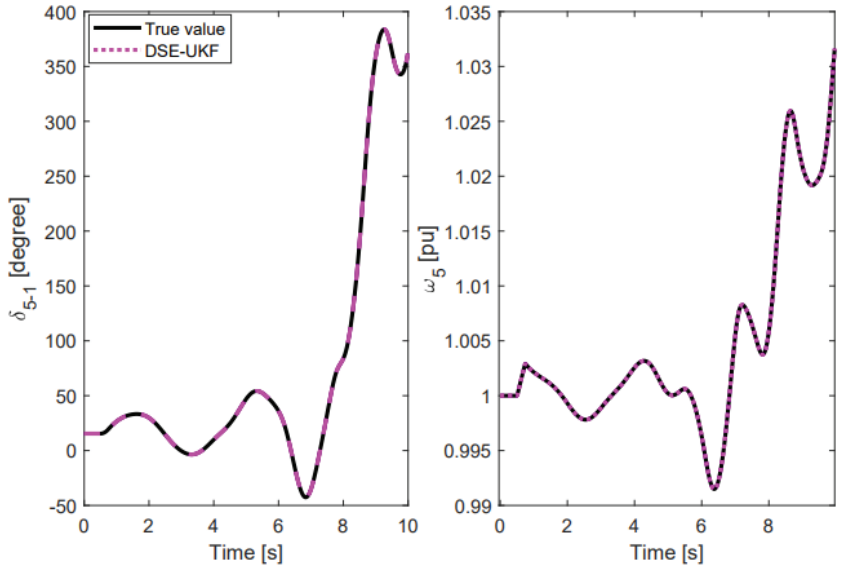

Fig. 8 DSE for an unstable system with high nonlinearity.

Dynamic stability assessment typically relies on a database that is built from offline simulations, wherein the evolution of the system dynamic states following different events is recorded. Then, an online classifier algorithm, e.g. decision tree or random forest, continuously compares real-time measurements with the database. If an evolving instability is detected, remedial control actions are initiated. This control philosophy is deployed in many power systems around the world. Due to its dependence on offline simulations, it is challenging to consider all possible operating scenarios during offline simulations [144]. This is particularly important with the increasing deployment of power electronics-interfaced DERs. DSE offers an alternative to these databases as it can provide a picture of the system dynamics in almost real-time, and can be used to compute transient stability indices, e.g., rotor angle stability [145]. This alternative control philosophy based on real-time information is yet in its infancy but seems to be

promising. Rotor angle stability can also be assessed via the sign of the system's maximal Lyapunov exponent [125], where the generator rotor angles provided by DSE would be of importance to predict system stability. To further demonstrate the capability of DSE in dealing with system instability, the same three-phase fault for the results in Fig. 6 is used but with 30 cycles of clearing time. This leads to system instability as shown in Fig. 8. The robust UKF-based DSE [112] is utilized to estimate and track generator rotor angle and speed.

We observe that even on the verge of losing stability, where the system response is highly nonlinear, DSE continues to track the evolution of the system states that can be used for emergency/ in extremis control schemes. On the other hand, DSE could benefit voltage stability assessment. From the short-term voltage stability perspective, DSE allows us to monitor the online states of synchronous generators' excitation system and induction generators/motors, and carry out stability assessment and controls. From the long-term voltage stability perspective, DSE can provide enhanced visibility of system states and snapshots [146]. In particular, the monitoring of the overexcitation limiters, and the detection of the failure of the excitation system and the topology changes would result in better early detection of voltage instability issues. For future power electronics-dominated systems, the frequency issue is of critical concern due to the reduced system inertia. DSE can provide online frequency information to enable a more effective system frequency stability assessment. However, there are very limited researches along with these directions and more investigations are needed.

4.3.4 DSE for Power Electronics-Interfaced Renewable Generation Visibility

Renewable energy sources (RESs) are typically integrated with the grid through power electronics converters. To achieve reliable and cost-effective RESs integration, dynamic visibility is needed. Compared with conventional synchronous generators, RESs exhibit a higher level of variability and uncertainty. Furthermore, the power converters and the control loops of RESs are very different from the synchronous machines. The power electronics have much smaller time constants than those of the synchronous generators, yielding much faster dynamics. As a result, the measurement system used for the monitoring of RESs should have a faster sampling rate and broader bandwidths for data transmission. It should be noted that besides the traditional voltage stability, rotor angle stability, and frequency stability, there is also converter-induced stability [147]. For monitoring and control such fast dynamics of the converters, DSE would be a good choice. For example, the UKF-based DSE is developed to extract the fundamental components of the point of common coupling voltage and load current for grid synchronization of PV systems in [148]. The doubly-fed induction generator (DFIG) wind generator's model can be put into the state-space form with their dynamic states estimated by DSE to achieve visibility. The DSE can be implemented via UKF, particle filter, and unscented particle filter [149]-[151]. Since there are errors with the wind speed measurements, DSE for DFIG with unknown wind speeds is addressed in [152]. The joint estimation of dynamic states and parameters of a permanent-magnet synchronous motor-based wind generator is investigated in [153]. It should be noted that the relation of estimated states via DSE with system dynamics and stability phenomena is still the subject of ongoing research. Except for the visibility of dynamic states, it is also important to detect any anomalies inside the RESs, such as control failures, erroneous tripping actions, etc. This would provide timely information for operators to take proactive control actions for maintaining system stability. For

example, due to the erroneous frequency and ROCOF measurements provided by the phase-locked-loop, several large solar farms have been incorrectly tripped in the 2016 California blue cut fire event [154]. The DSE would allow us to provide more accurate frequency and ROCOF estimates and visibility of abnormal behaviors by checking the model and measurement consistency. This is an open problem that needs more investigations.

4.4 Conclusions and Outlook

This section provides a comprehensive summary of the roles of DSE for power system modeling, monitoring, and operation. The relationships between SSE and DSE have been identified from the implementation requirements and related EMS functionalities. Several representative examples have been presented to highlight the critical importance of DSE for future power systems, especially for the development of the next-generation EMS.

Future research on DSE can be generally categorized into four key aspects: data infrastructure for DSE, DSE core functions, DSE applications, and its practical implementation to support the operation and planning of future power systems.

- **Data Infrastructure for DSE**: DSE, whether being implemented in a centralized or distributed/decentralized manner, needs real-time measurements, and these measurements need to be transferred to proper locations, such as a control center, a generation facility, or a substation. The power industry has been moving forward in the deployment of both sensors and communication networks. Research topics include: what are the data requirements such as data rates, signals, sensor placement? What are the data communication requirements, such as bandwidth, reliability, and redundancy for wide-area system applications? How to achieve more efficient and robust parallel and/or distributed implementations of DSE? And for a hierarchical system, how would the data communication network be structured, and where data should be sent to for the DSE application?
- **DSE Core Functions**: With the active efforts by many researchers for more than a decade, many DSE algorithms have been developed, and the DSE performance has been significantly improved, as summarized in this report. However, power systems are evolving to be more complex and different, and therefore DSE core functions should continue to improve to meet the operational requirements of future power systems. Research topics include: How to improve computational aspects of DSE to meet real-time requirements for large-scale systems? How to formulate DSE with fast inverter dynamics and potentially deal with mixed slow and fast dynamics? Can machine learning or other data analytical approaches help improve DSE performance in the context of a large amount of data and many system configurations? And how to break DSE into pieces in real-time for islanding situations, especially for a more resilient power system?
- **Development of DSE Applications**: DSE provides unprecedented detailed dynamic information, compared with SSE. A large number of applications in modeling, monitoring, and operation can benefit from DSE as mentioned in this report. Many more are emerging. There are conventional applications that can be enhanced by DSE-provided dynamic information and new applications that

can be enabled by DSE. Some of them include aggregated model calibration for wind/solar farms, loads, and DERs; oscillation source location; look-ahead DSA; visibility and detection of converter-induced instability; anomaly detection of DERs, where the complicated control loop may have fault or failures, etc.

- **The practicality of DSE Applications**: All the research efforts have a common goal which is to make DSE a practical part of the power system functions. Model calibration is an example of DSE applications, which are already in commercial tools, reliability standards, and industry practices. For most DSE applications, there are still significant gaps to address in terms of their practicality. Research questions include: How to transition from SSE to DSE while SSE and DSE will most likely co-exist for a significant period? How to make DSE compatible with the control room environment in terms of its information technology infrastructure and human-machine interface? For example, DSE results are updated too fast for operators to take action and how to present the critical information only to operators would be an important research need. This may be addressed by the development of advanced AI tools fed with DSE data streaming for visibility and stability assessment; What training should be developed and provided to prepare the workforce for DSE applications? And what new standards are needed to enable the DSE applications?

5. DSE for Power System Control and Protection

5.1 Introduction

Today's power systems are witnessing a rapid transition in generation technology from coal and gas-based non-renewable generation to wind and solar-energy-based renewable generation. Energy storage and modern power electronic loads penetrate power systems rapidly as well. As more and more of such converter-based resources (CBRs) are connected to the network, two major challenges emerge: (a) system response is faster and, therefore, its control should have a commensurate response speed, and (b) legacy protection functions that rely on the characteristics of conventional power systems (high fault currents and fault characteristics associated with synchronous generation) can be inadequate. Solutions to these challenges can be sought in DSE applications [109]. Specifically, DSE provides real-time operating states of the system at fast rates [155], which in turn can be utilized to fulfill the requirements for protection and control of modern power systems.

Traditional schemes for power system control and protection are primarily based on a deterministic system model with the majority of electricity coming from a few centralized and synchronous sources of generation [156]-[158], [147]. Such a system model has gradually become out of context due to the distributed, stochastic, and intermittent nature of renewable energy sources. In addition, stability, control and protection challenges introduced by the increased renewable integration include 1) reduced system inertia, and 2) extreme variation in the timescales of system dynamics – from a few milliseconds or lower in the case of CBRs to a few minutes or higher in the case of boiler and long-term dynamics of synchronous generation. To deal with these challenges, it is necessary to consider the control of each dynamic component in the system individually, and how different components influence each other's dynamics, and how they should be controlled together holistically. As DSE provides state

estimates at the required timescales, it can serve as a versatile tool to holistically control system trajectory, ensuring rotor-angle stability, frequency stability, voltage stability, resonance stability, and converter-driven stability [156].

With the increasing penetration of CBRs in power systems, traditional schemes for power system protection face the following challenges: 1) Many traditional protection schemes depend on abrupt changes of voltages/currents during faults, e.g. overcurrent/ undervoltage relays to detect faults; however, these characteristics may not be valid in systems with high penetration of CBRs [157]; 2) Phasor domain quantities are usually utilized in traditional relays, which can cause misoperation of relays during complex and unusual system transients in CBR-dominated power systems; 3) Traditional protection schemes usually require complex coordination among relays, e.g. time overcurrent relays and 3-step distance relays, resulting in risks of mis-coordination; 4) Hidden failures, such as failures of instrumentation channels, can lead to misoperation of protection relays [158]. DSE is a valuable tool to overcome the above limitations. First, DSE can accurately track complex dynamics and provide accurate estimates of the internal states of the system, enabling precise extraction of fault characteristics in both the phasor domain and time domain [109]. In addition, for a specific protection zone, DSE can formulate the protection logic by systematically checking the consistency between the measurement and the dynamic model of the protection zone without coordination among relays [8]. Finally, with redundant measurements, DSE can identify and reject bad data, and therefore prevent relays from misoperation during hidden failures.

With the development of advanced measurement devices and substation automation, high-quality synchrophasor measurements and synchronized sampled value (SV) measurements provide more information at higher rates and enable DSE-based advanced control and protection schemes. Towards this end, this section summarizes the joint efforts on DSE for power system control and protection. It has the following new insights: 1)) The existing DSE literature mainly focuses on electromechanical dynamics of synchronous machines while this paper extends it to consider the electromagnetic dynamics from CBRs; 2) The relationships and differences for observer and DSE using Kalman filters have been extensively compared and discussed to clarify their advantages and disadvantages; 3) the roles of DSE for control and protections have been thoroughly discussed with the support of numerical results, and 4) Several research directions have been offered to pave the way for further development.

5.2 DSE Formulation: Sampled Value Measurements versus PMU Measurements

Traditionally, power systems are dominated by synchronous generators. For these power systems, electromechanical oscillations with periods of a few seconds are very important. Although the detailed synchronous machine dynamic models involve electromagnetic transients, they are too fast as compared to the electromechanical oscillations and thus are neglected in the traditional dynamic studies and stability assessment [147]. With the increasing penetration of CBRs, DERs, and FACTS devices, to cite a few, the system dynamic responses are heavily dependent on the fast-response power electronic devices and their controls, and converter-induced dynamics and stability issues start to dominate the system [147], [154], [160]. In addition, power electronics devices cause waveform distortions and deviations from near sinusoidal waveforms. Note that the time-scale of the CBRs can range from a few microseconds to several milliseconds, due to switching operations of the power electronics. Conventional phasor representation or quasi sinusoidal approximation is usually used

for the study of electromechanical oscillations accounting for the synchronous machine oscillations and converter control dynamics (the dynamic phasors [161] or average models [162] could simplify the design of protection and control strategies for CBR systems). However, conventional phasor representation may not be suitable for the study of electromagnetic phenomena which represent the fast dynamics of the system. Hence, the formulation, measurement requirements, and potential applications of DSE are revisited in this paper, and the requirements for each application are defined.

Irrespective of the different time scales of power system dynamics, they can be described by the DAEs. Note that for models described through partial differential equations (PDEs), such as wave propagations in transmission lines, appropriate discretization methods need to be utilized to convert PDEs into (18).

$$\begin{cases} \dot{\boldsymbol{x}}(t) = \boldsymbol{f}(\boldsymbol{x}(t), \boldsymbol{y}(t), \boldsymbol{u}(t), \boldsymbol{p}(t)) \\ \boldsymbol{0} = \boldsymbol{g}(\boldsymbol{x}(t), \boldsymbol{y}(t), \boldsymbol{u}(t), \boldsymbol{p}(t)) \end{cases} \tag{18}$$

where $\boldsymbol{x}$ is the state vector; $\boldsymbol{y}$ is the algebraic variable vector; $\boldsymbol{u}$ is the input vector, $\boldsymbol{p}$ is the parameter vector; and $\boldsymbol{f}$ and $\boldsymbol{g}$ are nonlinear vector-valued functions. For power system applications, the measurements are sampled discretely, and thus, (18) needs to be discretized to be compatible with online measurements. To this end, the measurement function at time instant k can be written as $\boldsymbol{z}_k = \boldsymbol{h}(\boldsymbol{x}_k, \boldsymbol{y}_k, \boldsymbol{u}_k, \boldsymbol{p}_k)$, where $\boldsymbol{z}_k$ can come from PMUs, merging units (MUs), digital fault recorders, and in general IEDs; and $\boldsymbol{h}$ is a nonlinear vector-valued function. The way of solving (18) using DSE can be found in [109].

For capturing the electromechanical transients, phasor representation is leveraged while fast-electromagnetic transients are neglected. Measurement vector $\boldsymbol{z}_k$ usually includes time-synchronized phasor measurements from PMUs, such as voltage and current phasors, the calculated real and reactive powers, frequency, and RoCoF; and the state vector $\boldsymbol{x}$ includes internal dynamic variables of synchronous machines and dynamic loads. Note that the phasor measurements provide the fundamental frequency phasor voltages and currents, while the electromagnetic transients are filtered out. Thus, the model in (18) represents the electrical quantities with phasors, and the electromechanical system and control dynamics are formulated with differential equations.

To capture fast electromagnetic transients in a power electronics-dominated power system, there is an increasing need to use SV measurements directly. The synchronized SV measurements contain rich time-domain information and can be obtained from MUs, which can be standalone devices or embedded in non-conventional instrument transformers and other apparatus. The standard SV sampling rates in MUs are 80 or 256 samples per cycle according to the IEC61850-9-2LE standard [159]. Note that phasors and harmonics can be computed from SVs. Furthermore, electromagnetic transient models must be adopted to represent the fast dynamics of system components. The latter can include any components with electromagnetic transients, such as generators, transmission lines, transformers, CBRs, among others [8]. In this case, the voltages and currents are expressed using instantaneous SVs; the electromagnetic transients, such as fast electromagnetic transients of voltages or currents, are considered. Measurement vector $\boldsymbol{z}$ includes SV measurements, and the state vector $\boldsymbol{x}$ consists of instantaneous voltages, currents, generator speeds, and other internal states of the dynamic components.

The applications of DSE using PMU measurements for electromechanical transients include both control and protection. For control applications, For control applications, DSE contributes to the enhancement of the visibility of the system operations and the

validation and calibration of the control models. Furthermore, it provides essential feedback state signals and accurate measurements for controls. It is shown in the literature that DSE-based out-of-step protection provides more benefits for fast and reliable relay actions than traditional approaches.

DSE using SV measurements for both electromagnetic and electromechanical transients also enables advanced control and protection applications. For the control applications, it can 1) provide essential state feedback signals for CBR control, including both grid following and grid forming controls to enhance system stability; 2) identify unknown parameters and help calibrate electromagnetic models; 3) detect and diagnose anomalies locally, especially for converter-interfaced resources; and 4) provide accurate frequency measurements even in the presence of large disturbances. The widely used phase-lock-loop is well-known to be vulnerable to large disturbance and can trigger erroneous relay actions, for example, see the 2016 California blue-cut fire events [154]. For protection applications, it allows us to 1) design protective relays with improved dependability, security, sensitivity, and speed; 2) develop fault locators that work with short data window with improved fault location accuracy, and 3) enable cyber intrusion/hidden failure detection of protective relays. These issues will be discussed in subsequent sections.

5.3 Controller Options: DSE versus Observer

Both observers and DSE can be used to provide state feedback signals for control. In this section, the advantages and disadvantages of these two methods are discussed. Note that the detailed formulations of observers and DSE can be found in [109] and [163].

Operational principle: Observers are based on sensor outputs measured from the physical system and are usually based on the Luenberger criterion [163]. The sliding mode observer and the observer using the Koopman-based model of the process are also proposed [164]. DSE is based on the minimum variance estimation criterion from a statistics point of view and it fuses both the physical model predictions and the sensor outputs. Although these two approaches fundamentally differ in their assumptions and algorithmic details, both can be used to estimate the state of a dynamic system.

Addressing stochastic systems: The majority of designed observers in the literature do not assume statistical distributions for the process and measurement models. Most control-theoretic observer designs assume the existence of unknown inputs and sensor noise in a deterministic way without associating any distribution to these uncertainties. This is because deterministic observers still perform well in the presence of various noise distribution types. Note that gain matrix design for an observer can be challenging for large nonlinear systems due to high nonlinearity in state transition [165]. A good observer design can provide robustness to exogenous disturbances, though its performance cannot adapt to time-varying changes unless it evolves with time. Furthermore, if the noise distribution deviates from assumptions, such as Gaussian distribution, an observer may obtain better performances than the traditional DSEs using Kalman filters since an observer only requires the bounds for noise. During information extraction from data, there are random fluctuations or measurement errors in the data that are not subject to any models. They are called stochastic noises. When the phenomenon being modeled is too complex and some approximations are applied, errors are induced and they are called deterministic noises or biases (i.e., model uncertainty/error). Both DSE and observer need to be designed to handle both types of noises. The comparisons of robust DSE and observer considering different types of noises, i.e., both deterministic and stochastic need further investigations.

Sensitivity to outliers: Measurements are frequently subjected to outliers and the model outputs can be corrupted by gross errors due to control failures, incorrect model

inputs, parameter errors, etc. [28]. In the presence of outliers, both state observers and DSE may provide biased results. To mitigate the influence of outliers, an observer needs to increase the assumed error bounds, which would significantly decrease its performance in the absence of outliers. In contrast, by adopting a statistical test or developing robust DSEs, outliers can be automatically detected and suppressed without affecting DSE performance when there are no outliers [109], [28].

Computational efficiency: The majority of DSE designs recursively compute gains; this involves matrix multiplications and inversions at each time step. In contrast, once the observer is designed offline, state estimation can be performed with a significantly smaller number of matrix multiplications, as the calculations of observer gain are usually done offline assuming certain error bounds of process and measurement models [166]. This offline calculation involves computationally costly linear matrix inequalities and convex semidefinite programs. Thus, recalculation of observer gains is time-consuming in the presence of changes in the network topology or parameters, whereas DSE can update such new information more efficiently at each time step.

Sensor requirements*:* Both DSE and observers require the system/states to be observable as a prerequisite from the dynamical system perspective [109]. For DSE, more sensors would lead to better statistical efficiency of the state estimates. Observers usually suffer from a key limitation regarding the required number of sensors, which can lead to infeasible observers [167]-[168], theoretically infinite estimation error, or practically unusable estimates. Kalman filters, however, still produce some useful results even with a limited number of sensors.

Handling system nonlinearity: Both DSE and observers can be designed to deal with nonlinear systems. However, designing a good observer when the system is subjected to complex nonlinearities is very challenging as it involves nonlinear optimization [168]. Also, the Jacobian matrix is needed for some nonlinear observer designs. However, magnetic saturation in synchronous machines is frequently encountered in power systems [155], making infeasible the computation of Jacobians and subsequent observer design. In contrast, there exist derivative-free nonlinear Kalman filter-based DSEs, such as unscented Kalman filter, ensemble Kalman filter, particle filter, etc. [109], which avoid the use of Jacobian matrix and thus handle system nonlinearity better.

Sensitivity to initial conditions: For DSE, a good initial condition is usually needed, otherwise, it takes some time to converge to the true value. This, in general, is not an issue since DSE runs continuously and in the long run, once it has converged, the initial condition is the state estimate of the system at the prior time step, which is an accurate initial condition. For state observers, irrespective of the initial condition, fast convergence of the estimated states to their accurate values is guaranteed as long as a proper observer gain is determined, and the system is observable. It should be noted that practically, a reasonable initial condition can typically be obtained by utilizing power flow calculations or state estimation, or engineering judgments or experiences.

5.4 Control Applications of DSE

Overview of control: Control of different components in a power system is performed by controlling the devices which govern their power and voltages. For a synchronous generator, these devices are the governor (which controls the mechanical power input) and the AVR (which controls the excitation voltage). For CBR, on the other hand, these devices are the power electronics converters, which have a few control options, for example, maximum power tracking and voltage control, real and reactive power control, real power and voltage control, and AC/DC voltage control. In addition, depending on operating conditions, the controls can switch to low voltage ride through

logic, storage control, etc. Since synchronous generator controls are slower than converter controls, DSE must provide feedback to the controllers on a commensurate time scale. DSE operating at a cycle scale can meet the requirements of controllers for synchronous machines and converter control. For other applications such as protection and associated controls, DSE needs to operate at faster time scales and typically uses SV measurements or dynamic phasors. An overall scheme for the implementation of DSE-based control of power systems is shown in Fig. 9. It should be noted that the "traditional phasors" assume steady-state operation of the system, while the "synchrophasors" obtained from PMUs are time-synchronized phasors with fast-varying amplitudes and phase angles, which can better describe the dynamics of the system [169]. However, the synchrophasors are still based on the framework of phasors, which assumes sinusoidal-shape waveform, but with much faster update rates (hundreds of samples per second). By contrast, SV measurements directly utilize measured values from the waveforms at each sample, with a full description of measurement transients. Thus, PMU measurements and SV measurements are two options for controls with fast time scales.

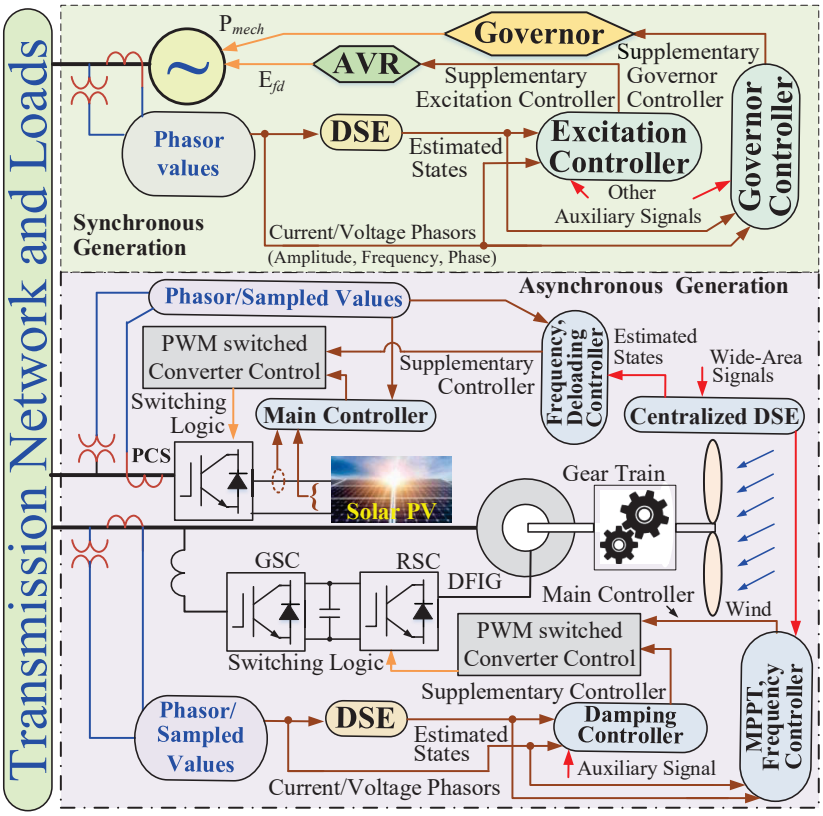

Fig. 9. An example implementation of DSE-based control architecture

5.4.1 DSE-Based Control using PMU Measurements

1) DSE-based Control of Rotor Angle Stability

As synchronous generators form the backbone of today's AC power system, they are the main points of control actuation and can be directly controlled using excitation systems & governors. Other important actuators are the transmission paths, controlled using FACTS devices and transformer taps. DSE-based control design can be centralized, decentralized, or hierarchical (Fig. 10).

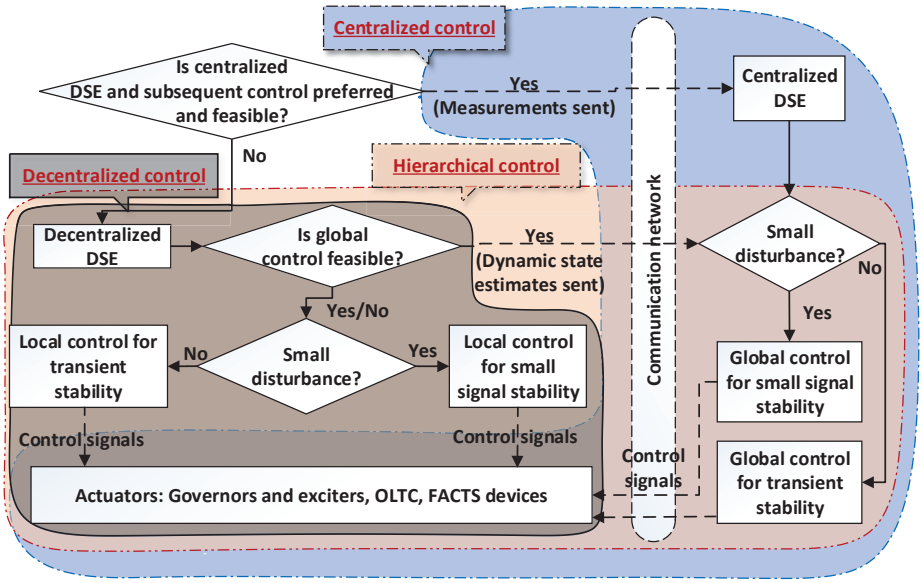

Fig. 10. DSE-based control decision and design process for rotor angle stability

Centralized and Hierarchical Control

In DSE-based centralized control, measurements from across the system are transmitted to a central location, and DSE for the whole system is performed [170]-[171], [17], as shown in Fig. 10. A control law is then obtained using the system model and the dynamic state estimates via various control techniques, including L_∞ robust control that models disturbances as L_∞ bounded inputs and finds a state-feedback control law using nonconvex optimization [170]; linear quadratic regulator (LQR) where the quadratic costs of control and state-deviation are optimized with pole-placement for crucial system eigenvalues using state-feedback [17]; and residue-based control, where pole-placement is explicitly done using power system stabilizers (PSSs)/power oscillation dampers [171]. Some limitations of centralized control that restrict its field implementation are: communication latencies can impact performance, an accurate model of the whole system at the central location is required, and communication failures and bottlenecks can create serious issues.

A partial solution to the problems of centralized control is hierarchical control in which decentralized DSE is performed at machine locations and the estimates are sent to a central location (or PMU measurements are sent to a central location for performing DSE in a decentralized manner using a federation of estimators [102]). Global control laws are then developed at the central location along with local control laws for decentralized locations. The local and global controls form the two levels of hierarchical control, as shown in Fig. 10, and are implemented using actuators, such as FACTS devices and excitation systems of synchronous generators [68] [172]. In the worst-case scenario, such control can also be used to shed run-away generators on the fly to prevent instability [145]. The hierarchical control approach also requires knowledge of a complete system model at the central location.

Decentralized Linear Control

In decentralized control, each generator is controlled independently, requiring only local measurements for both DSE and control. By controlling local machine dynamics, some aspects of global system dynamics may also be controlled. This eliminates communication requirements, but in many cases, it suffers from limited system-level controllability/observability. As a result, special techniques are needed to establish

system stability. Both linear and nonlinear methods can be used to implement such control.

Linear methods of DSE-based decentralized control are valid only for small-signal dynamics [147], and are similar to the traditional PSSs: in PSSs the control parameters are tuned offline, while DSE-based methods do so online. Such a 'dynamic tuning' of control parameters can be done using various methods, such as decentralized L_∞ [170], in which a convex approximation of centralized L_∞ formulation ensures that only local machine states are needed for control; and extended LQR [20], in which the costs of voltage phasors (as exogenous inputs) are included in the LQR costs to find control gains. A drawback of linear methods is that the asymptotic stability of the whole system cannot be guaranteed. However, this is usually not an issue as linear methods are applicable only for small disturbances, which usually do not alter the asymptotic stability.

Another linear control approach is to use data-driven DSE, where local measurements are used to find a linear Koopman predictor [164] to mimic system dynamics, which is then used to perform DSE (similar to an observer) and to design model predictive control (MPC). The estimated rotor speed of each generator is used as a feedback signal in the MPC for excitation control. To build the Koopman predictor, the data of all the states and measurements are collected in matrixes $\boldsymbol{X}$ and $\boldsymbol{Y}$, respectively, for different trajectories of the system, while inputs are collected in matrix U. Lifting radial basis functions (RBFs), $\psi(\boldsymbol{x})$, are used for lifting $\boldsymbol{X}$ and $\boldsymbol{Y}$, and are defined as follows (with the centers $\boldsymbol{x}_0$ obtained randomly from a uniform distribution in [-1,1]) [164]:

$$\psi(\boldsymbol{x}) = \|\boldsymbol{x} - \boldsymbol{x}_0\|^2 \cdot \log(\|\boldsymbol{x} - \boldsymbol{x}_0\|)$$

After data lifting, extended dynamic mode decomposition is used to compute the lifted matrices, which represent the predicted model used to design the MPC controller. The lifted matrices ($\boldsymbol{A}$, $\boldsymbol{B}$, $\boldsymbol{C}$) are the solution to the following optimization problem [164], with $\boldsymbol{X}_{lift}$ and $\boldsymbol{Y}_{lift}$ denoting the lifted states and measurements, respectively, and $\boldsymbol{U}$ denoting the inputs.

$$\min_{\boldsymbol{A},\boldsymbol{B}} \sum_{J=1}^{k} \left\| \boldsymbol{Y}_{lift} - \boldsymbol{A}\boldsymbol{X}_{lift} - \boldsymbol{B}\boldsymbol{U} \right\|^2$$

$$\min_{\boldsymbol{C}} \sum_{J=1}^{k} \left\| \boldsymbol{X}_{lift} - \boldsymbol{C}\boldsymbol{X}_{lift} \right\|_2^2$$

Fig. 11 shows that the proposed Koopman MPC (KMPC) provides a much better oscillation damping performance as compared to the classical PSS, after a 100 ms symmetrical three-phase fault at the infinite bus in a single machine infinite bus system (ω_1 denotes the rotor speed of the machine, while V_t denotes its terminal voltage). This example uses a highly accurate Koopman model trained with random excitations, with dimension N=108 (8 physical states plus 100 RBFs) [164]. System trajectories are generated through simulations after applying random control signal inputs to generate the trajectories. The control input for each trajectory is selected randomly from a uniform distribution in [-1,1]. The parameters for the two-stage lead-lag PSS with a washout filter used in this example are (parameters found using the standard root-locus method [173]): K_{PSS}=5.2450, T_1=0.5603, T_2=0.0145, T_3=0.6614, T_4=0.0415, T_W=10.

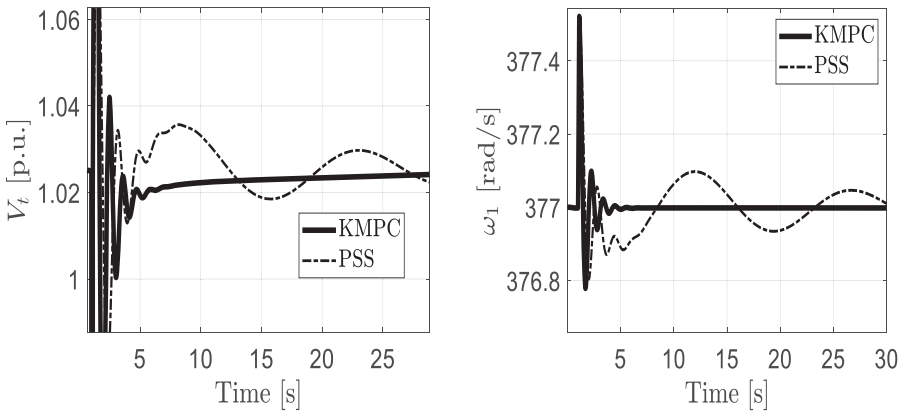

Fig. 11. Rotor speed response of KMPC vs PSS

Decentralized Nonlinear Control

Nonlinear control methods are needed to ensure the stability of the system against large disturbances, i.e. when a linear approximation of the system is no longer valid. These methods either find a partially linear transformation of system dynamics, called feedback linearization [19], [174], or find a positive scalar with a negative time derivative, called a Lyapunov function [175]- [176]. Feedback linearization is easier to formulate and use than Lyapunov functions, but the latter has better asymptotic stability characteristics. In [19], detailed generator modeling has been used to implement feedback linearization-based excitation control to ensure transient stability, while [174] considers detailed load modeling for the same. In [175], a Lyapunov function is constructed for excitation and governor control, and [176] proposes an optimal Lyapunov formulation for excitation control and uses neural networks for computational efficiency.

Although nonlinear control works well even for small disturbances, its control costs (given by the time integral of a weighted sum of the squares of control inputs) are much higher than the linear control costs. Hence, it is practical to activate nonlinear control only for large disturbances. Based on this idea, a hybrid decentralized control is proposed in which RoCoF estimation is used to infer if a large disturbance has occurred. To do this, the DSE-based RoCoF estimate obtained using [117] is multiplied with the machine's inertia to get a switching signal: if the absolute value of this signal is greater than a predefined value (say 0.5 p.u.) for two cycles, then the control is switched to the nonlinear control given in [19]. Control is switched to the linear control given in [20] only if the switching signal stays within ±0.5 p.u. continuously for 5 s.

The comparison of performances of the hybrid decentralized control and classical PSS control is shown in Fig. 12. Test system model, simulation conditions, and controller parameters are the same as in [19]. The test system starts from a steady state, and at t = 1s a small disturbance takes place in form of a step load change by doubling the load on bus 53. At t=20s, a large disturbance takes place in form of a solid three-phase fault on bus 54, which is cleared after 200 ms by opening of circuit breakers on line 54–53. The difference between rotor speeds of machines 1 and 16 ($\omega_1 - \omega_{16}$) has been plotted in Fig. 12 corresponding to the two control methods. Tables II and III also present the modal analysis of three interarea modes (for comparing small-signal performance of different control methods) and the critical clearing times (CCTs) (for comparing transient stability performance), respectively. It can be seen that hybrid control can ensure both small-signal stability and transient stability of the system, and exhibits the best properties of both linear and nonlinear control – it adequately damps

interarea modes without significantly changing the modal frequencies (unlike nonlinear control), and its critical clearing time is similar to nonlinear control.

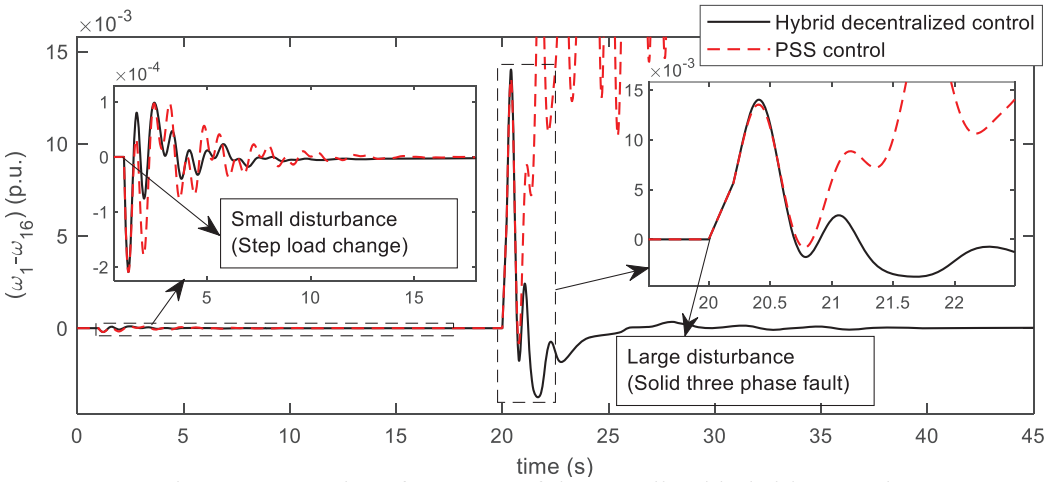

Fig. 12. Control performance of decentralized hybrid-control

TABLE II
MODAL ANALYSIS OF INTERAREA MODES

	OPEN-LOOP	PSS	ELQR [20]	NONLINEAR CONTROL [19]	HYBRID CONTROL
Mode-1 frequency (Hz)	0.39	0.43	0.31	0.12	0.31
Mode-1 damping ratio (%)	0.9	11.4	18.7	47.2	18.7
Mode-2 frequency (Hz)	0.52	0.54	0.47	0.20	0.47
Mode-2 damping ratio (%)	2.1	6.3	9.8	92.8	9.8
Mode-3 frequency (Hz)	0.60	0.63	0.54	0.21	0.54
Mode-3 damping ratio (%)	1.2	5.7	11.0	91.0	11.0

TABLE III
TRANSIENT STABILITY PERFORMANCE

	PSS	ELQR [20]	NONLINEAR CONTROL [19]	HYBRID CONTROL
Critical clearing time (ms)	179	92	210	209

2) DSE-based Control of Frequency Stability

Unpredictable load fluctuations, intermittency due to stochastic generation, and random system disturbances may result in continuous fluctuations in system frequency and tie-line-power exchanges causing them to deviate from their nominal values. These variations are corrected by governor-based load frequency controller (LFC) action [177]. The performance of LFCs is significantly affected by the inherent governor dead-band (GDB) and generation rate constraint (GRC) [128], [178]-[179]. In contrast, DSE-enabled LFC [180] (Fig. 9) is not affected by the GDB or GRC and uses PMU measurements to derive the auxiliary signal for the governor loop. However, communication impediments hinder the applicability of such LFCs. To address this

issue, it is proposed that traditional LFCs should be assisted by a supplementary stabilizer, in which turbine-governor dynamics are estimated using decentralized DSE to derive the control signal. This improves the frequency stability margins compared to observer-based conventional LFCs (as in [181]) and is illustrated in Fig. 13.

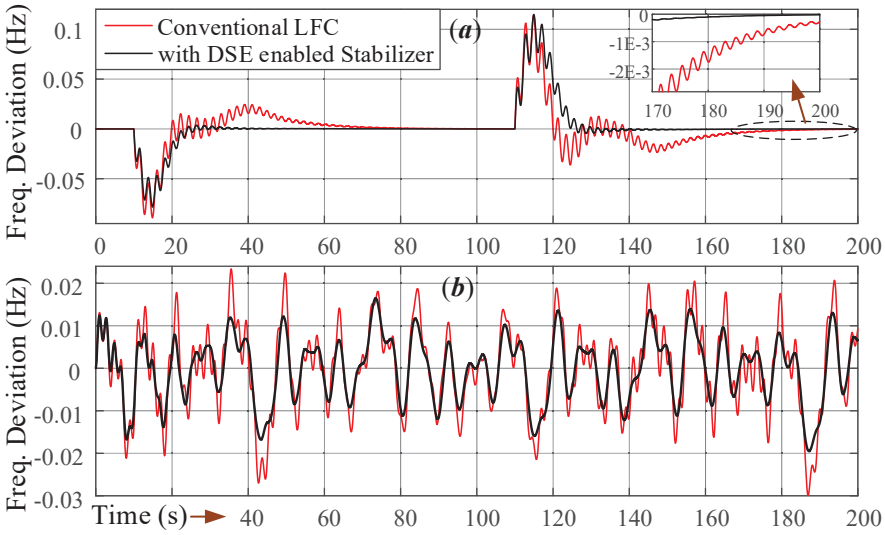

Fig. 13. Frequency Stability: DSE-Stabilizer vs conventional LFC

Fig. 13. (a) depicts the frequency response in Area 1 of the IEEE 10 machine 39 bus system (system details are shown in [182]) following a stepped load increment of 2% of load at Bus 15 at t=10s followed by a decrement of 2.5% at t=110s. Fig. 13. (b) depicts the frequency response for the system under fluctuating wind power output which was simulated by considering a realistic wind speed profile (please see [178] and [179] for the details of wind modeling). The details of the turbine and governor model, including nonlinearities like GDB and GRC, are given in Appendix of [128]. The auxiliary frequency control law uses turbine states (valve opening, turbine power, and reheater output), which are estimated through DSE [128], as inputs to derive the corrective control signal. The gain vector for this control signal is obtained by modeling the stochastic generation and load perturbations as unmatched perturbations and solving the resulting nonlinear equation following the same procedure as detailed in [183]. Since the time evolution of the governor states is relatively slow, the estimated states need to be supplied to the auxiliary stabilizer at a slower rate (10Hz or less) compared to a reporting rate of the PMUs (100Hz or above) using a zero-order hold.

The response in Fig. 13. (a) illustrates that the stabilization time of the frequency improves by many folds (about 3 times) via the DSE-enabled supplementary stabilizer in the event of stepped load changes. In the event of continuous parity between generation and load due to the stochastic nature of renewables, the frequency excursions are reduced significantly by employing the DSE-enabled stabilizer compared to traditional LFC as illustrated by Fig. 13. (b). Therefore, DSE-enabled frequency stabilizers can help in improving the frequency control indices manifold.

3) DSE-based Control of Voltage Stability

Real-time voltage instability detection and control methods that are the best candidates to take advantage of DSE are those that use snapshots of evolving system trajectories, captured either by dedicated measurement/communication system or by a tracking state estimator [146], [184]-[185]. In principle, those methods can use the system snapshots provided by a DSE giving access, for instance, to the excitation

system status of generators (namely: is the generator controlling its voltage or is it under field or armature current limit?) and system frequency. The same holds for other voltage controlling components such as static VAr compensators or STATCOMS. Long-term voltage instability detection and control can use originally proposed approaches (like sensitivities in [146] and modal analysis in [185]). In addition to the dynamic states, the network state and topology are required to monitor, detect, and control voltage instability. In this respect, the local DSE approaches discussed in [109] are combined with network state estimation, which can be fully based on PMUs or multi-rate measurements [184]. In principle, for long-term voltage instability, the system state can be updated at low rates (less than 10 times per second). One of the advantages of DSE is its ability to provide full state estimates, thus enabling full-state feedback MPC controllers [186].

An example of emergency control against long-term voltage instabilities [187], which can be adapted to take advantage of DSE outputs and be used for long-term instability detection, is illustrated in Fig. 14.

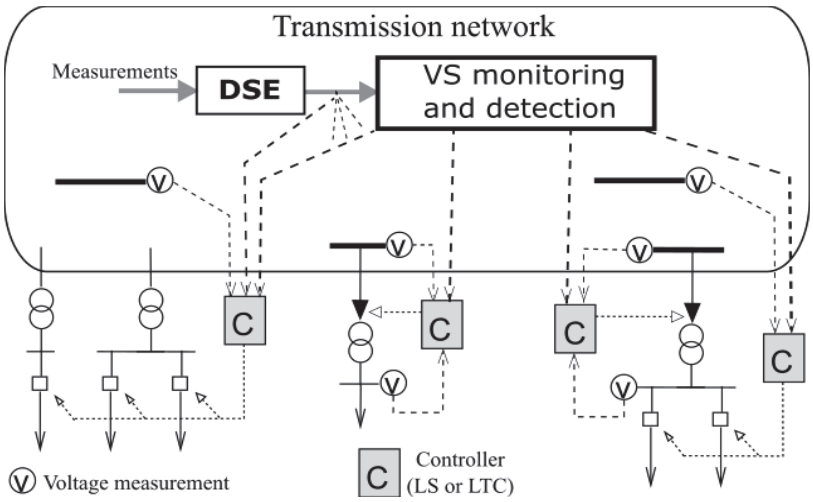

Fig. 14. A framework for two-level long-term voltage stability (VS) monitoring, instability detection, and emergency control

It is a two-level scheme. The upper level is in charge of wide-area monitoring, while the lower level controllers provide remedial actions such as Load Shedding (LS) or modified Load Tap Changer (LTC) control. In an emergency voltage situation, the upper level relies on the voltage instability detection method of [146] (DSE can replace the dedicated PMU measurements) and provides the lower-level controllers with minimum transmission voltages to maintain. Those voltages correspond to the point where long-term voltage instability is detected [187].

In terms of short-term voltage instability detection and control, the voltage control statuses of synchronous generators or compensators are crucial information. The phenomenon of concern is faster and a DSE used for this purpose must provide the system dynamic states at a high rate (10 to 60 times per second); a PMU-based network state estimation appears to be mandatory for this application.

Increased penetration of grid-connected CBRs (particularly when connected to weak grids) brings concerns to voltage instability (both long- and short-term). This requires even more rigorous metering infrastructure and DSE should use a detailed model with the full complement of state variables for the CBRs to solve voltage instability problems.

4) DSE for CBR Control

The intermittent and asynchronous nature of variable CBRs, mainly wind and solar, poses several pressing challenges in today's energy systems research [147], [160], especially for CBR-DSE and control. Several methods for DSE-based control of CBRs have been proposed in the literature. A UKF-based DSE is developed to estimate doubly-fed induction generator (DFIG) flux dynamics and this allows for the development of a flux estimation-based control scheme [188], which achieves a better fault recovery response than traditional control methods. In [189], DSE has been used to estimate the electromechanical dynamics of a DFIG and the estimated states have been used to derive the supplementary signal for damping of electromechanical oscillations (Fig 9). The aforementioned stabilizers improve the fault recovery response significantly, however, crowbar intervention (hardware protection) for few cycles may be required to limit potentially dangerous overcurrents in the DFIG rotor circuit following a severe/extreme low voltage condition [189]. DSE-based sliding mode control for DFIG-integrated power systems is developed in [190] for maximum energy extraction and power quality enhancement. The idea is further extended to the DSE-based frequency restoration method considering solar irradiance variations [191]. DSE-based control can also be used to damp sub-synchronous oscillations in series-compensated lines with wind generation [192].

5.4.2 DSE-based Control using SV Measurements

Traditional generator controls are mostly decentralized as the local frequency and voltage information act as a medium to bring the information of the rest of the grid to the local generator. Modern power systems are evolving with lower inertia and more complex transients with CBRs. In this case, controls with local frequency and voltage information may not be sufficient; remote side information such as frequency, RoCoF, and waveform distortion can also help minimize the transients and prevent damage/shut-down of converters during disturbances. However, remote side information usually requires communication channels, resulting in increased cost and compromised reliability of the system. With the help of SV measurements and the accurate time-domain transmission line model, DSE can effectively estimate the voltages and currents at the remote side of the transmission line using local information only, without any physical communication channels between the two terminals of a transmission line [193]-[194]. Afterward, remote side information such as frequency, RoCoF, and waveform distortion is extracted from the estimated voltages and currents and is utilized as the input to CBR control. Fig. 15 depicts an example of a DSE-based converter control system using SV measurements.

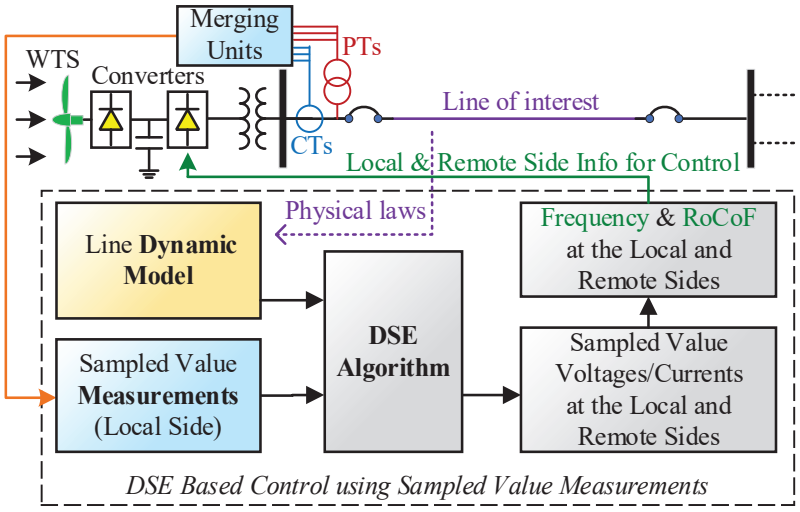

Fig. 15. DSE based converter control system using SV measurements

In this example, the local voltage and current SV measurements are first obtained via potential transformers (PTs), current transformers (CTs), and MUs. Next, using the DAEs of the line of interest, DSE estimates the dynamic states of the system, including SV voltages and currents at the remote side. Finally, the frequency and the RoCoF at the local and remote sides are extracted from the estimated SV measurements. These are fed into the local converter controller to initiate supplementary control using local and remote frequency and RoCoF to minimize transients during system oscillations and keep the converter synchronized with the system. Note that the remote side frequency information could also be approximated using phasor domain methods [195]. In addition, estimated SV states of the system can also be used for other applications such as fast control of converters, harmonics filtering, etc.

5.5 Protection Applications of DSE

When a fault occurs on power system components, protective relays need to immediately operate, to isolate the faulty components, minimize the power outage, and ensure the safety of human beings and the overall power system. Protective relays are evolving with improved reliability. However, statistically, the industry in the U.S. and abroad are still experiencing around 10 percent misoperation on average [196]. These are due to limited measurements, mis-coordination among relays, or faults that are hard to be quickly and reliably detected, such as high impedance faults, faults near neutrals, etc. In addition, most protective relays are based on fundamental frequency measurements, which limit their operational speed as well as applicability to DC systems. The proliferation of CBRs has also generated new challenges for legacy protection systems. Most relay settings are fixed; but with reduced system inertia, the settings need adjustment to distinguish stable and unstable swings. DSE-based protection provides a new approach to deal with these challenges. DSE is a powerful tool in tracking power system transients (including electromechanical and electromagnetic transients) and therefore enables protective relays with improved operational speed, sensitivity, and reliability.

5.5.1 DSE-based Protection using PMU Measurements

1) Out-of-step Protection using Direct Stability Assessment

DSE for electromechanical dynamics has been used to monitor the stability of

generators and to detect instability when it occurs. This provides better system protection for stability. Specifically, generator instability is a serious problem for power systems; generators must be protected against this condition; out-of-step (OOS) relaying is used to detect and protect the generator when it spins into instability. Present out-of-step protective relays typically monitor the apparent impedance at the terminals of a generator. When instability occurs the impedance moves from the right-hand side of the impedance diagram to the left-hand side. Upon this detection, the relay will schedule to trip the generator when the generator swings another 120 to 150 degrees, which will minimize the transients in the breaker (transient recovery voltage) and allow the reliable opening of the breaker. Because of this timetable (i.e. detection of the instability and then a delay for favorable conditions to trip the generator), the period during which the generator experiences severe current flow due to the oscillation is long.

A new DSE-based protection method has been introduced to detect the onset of instability much faster than the impedance-based approach described above [11], [23]. The basic idea is quite simple: DSE is used to estimate the full dynamic state of the generator and the immediate network to which the generator is connected. The DSE provides the speed of the generator [195], the frequency, and RoCoF at each bus of the system. A simple calculation provides the center of oscillation (CoO). The CoO is characterized by the fact that the frequency at that point does not oscillate (it may be linearly changing with time) and the frequency at the nearest two buses oscillates approximately 180 degrees out of phase. Knowledge of the generator speed and the location of the CoO enables the computation of the total energy of the generator,

$$E_{total} = E_p + E_k = -\int_{\delta_{coo}}^{\delta} \left(P_m - P_e(x)\right) dx + \frac{1}{2} M \omega^2 \tag{19}$$

where E_{total}, E_p and E_k are the total energy, potential energy, and kinetic energy of the generator, respectively. $M = 2H/\omega_s$, H is the per-unit inertia constant, δ is the generator position, ω is the rotor speed, and ω_s is the synchronous speed.

The stability of the generator is determined by the total energy using classical Lyapunov's theory. The theory states that when the total energy reaches the value of the peak potential energy (stability barrier) the generator becomes unstable. The dynamic state estimator provides the total energy of the generator as well as the potential energy function and asserts instability when the total energy reaches the stability barrier. It turns out that the assertion of generator instability occurs before the generator has swung away from the system and therefore can be tripped immediately, avoiding severe transients of an unstable generator. Next, we present a simplified example to illustrate the performance of this method.

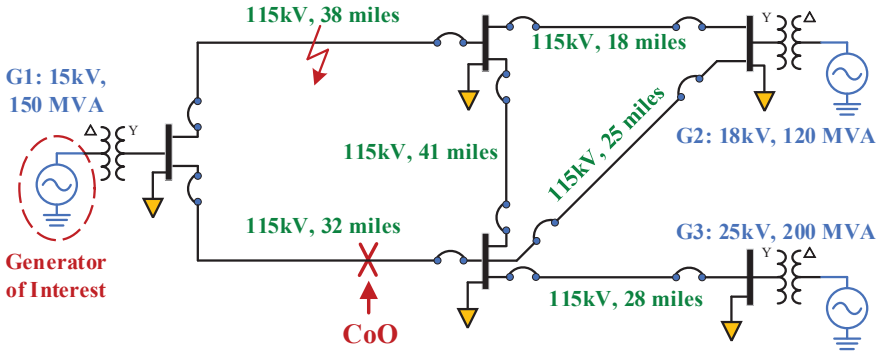

Fig. 16. Single-line diagram of the example test system

The example test system is illustrated in Fig. 16. It consists of three generators, three transformers, six transmission lines, five loads, and 12 breakers. The parameters of the

generators, transformers, lines, etc. are typical. We consider a fault on the 115 kV, a 38-mile-long line that is successfully cleared by the protection system of the line. The fault disturbs the system and oscillations are triggered.

Fig. 17 illustrates the results of the DSE and computed trajectory of the impedance of the generator as "seen" at the terminal of the generator. The trajectory is superimposed on the characteristics of an OOS legacy protective relay to compare the DSE-based protection results with the legacy protection. The apparent impedance moves to a value very close to the origin upon fault initiation at time t=1 s. During the fault, as the generator and the system oscillate, the trajectory moves. The fault is cleared 0.25 s after the occurrence of the fault (i.e. t=1.25 s) by disconnecting the faulted transmission line. For this system, the critical clearing time is 0.2 s. This means that the generator enters instability at time t=1.2 s. The legacy relay will alarm the condition at time t=1.43 s and will assert instability at t=1.51 s while the generator rotor is at 216.2 degrees. At this angle, the generator cannot be tripped immediately (due to concerns over transient recovery voltage at the generator breaker and the possibility of restrike) but need to wait until the phase angle goes to a smaller value. The DSE estimates the potential energy after the clearing of the fault and due to computational latencies, it asserts instability at t=1.29 s when the generator rotor is at 118.4 degrees out of phase with the center of oscillation. At this phase angle, the generator can be tripped immediately, avoiding any additional stress on the generator.

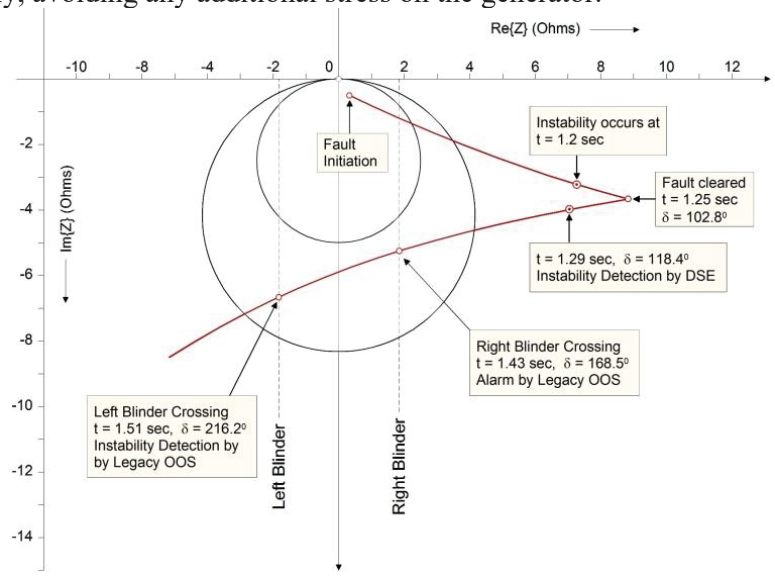

Fig. 17. Instability assertion time via DSE and comparison to legacy OOS Protection

2) Adaptive OOS Relay Settings Approach

Adaptive OOS settings based on dynamic model parameters estimation preserves existing industrial practice, and it is assisted by DSE for electromechanical dynamics. The OOS settings are mainly influenced by the direct axis transient reactance, quadrature axis speed voltage, and generator inertia. As seen by the relay, these parameters vary with time in the modern grid architecture with high penetration of power electronic interfaced technologies. The approach reported in [93] can be used to provide this real-time information for OOS relay settings recalculation. DSE is used to estimate dynamic model parameters which are used to recalculate the setting of OOS to adapt the relay sensitivity towards the generator instability with the system operating condition before the disturbance. This approach has been reported in [21]. In the paper, the settings of OOS are recalculated based on the extended equal area criterion method and demonstrated to be more effective OOS condition detection and protection.

5.5.2 DSE-based Protection and Fault Location Using SV measurements

1) DSE-based Protection Using SV Measurements

Compared to the synchrophasor measurements from PMUs, synchronized SV measurements from state-of-the-art MUs capture system dynamics in the time domain. DSE can be utilized to extract the system information embedded in SV measurements, to provide reliable detection of fault conditions that are not reflected by fault current levels, distortion of waveforms, and characteristics of fault currents. In addition, the use of SV measurements provides detection of faulty conditions much faster than legacy protection functions (such as overcurrent protection, distance protection, current differential protection, etc.), which usually require the collection of enough data to compute phasors, resulting in fault detection delays.

DSE-based protection methods using SV measurements have been introduced in [8]. These methods were inspired by the widely adopted current differential protection. The latter examines whether the phasor domain KCLs of the protection zone is satisfied; many but not all internal faults will violate KCL allowing differential protection to detect these faults and trip the component. By contrast, DSE-based protection examines whether all the physical laws of the specific protection zone are satisfied and an internal fault is detected with any violation of any physical law. Depending on the protection zone, physical laws may include KCLs, KVLs, motion laws, thermodynamic laws, etc. The primary improvements of the DSE based protection compared to the existing protection approaches (such as current differential protection) include: 1) speed: DSE based protection approach utilizes time-domain SV measurements instead of phasor/spectral domain synchrophasor measurements, which enables faster fault detection; 2) applicability to DC systems; 3) DSE based protection approach checks all the physical laws (instead of KCLs only), and therefore can detect internal faults with improved sensitivity and reliability. Note that current differential protection fails to detect some faults, for example, inter-turn faults in transformers, etc.

A systematic procedure for DSE-based protection is as follows: 1) building the dynamic model that encapsulates all the physical laws of the protection zone in the time domain; the model uses differential and algebraic equations (DAEs) that could include electromechanical, electromagnetic, and thermal transients; the model represents a high fidelity time-domain representation of the protection zone; 2) applying DSE for estimating dynamic states and checking the consistency between the available measurements and the dynamic model. Low consistency indicates that some of the physical laws are violated and therefore an internal fault is detected. The validity of the DSE-based protection comes from the following key advantages of DSE: 1) accurately tracking the dynamics of the system; 2) systematically checking the consistency between the measurements and the dynamic model through the residuals, and 3) effectively filtering out measurement errors. DSE based protection schemes have been applied to transmission lines [9], [197], microgrids [194], transformers [198], etc. With increased security and dependability compared to legacy methods, the DSE-based protection can be utilized as the main protection of the component of interest (protection zone). Additionally, the DSE-based protection is capable of detecting bad data through centralized substation protection.

The implementation of an example DSE-based protective relay with a two-terminal transmission line as the protection zone is shown in Fig. 18. Due to space limitations, the figure only demonstrates the relay on the left terminal of the line, with the inter-trip signal connected to the left side breaker (the relay on the right terminal is equivalent).

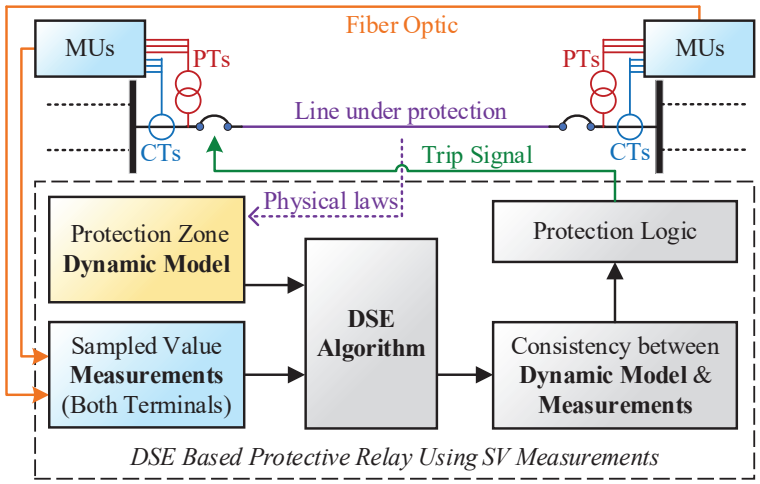

Fig. 18. An example DSE based protective relay using SV measurements at the left terminal, with a 2-terminal line as the protection zone

The two-terminal voltage and current SV measurements are obtained through PTs, CTs, and the MUs. The dynamic model of the protection zone is established by describing all the physical laws of the line under protection using DAEs. Afterward, DSE combines the dynamic model and the SV measurements, solves the dynamic states of the system, and computes the consistency between the dynamic model and the measurements (via the well-known chi-square test). Finally, the trip signal is issued to open the circuit breaker of the transmission line if an internal fault is detected. Using such an approach high impedance, or arcing faults are easily detected. A similar approach can be used to design smart auto-reclosure procedures [199].

2) DSE-based Fault Location Using SV Measurements

Fault Location is another important function when the fault occurs in a protection zone. Specifically, the exact fault location should be determined to minimize the time spent searching for the fault location by repair crews, yielding reduced power outage time and operating costs. With the development of fast-tripping techniques of protective relays, the time window of available measurements during faults for fault location is further shortened to the order of milliseconds. In addition, during this short time window, the available measurements usually experience severe transients. This leads to compromised accuracy of calculated phasors and therefore increases the fault location errors for legacy phasor domain-based fault location approaches.

To deal with these challenges, DSE-based fault location approaches using SV measurements have been proposed in [200]-[201]. They were inspired by the widely adopted traditional phasor domain fault location methods. Traditional phasor domain methods build the relationship between the available phasor domain measurements and the location of the fault using algebraic equations, which are afterward solved to identify the location of the fault. DSE-based fault location methods first describe the relationship between the available time-domain measurements and the location using an accurate time-domain dynamic model of the transmission line with fault. The time-domain model can also include the model of the arc [202]. The dynamic model is a set of DAEs, which typically include instantaneous voltages and currents through the transmission line as dynamic states of the system, and also the location of the fault as an extended state. Then, DSE is applied to systematically estimate the location of the fault. The primary advantages of DSE based fault location approach over traditional phasor domain approaches are 1) the DSE based methods make full use of information embedded in SV measurements and systematically filter out measurement errors; 2)

time-domain algorithms typically possess faster convergence compared to phasor domain algorithms; 3) time-domain algorithms are not sensitive to complex harmonics distortions and are capable of accurate tracking severe dynamics during faults [202].

3) Hidden Failure Detection of Protective Relays using DSE

DSE-based protection schemes have also been applied at the substation level to achieve centralized substation protection [203], to detect compromised devices such as MUs and relays. The main idea is to utilize all the measurements in a substation, resulting in high data redundancy; this enables surgical detection of bad/missing data and validation of the source of anomalies (i.e. actual fault in the system, instrumentation faults, bad data injection cyber-attacks, etc.) via systematic hypothesis testing. Instrumentation faults (blown fuses, shorted CT, incorrect instrumental transformer ratios, etc.) known as hidden failures are a real problem in any protection system. DSE offers another advantage: upon detecting a hidden failure and bad data, the compromised data can be replaced in real-time by estimated values to ensure the resilient and reliable operation of the protection system.

5.6 Conclusions and Outlook

This Section has explored the usefulness and the advantages of DSE on many control and protection applications for modern power systems. It has been shown how DSE-based solutions comprehensively respond to challenges in the control and protection of modern power systems holistically. In addition, several gaps in the existing literature have also been identified and several new DSE-based control and protection methods have been proposed as possible solutions. Future research on DSE applications on control and protection are categorized into the following key areas:

- **Role of AI/machine learning**: DSE enables the validation and calibration of system dynamic models, but there are still scenarios that good calibrations cannot be achieved due to the lack of high-quality large disturbances. As a result, the dynamic model may create deficiencies, yielding unreliable control, and protection. By mining the historical operational characteristics, advanced AI and machine learning tools may be able to compensate for these deficiencies. This further allows us to develop deep reinforcement learning algorithms that interact with the compensated DSE model outputs for system protection, control, and stability enhancement.
- **Enhancement of DSE and Observer**: Although the advantages and disadvantages of observer and DSE have been discussed, there is still a need to develop computationally efficient and robust alternatives in terms of handling sensor quality, model uncertainties, and nonlinearities. The practical implementation challenges for them need to be further investigated as well when designing state-feedback controls.
- **Management of distributed energy resources (DERs)**: In cases where fully decentralized DSE-based protection and control for all DERs do not cover all protection and control needs, as in cases of grid forming converters, multi-agent distributed DSE-based approaches need to be investigated, so as to share and transmit key information for frequency and voltage control, and protective actions.
- **DSE-based control for inertia emulation:** One possible solution for the decreasing system inertia due to an increase in CBRs can be through estimation of the states as well as the frequency, rate of change of frequency of the CBRs using DSE. These estimates can be utilized to control the power output of the CBRs in an intelligent manner such that the CBRs can provide an inertial response to the grid and, to some extent, also participate in its frequency control.

- **DSE-based protection with high penetration of CBRs:** For systems with high penetration of CBRs, protection systems encounter additional challenges with the extremely fast electromagnetic transients. Therefore, DSE tools should be carefully validated to ensure their capability of tracking electromagnetic transients in those conditions. In addition, parameter identification of CBRs using DSE can also improve the visibility of the system and therefore benefit the protection design. Moreover, the computational complexity of DSE should be considered to ensure real-time protection operation.
- **DSE-based optimal operations of a distributed microgrid:** DSE has already been used for estimating and controlling solar power sources, wind energy power sources, traditional generation units, and monitoring and estimation of batteries. Aided by MPC and data-driven methods, the applications of DSE can be extended to microgrids' stability and operation, synergistically achieving optimal operations of renewable energy microgrids. Overall, this will help supply the electricity in an economic, reliable, and sustainable manner.
- **Design of fault-tolerant and reconfigurable controls:** It is reasonable to expect that DSE becomes a key enabler to design fault-tolerant and reconfigurable controls particularly for long-term phenomena (like long-term voltage instability). A good starting point is to take advantage of similar and proven approaches from other engineering fields [204]. The ability of DSEs to detect and handle bad measurements (failure) and topology changes (errors in the model) would further simplify this problem focusing on control failures.
- **DSE enabled control of energy storage state-of-charge for grid-scale applications:** Reliability, longevity, and efficiency of electrochemical energy storage systems like battery storage deployed for grid-scale applications, such as intermittency mitigation, frequency control, etc., can be enhanced by utilizing its internal states like state-of-charge (SoC) in modulating the flow of energy from/to the energy storage via control of its power conditioning circuit. DSE can utilize the terminal measurements of the energy storage unit to dynamically estimate the SoC (otherwise unmeasurable directly) to ensure optimal flow of energy from/to the energy storage system while keeping overcharge/over-discharge in check to avoid its degradation thereby prolong its life expectancy.
- **Practical implementation**: Practical implementations should address issues of response time commensurate with the application. DSE applications need to be supported by adequate computing resources or distributed to achieve practical and acceptable performance in real-time. Many DSE applications of control and protection lack examples of their practical implementation in the field. Research topics include: How to ensure interoperability with currently used tools of control and protection? How to make them compatible with the current control room environment? What level of centralized or distributed computing is needed? What response times are desirable? What information should be communicated between remote sites and control rooms? What training should be developed and provided to power engineers? And what new standards are needed?

6. Demonstrative Examples

6.1 DSE-based Protection Using SV Measurements

6.1.1 System Description

A 500kV/1000MVA three-phase AC transmission system is built in PSCAD/EMTDC, as shown in Fig. 19. Here Line 1 is protected by the DSE-based protection Using SV Measurements. The line under protection (Line 1) is a 200 km overhead transmission line, with SV voltage and current measurements installed at dual ends. The length of Line 2 and Line 3 are 120 km and 180 km, respectively. The sampling rates of the SV measurements are 4000 samples per second (50 Hz nominal frequency, 80 samples per cycle according to IEC 61850-9-2 standard [158]).

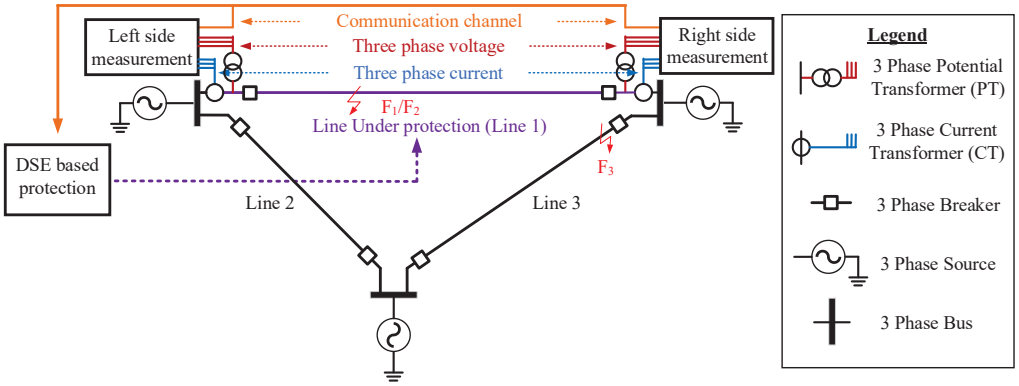

Fig. 19. Example transmission system

Trip logic and Settings of the Protective Relay

The detailed trip logic of the DSE-based protection is shown as follows. The dynamic state estimation finds the best estimates of the states of the line under protection at time t. Afterward, those estimated states are substituted into the dynamic model of the transmission line for the calculation of the "chi-square value" $J(t)$. The chi-square value is defined as the weighted sum of the squares of the residual (difference between the actual measurements and the estimated measurements). A large chi-square value indicates a large possibility of internal faults, while a low chi-square value indicates that the line is healthy. Therefore, a user-defined threshold (a "setting" of the relay) J_{set} is introduced, and the chi-square value is compared to this value,

$$test(t) = \begin{cases} 1, \ if \ J(t) > J_{\text{set}} \\ 0, \ if \ J(t) < J_{\text{set}} \end{cases} \tag{20}$$

where test(t) indicates the possibility of an internal fault.

To further ensure the reliability of the DSE-based protection method, integration of the value $test(t)$ is introduced for trip decision,

$$trip(t) = \begin{cases} 1, \int_{t-T_{\text{delay}}}^{t} test(\tau)d\tau > T_{\text{set}} \\ 0, \int_{t-T_{\text{delay}}}^{t} test(\tau)d\tau \le T_{\text{set}} \end{cases} \tag{21}$$

where T_{delay} and T_{set} are two settings of the relay. The meaning of (21) is as follows: if within the time window of T_{delay}, the value of *test*(*t*) keeps 1 for T_{set}, the trip signal is issued.

For this example test system, the settings of the DSE-based protection is selected as follows: J_{set} = 500, T_{delay} = 10 ms, T_{set} = 5 ms.

6.1.2 Test Cases and Results

This section introduces 3 example fault events to demonstrate the dependability and the security of the DSE-based protection method, including a low impedance internal fault, a high impedance internal fault, and a low impedance external fault. For the two internal faults, the DSE-based protection should be able to dependably trip the line under protection with high speeds; for the external fault, the DSE-based protection should securely ignore this transient and no trip signal should be issued.

Fault Event 1: Low Impedance Internal Fault F_1

A low impedance phase A to ground internal fault occurs at 80 km away from the left end of the line at time 0.3 s. The fault impedance is 0.01 ohm, indicating that this is a severe internal fault. Fig. 20 shows the three-phase voltage and current SV measurements before and during the fault. One can observe that the phase A current increases dramatically during this severe internal fault.

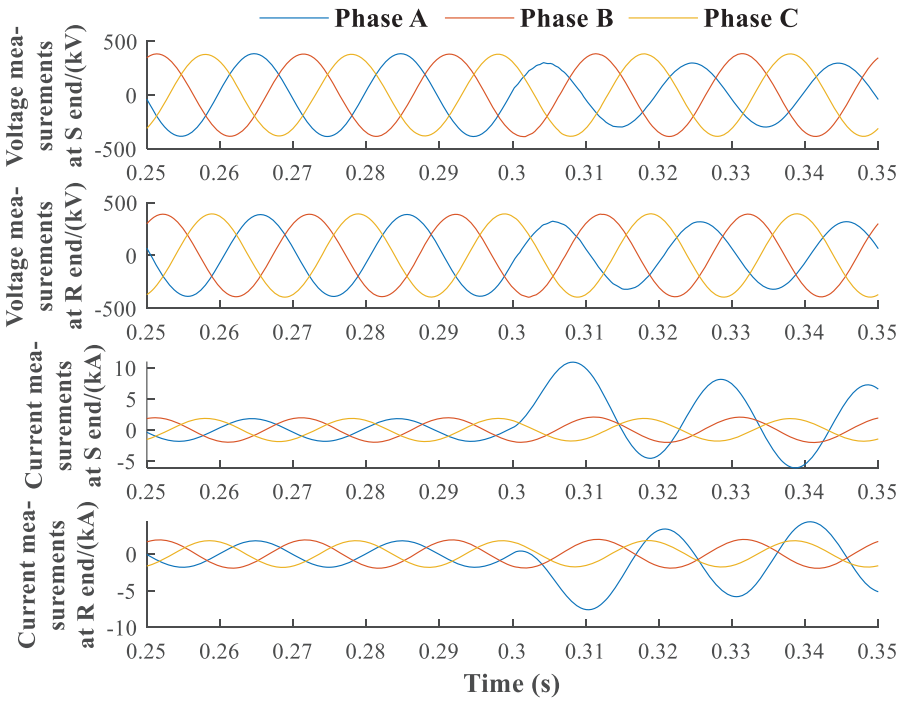

Fig. 20. Three-phase voltage and current SV measurements at both terminals, fault event 1

The performances of the DSE-based protection method are shown in Figs. 21 and 22. Fig. 21 takes the voltages at terminal R as examples and shows the actual measurements, estimated measurements, residuals and normalized residuals of three-phase voltages at terminal R. One can observe that, before the occurrence of the fault, the residuals and normalized residuals are very small (the differences between the actual and estimated measurements are very small), indicating high consistency between the measurement and the dynamic model, and therefore a healthy condition of the line under protection. During the internal fault, the residuals and normalized residuals increase dramatically, implying an internal fault.

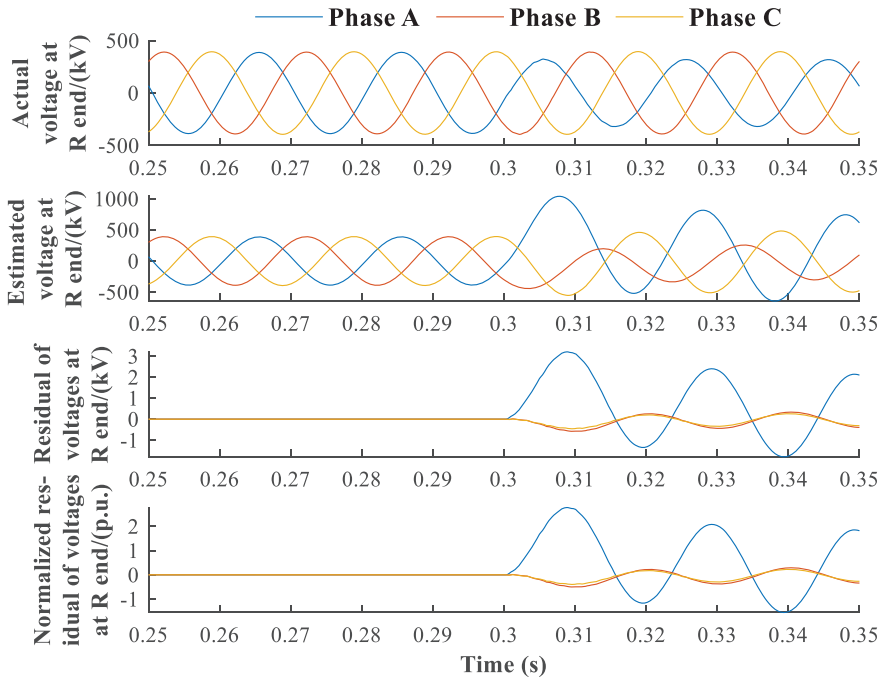

Fig. 21. Actual measurements, estimated measurements, residuals, and normalized residuals of three-phase voltages at R end, fault event 1

Fig. 22 demonstrates the chi-square values, the test values, and the trip values corresponding to fault event 1. It can be observed that the chi-square values are very small before the fault, and increase dramatically during the fault. As a result, the test values keep 0 before the fault, and jump from 0 to 1 at 0.301 s, meaning that the fault detection time is only 1 ms. Afterward, the test values remain to be 1 during the fault. Therefore, the trip decision is made with the user-defined time delay and the line is tripped at 0.306 s. This event proves that the DSE-based protection can dependably detect the low impedance internal fault with very high speed.

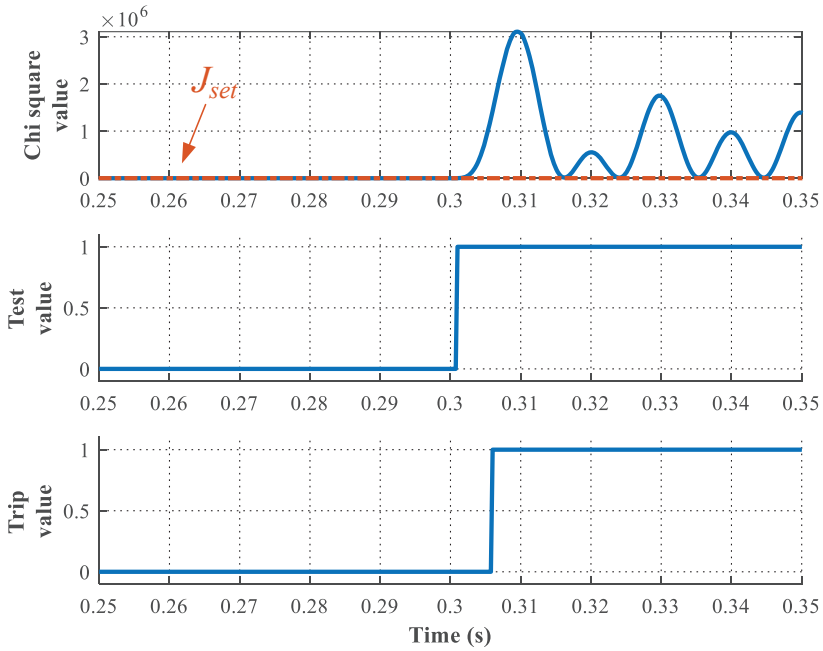

Fig. 22. Protection performance, fault event 1

Fault Event 2: High Impedance Internal Fault F_2

A high impedance phase A to ground internal fault occurs at 80 km away from the left end of the line at time 0.3 s. The fault impedance is 500 ohm. This fault is extremely mild in practical transmission systems and is difficult to be detected by legacy protection functions. Fig. 23 shows the three-phase voltage and current SV measurements before and during the fault. One can observe that the currents and voltages do not change much after the occurrence of the fault.

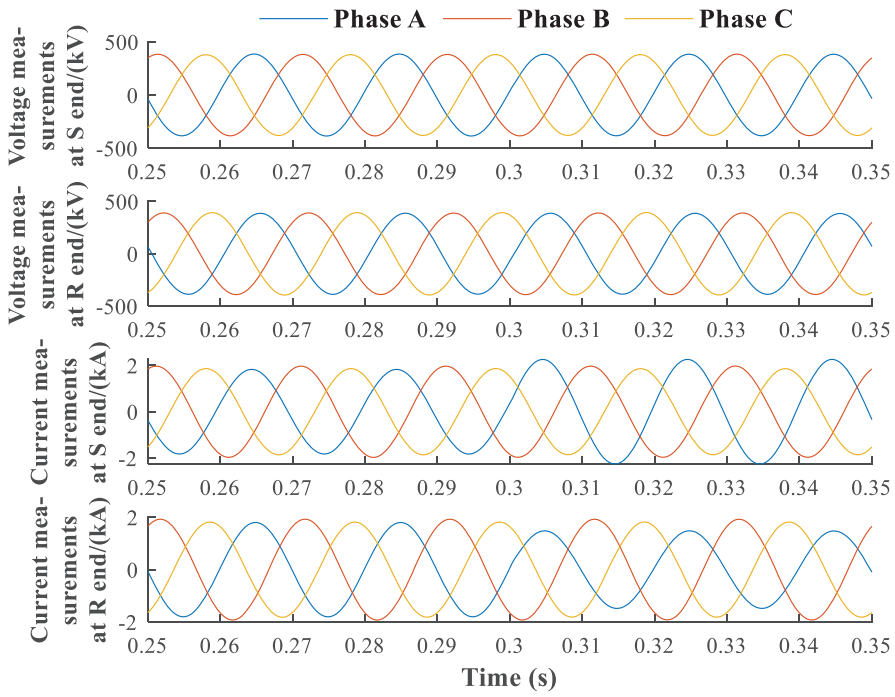

Fig. 23. Three-phase voltage and current SV measurements at both terminals, fault event 2

The performances of the DSE-based protection method are shown in Figs. 24 and 25. Fig. 24 shows the actual measurements, estimated measurements, residuals, and normalized residuals of three-phase voltages at terminal R. Similarly, before the occurrence of the fault, the residuals and normalized residuals are very small, indicating high consistency between the measurement and the dynamic model, and therefore a healthy condition of the line under protection. During the internal fault, the residuals and normalized residuals increase dramatically, implying an internal fault.

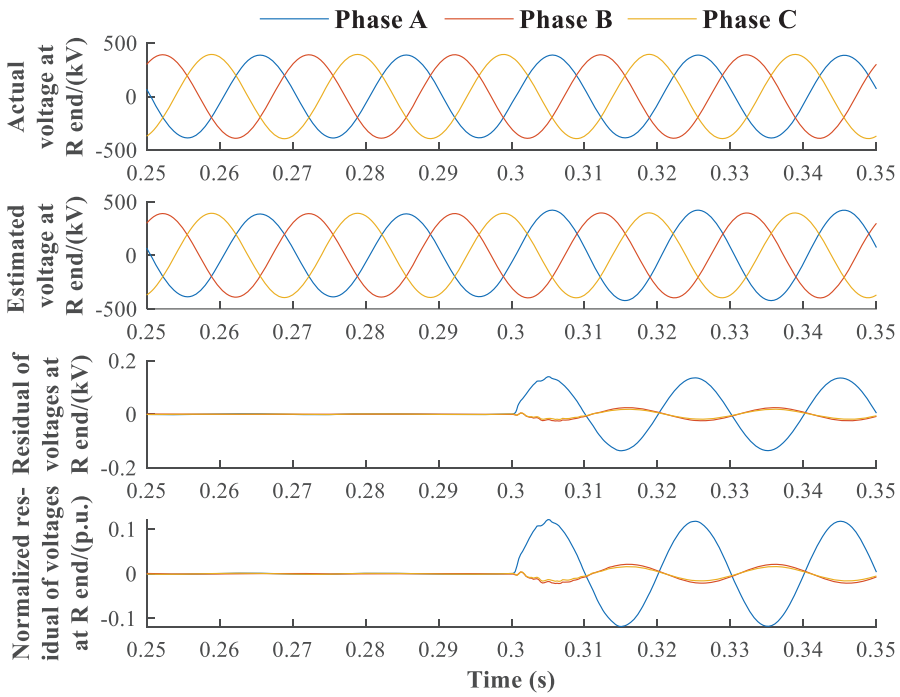

Fig. 24. Actual measurements, estimated measurements, residuals, and normalized residuals of three-phase voltages at R end, fault event 2

Fig. 25 demonstrates the chi-square values, the test values, and the trip values corresponding to fault event 2. Similarly, it can be observed that the chi-square values are very small before the fault, and increase dramatically during the fault. As a result, the test values keep 0 before the fault, and jump from 0 to 1 at 0.3018 s, meaning that the fault detection time is only 1.8 ms. It is worth noting that, since this is a high impedance internal fault, the test values vary between 0 and 1 during the fault (test value stays 1 for the majority of the time). However, this is still a clear indication of abnormality in comparison to continuous low chi-square values for a long time. Therefore, the trip decision is made with the user-defined time delay and the line is tripped at 0.3068 s. This event proves that the DSE-based protection can also sensitively and dependably detect the high impedance of the internal fault with very high speed.

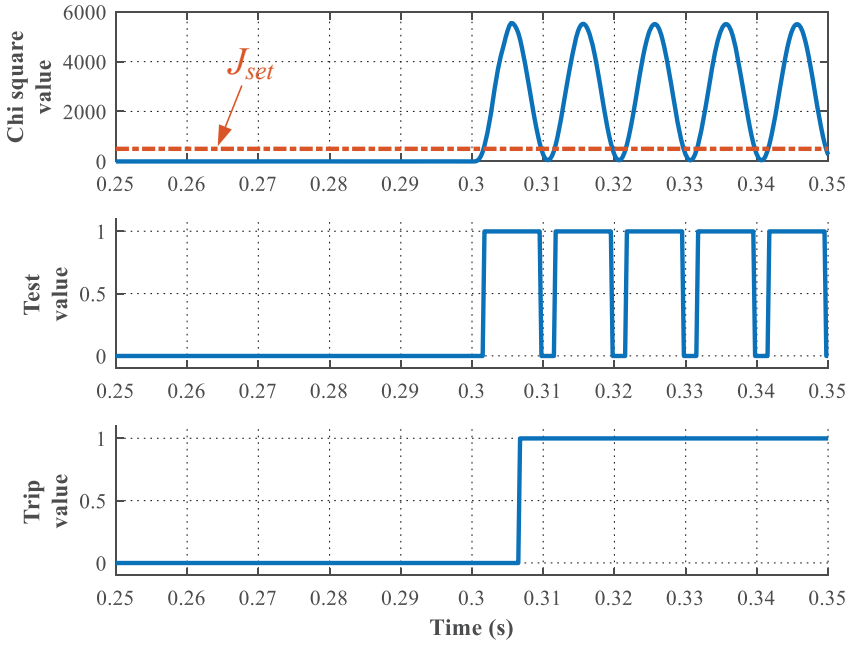

Fig. 25. Protection performance, fault event 2

Fault Event 3: Low Impedance External Fault F_3

A low impedance phase A to ground external fault occurs at 1 km away from the right end of Line 1 (within Line 3) at time 0.3s. The fault impedance is 0.01 ohm. This fault is a severe external fault, which will generate severe transients within the line under protection (Line 1). Fig. 26 shows the three-phase voltage and current SV measurements before and during the fault. One can observe that the phase A current also increases dramatically after the occurrence of the fault (similar to fault event 1). However, since this is an external fault, according to the requirement of the protective relay, this fault should not be identified as an internal fault and the DSE-based protection should not trip this external fault.

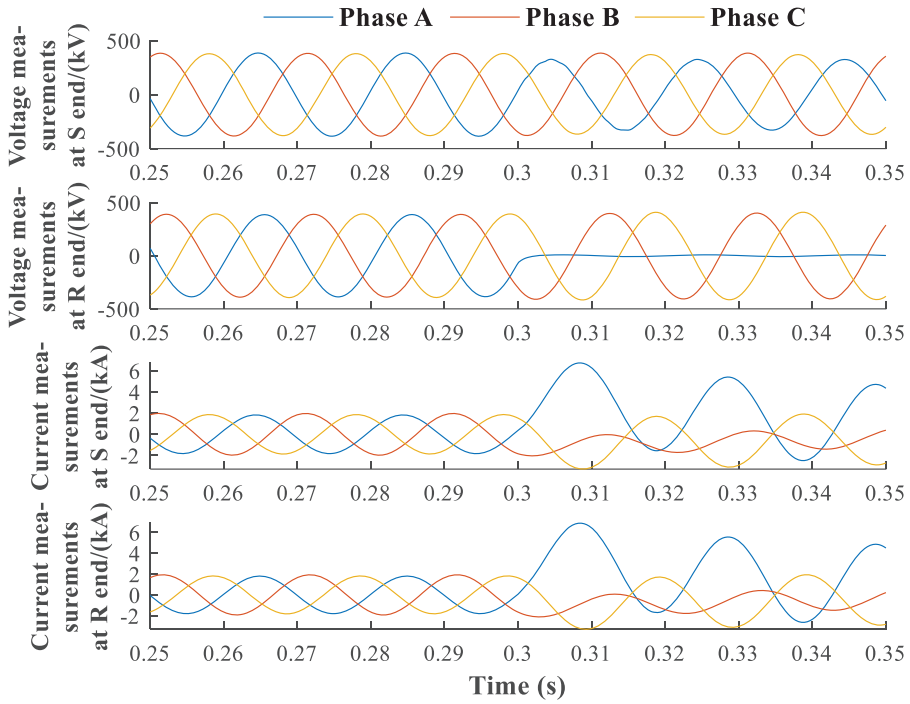

Fig. 26. Three-phase voltage and current SV measurements at both terminals, fault event 3

The performances of the DSE-based protection method are shown in Fig. 27 and 28. Fig. 27 shows the actual measurements, estimated measurements, residuals and normalized residuals of three-phase voltages at terminal R. One can observe that the residuals and normalized residuals are both very small before and during this external fault, implying high consistency between the measurement and the dynamic model even during the fault. Therefore, one can conclude that the line remains healthy during this event.

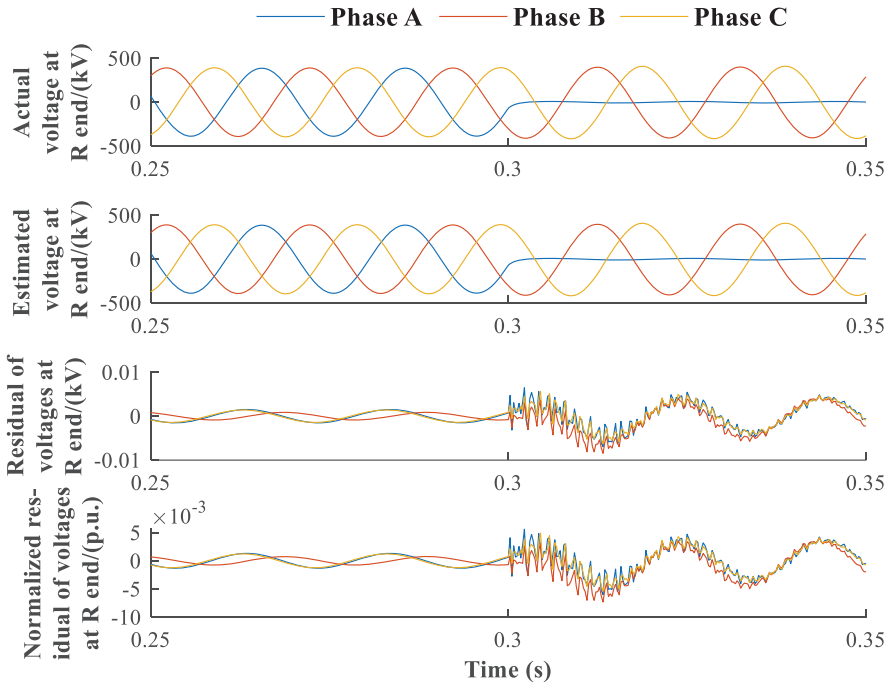

Fig. 27. Actual measurements, estimated measurements, residuals, and normalized residuals of three-phase voltages at R end, fault event 3

To further quantify this consistency, Fig. 28 demonstrates the chi-square values, the test values, and the trip values corresponding to fault event 3. It can be observed that the chi-square values increase very slightly during the fault (the increase is caused by the severe transients). However, the chi-square values are still way below the threshold, meaning that the line is without internal faults. Therefore, no trip decision is made during this severe external fault. This event proves that the DSE-based protection can securely ignore severe external faults.

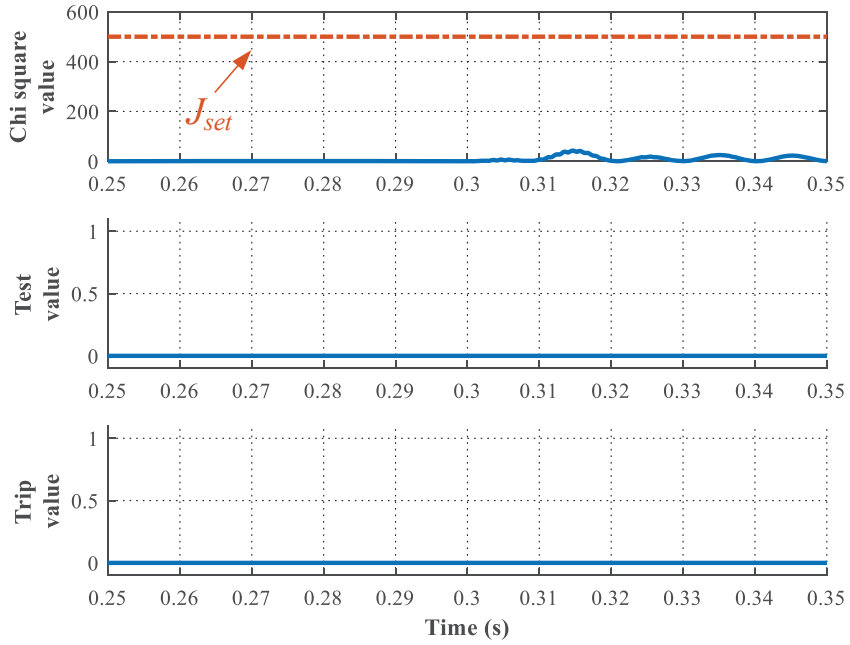

Fig. 28. Protection performance, fault event 3

6.1.3 Summary

To sum up, with the example test system and above fault events, the DSE-based protection can dependably operate during internal faults (even high impedance faults) with high speeds, and can securely refuse to operate during severe external faults. The effectiveness of the DSE-based protective relay comes from the advantages of DSE that it can accurately track fast dynamics (even electromagnetic dynamics) of the line under protection, can systematically check the consistency between the measurements and the dynamic model of the line under protection, and can filter out measurement noises.

6.2 DSE-based Adaptive-Phasor Approach to PMU Measurement Rectification for LFOD Enhancement

6.2.1 Overview of DSE Adaptive-phasor-based Data Recovery Method

In [205], a DSE-based integral local data processing and central data recovery scheme is proposed. The data processing procedure is to detect and eliminate bad data and verify PMU measurements, whereas the data recovery scheme is to compensate for data transmission delays and restore missing and disordered data. The recovered PMU measurements are then utilized in a low-frequency oscillation damping (LFOD) enhancement scheme, which is achieved by a modified PI PSS mechanism embedded in the automatic voltage regulator structure of a synchronous generator.

The proposed measurement processing and restoration and LFOD enhancement strategy, as shown in Fig. 28, comprises (i) a DSE-based bad data detection and elimination [149] and measurement verification mechanism, collocated with PMUs at each generator bus-bar, (ii) a data recovery block, which can decompose oscillatory PMU measurements and restore the measurement data after time-varying communication delays, and data loss and disorder, with dedicated channels for each synchrophasor, (iii) an LFOD enhancer (PI-PSS) connected to the AVR structure of a selected synchronous generator (G_M in Fig. 28), and (iv) a parameter optimization block to obtain the optimal set of parameters for the PI-PSS.

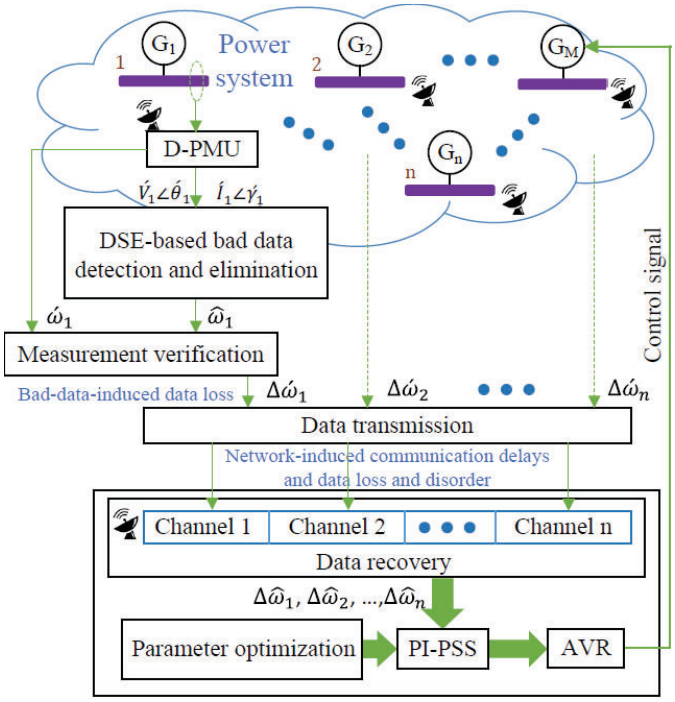

Fig. 28 Overview of the proposed DSE-based PMU measurement rectification and LFOD control mechanism

In detail, an adaptive-phasor-based delay compensation method is proposed to achieve the measurement data recovery purpose. To address the missing data issue, which is caused either by bad measurement of the PMUs or network-induced reasons, as well as data disorder issue, we consider missing data as increased communication delay and data disorder as decreased communication delay, so that the proposed method can cope

with all these situations. Note that, for the data-bearing time stamps that are earlier than the timestamp of the most recent stored datum will be directly discarded, i.e., the data that arrive late due to data disorder will be abandoned without further processing. The proposed AP-based data recovery method is only aware of the consistency of the received data, and when the data flow is smooth, we consider the data transmission process has a constant delay; otherwise if data is empty or data flow is inconsistent, communication latency is deemed changing.

The fundamental assumption of this method is that when a power system is subjected to small disturbances the low-frequency oscillatory signals $\chi(t)$can be decomposed into an average component and an oscillatory component, which is shown as follows,

$$\chi(t) = \chi_{av}(t) + \chi_{osc}(t),\ \ \chi_{osc}(t) = Re\{\boldsymbol{\chi_{ph}} e^{j\Omega t}\},$$

where χ_{av} and $\chi_{osc}(t)$ are the average and oscillatory components of the decomposed signal. Terms $\boldsymbol{\chi_{ph}}$ and Ω are respectively the phasor and angular frequency of the oscillatory signal, i.e., the frequency of LFO. Then through adaptively rotating the reference frame of the phasor component based on the time latency T_d, the time-varying latencies can be compensated. Fig.29 shows the overall AP-based signal restoration method, which consists of three major components: signal decomposition, frequency adaptation, and signal recovery. For detailed procedures, analysis, and mathematical derivations, see [205] for enhanced PMU data recovery and [206] for communication delay compensation.

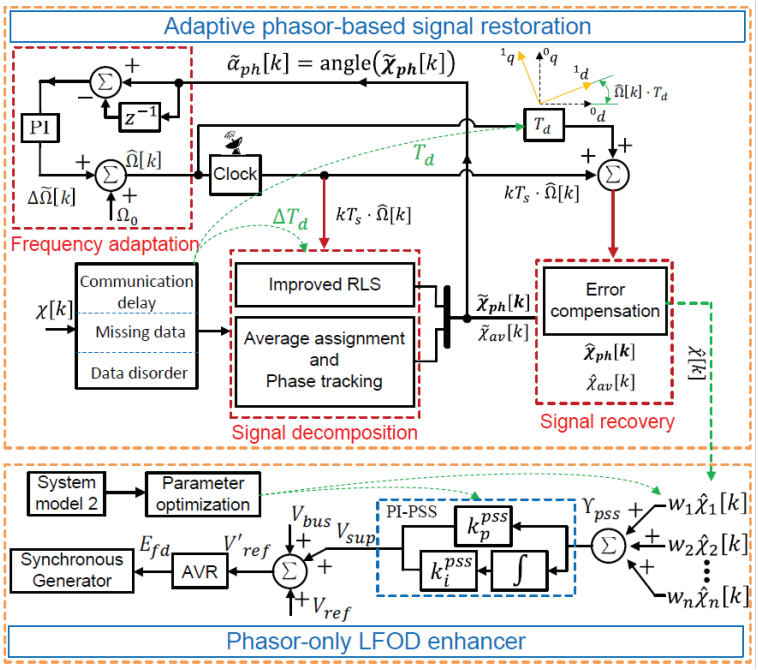

Fig. 29 Proposed DSE-based adaptive phasor method for PMU data recovery

6.2.2 Case study and simulation results

A. Simulation Condition

A 2-area, 4-machine power system modified from [207] is employed to test the functionality of the measurement rectification and LFOD enhancement strategies. The test system runs in steady-state until $t = 1.0$s when a sudden load decrease, i.e., $P_7 = P_7^{ini} - 0.1$ p.u., happens at the load connected to bus 7.

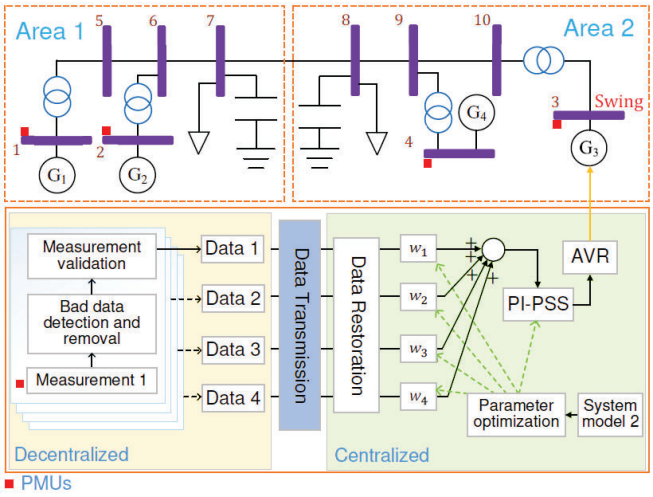

Fig. 30 Two-area four-machine test system with the proposed data rectification and LFOD enhancement strategy

Four PMUs are individually installed in all generator buses, and the control center is placed at bus 3. All PMUs, except the one that is locally installed at bus 3, are connected to the control center via communication links subjected to random time-varying latencies, data loss, and data disorder. The random communication latencies are generated with the generalized Pareto distribution model with empirical PMU latencies seen in practical situations [208]. Note that the mean values of the communication latencies are proportional to the geographical distance between the control center and the PMUs, and the communication latency between the control center and the PMU located in bus 3 is ignored.

B. Simulation Results

DSE and Local Data Processing: Figs. 31(a)–(b) demonstrate the selected state estimation results generated by the decentralized UKF-based DSE algorithm from G1. It is evident that the UKF algorithm can track the dynamic states using local voltage and current measurements infected with bad data obtained from PMUs. The bad data detection functionality has also been examined by injecting random perturbations into the measurement signals at selected time instances, i.e., $t = \{2, 4, 6, 8\}$s. As shown in Figs. 31(c)–(d), outstanding readings are found from the deviation ratios at G1 at $t = \{2, 4, 6, 8\}$s, indicating bad data are detected, which are then removed. See [149] and [74] for the discussion on classifying bad data with the deviation ratios.

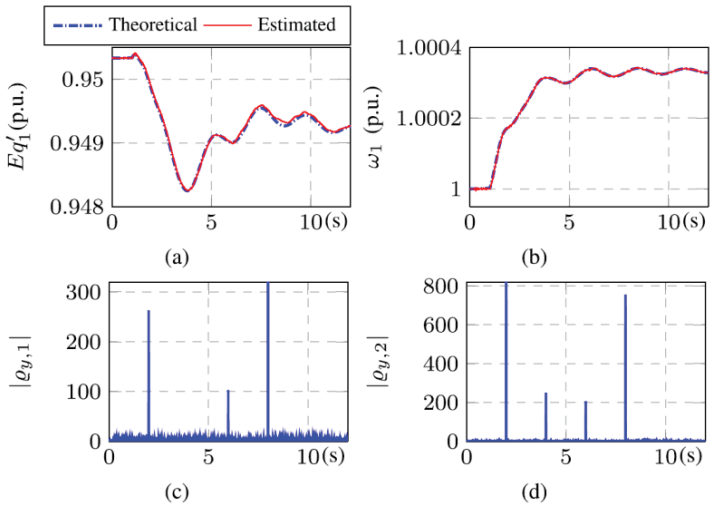

Fig. 31 (a) and (b): Decentralized UKF-based DSE; (c) and (d): absolute values of normalized deviation ratios G1.

Signal Decomposition and Restoration: The frequency deviation signal of G1 is shown in Fig. 32, where the solid line shows the signal captured from the PMU, the dotted line is the uncompensated signal retrieved from the control center and the remaining curve represents the compensated signal to be fed into the PI-PSS controller. Comparing the original signal to the uncompensated signal from the enlarged graphics in Figs. 32 (a)-(d), distortions can be observed from the uncompensated signal, which are caused by data loss, data disorder, and time-varying delays. Evidently, the AP-based signal recovery algorithm can restore the distorted frequency deviation signal to be input into the PI-PSS structure for the best control outcome.

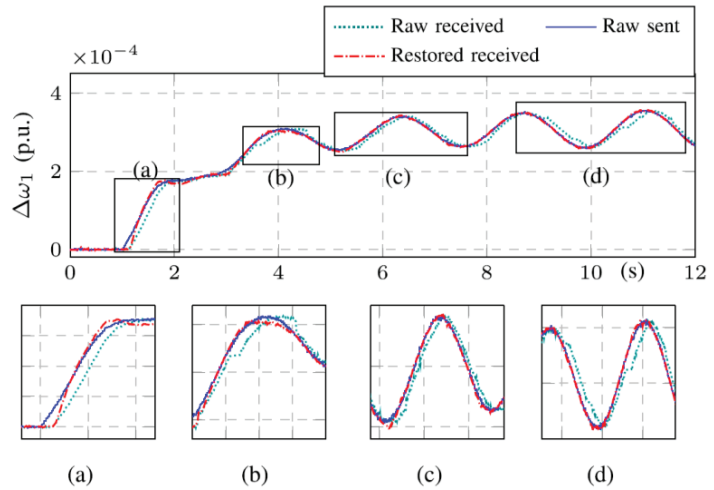

Fig. 32 Noisy frequency deviation measurement of G1

Fig. 33 demonstrates the decomposed oscillatory component of the frequency deviation signal of G1 with and without the proposed measurement rectification method. It is noteworthy that the extracted oscillatory signal oscillates at the frequency obtained through the modal analysis. The result also indicates the functionality of the signal decomposition strategy.

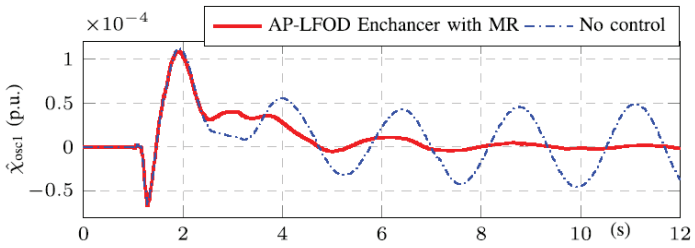

Fig. 33 Oscillatory component of frequency deviation from G1

LFOD Enhancement: Fig. 33 also shows the difference between the oscillatory component of the restored signal with and without LFOD enhancer. It is clear that with the proposed AP-LFOD enhancement method, the oscillatory component of the measured signal subsides substantially faster than without the proposed control scheme. In addition, Figs. 34 (a) and (b) demonstrate the differences in the LFO mitigation with and without the proposed measurement rectification method (marked with MR in the figures). Without any control strategies enforced, the frequency deviation signals fluctuate within increasing amplitudes due to system instability, whereas the system with the AP-LFOD enhancer and the proposed MR methodology has shown significant improvement in LFO alleviation. It can also be seen that the LFOD controller with MR performs more favorably than without MR, which suppresses oscillations before the frequency signal settles, hence a better primary frequency response. This reveals that the newly proposed measurement rectification method can effectively eliminate the unwanted PMU measurements and ensures the AP-LFOD enhancer has valid input data, which in turn enhances the stability of the power system.

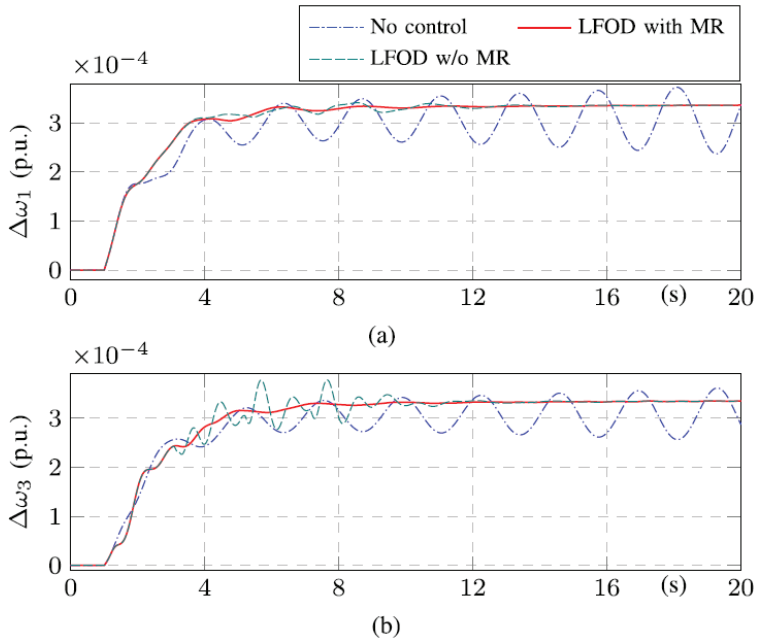

Fig. 34 Frequency deviations of (a) G1 and (b) G3 with proposed LFOD enhancer

6.2.3 Summary

A DSE-based measurement rectification, comprising local measurement processing and central data recovery functions, has been proposed based on the adaptive phasor concept. The recovered PMU measurements are imported into a dedicated central PI-PSS mechanism, which realizes LFOD enhancement. The proposed method is intended to improve the quality of synchrophasors obtained from PMU so that the designed controller can generate expected, satisfactory control performances, which would otherwise be compromised when using unprocessed data as demonstrated in the case study. Time-domain studies have shown the functionality of the proposed measurement rectification strategy and demonstrated the effectiveness of the LFOD enhancer that improves the small-signal stability of the overall power system.

7. Conclusion

This technical report provides a clear definition of DSE and classifies its relationships and differences with other existing SE formulations. Different methods for implementing DSE as well as its practical implementation using commercial software are discussed. Its roles for power systems modeling, monitoring, operation, control, and protection have been thoroughly discussed and many numerical results have also been presented. Future research directions on DSE algorithms, implementations, and applications have been carefully discussed. It is expected that this technical report will play as the foundation in using DSE for future power electronics-dominated clean energy systems.

8. References

[1] M. D. Ilić and S. Liu, *Hierarchical Power Systems Control*. London: Springer London, 1996.

[2] P. Kundur *et al.*, “Definition and classification of power system stability IEEE/CIGRE joint task force on stability terms and definitions,” *IEEE Trans. Power Syst.*, vol. 19, no. 3, pp. 1387–1401, 2004, doi: 10.1109/TPWRS.2004.825981.

[3] F. C. Schweppe and J. Wildes, “Power System Static-State Estimation, Part I: Exact Model,” *IEEE Trans. Power Appar. Syst.*, vol. PAS-89, no. 1, pp. 120–125, 1970, doi: 10.1109/TPAS.1970.292678.

[4] F. C. Schweppe and D. B. Rom, “Power System Static-State Estimation, Part II: Approximate Model,” *IEEE Trans. Power Appar. Syst.*, vol. PAS-89, no. 1, pp. 125–130, 1970, doi: 10.1109/TPAS.1970.292679.

[5] F. C. Schweppe, “Power System Static-State Estimation, Part III: Implementation,” *IEEE Trans. Power Appar. Syst.*, vol. PAS-89, no. 1, pp. 130–135, 1970, doi: 10.1109/TPAS.1970.292680.

[6] A. Abur and A. Gomez-Expósito, *Power System State Estimation: Theory and Applications*. CRC Press, 2004.

[7] H. Modir and R. A. Schlueter, “A Dynamic State Estimator for Dynamic Security Assessment,” *IEEE Trans. Power Appar. Syst.*, vol. PAS-100, no. 11, pp. 4644–4652, 1981, doi: 10.1109/TPAS.1981.316806.

[8] A. P. S. Meliopoulos *et al.*, “Dynamic State Estimation-Based Protection: Status

and Promise," *IEEE Trans. Power Deliv.*, vol. 32, no. 1, pp. 320–330, 2017, doi: 10.1109/TPWRD.2016.2613411.

[9] Y. Liu, A. P. S. Meliopoulos, R. Fan, L. Sun, and Z. Tan, "Dynamic State Estimation Based Protection on Series Compensated Transmission Lines," *IEEE Trans. Power Deliv.*, vol. 32, no. 5, pp. 2199–2209, 2017, doi: 10.1109/TPWRD.2016.2633410.

[10] R. Fan, A. P. S. Meliopoulos, G. J. Cokkinides, L. Sun, and L. Yu, "Dynamic state estimation-based protection of power transformers," in *2015 IEEE Power & Energy Society General Meeting*, 2015, pp. 1–5, doi: 10.1109/PESGM.2015.7286463.

[11] Y. Cui, R. G. Kavasseri, and S. M. Brahma, "Dynamic State Estimation Assisted Out-of-Step Detection for Generators Using Angular Difference," *IEEE Trans. Power Deliv.*, vol. 32, no. 3, pp. 1441–1449, 2017, doi: 10.1109/TPWRD.2016.2615594.

[12] J. D. La Ree, V. Centeno, J. S. Thorp, and A. G. Phadke, "Synchronized Phasor Measurement Applications in Power Systems," *IEEE Trans. Smart Grid*, vol. 1, no. 1, pp. 20–27, 2010, doi: 10.1109/TSG.2010.2044815.

[13] V. Terzija *et al.*, "Wide-Area Monitoring, Protection, and Control of Future Electric Power Networks," *Proc. IEEE*, vol. 99, no. 1, pp. 80–93, 2011, doi: 10.1109/JPROC.2010.2060450.

[14] J. J. Sanchez-Gasca (Chair), "Identification of Electromechanical Modes in Power Systems," IEEE Technical Report PES-TR15, 2012.

[15] Y. Chen, M. Rice, K. Glaesemann, and Z. Huang, "Sub-second state estimation implementation and its evaluation with real data," in *2015 IEEE Power & Energy Society General Meeting*, 2015, pp. 1–5, doi: 10.1109/PESGM.2015.7285996.

[16] S. Jin, Z. Huang, R. Diao, D. Wu, and Y. Chen, "Comparative Implementation of High Performance Computing for Power System Dynamic Simulations," *IEEE Trans. Smart Grid*, vol. 8, no. 3, pp. 1387–1395, May 2017, doi: 10.1109/TSG.2016.2647220.

[17] A. K. Singh, R. Singh, and B. C. Pal, "Stability analysis of networked control in smart grids," *IEEE Trans. Smart Grid*, vol. 6, no. 1, pp. 381–390, Jan. 2015, doi: 10.1109/TSG.2014.2314494.

[18] M. Ghandhari, G. Andersson, and I. A. Hiskens, "Control Lyapunov functions for controllable series devices," *IEEE Trans. Power Syst.*, vol. 16, no. 4, pp. 689–694, 2001, doi: 10.1109/59.962414.

[19] A. K. Singh and B. C. Pal, "Decentralized Nonlinear Control for Power Systems Using Normal Forms and Detailed Models," *IEEE Trans. Power Syst.*, vol. 33, no. 2, pp. 1160–1172, 2018, doi: 10.1109/TPWRS.2017.2724022.

[20] A. Singh and B. Pal, "Decentralized control of oscillatory dynamics in power systems using an extended LQR," in *2016 IEEE Power and Energy Society General Meeting (PESGM)*, 2016, p. 1, doi: 10.1109/PESGM.2016.7741163.

[21] M. A. M. Ariff and B. C. Pal, "Adaptive Protection and Control in the Power System for Wide-Area Blackout Prevention," *IEEE Trans. Power Deliv.*, vol. 31, no. 4, pp. 1815–1825, 2016, doi: 10.1109/TPWRD.2016.2518080.

[22] H. F. Albinali and A. P. Meliopoulos, "A Centralized Substation Protection Scheme that detects hidden failures," in *2016 IEEE Power and Energy Society General Meeting (PESGM)*, 2016, pp. 1–5, doi: 10.1109/PESGM.2016.7741559.

[23] E. Farantatos, R. Huang, G. J. Cokkinides, and A. P. Meliopoulos, "A Predictive Generator Out-of-Step Protection and Transient Stability Monitoring Scheme

Enabled by a Distributed Dynamic State Estimator," *IEEE Trans. Power Deliv.*, vol. 31, no. 4, pp. 1826–1835, 2016, doi: 10.1109/TPWRD.2015.2512268.

[24] V. Vittal (Project Leader), "Next Generation On-Line Dynamic Security Assessment," PSERC Final Project Technical Report, 2011.

[25] "Power Plant Dynamic Model Verification using PMUs," NERC Reliability Guideline, 2016.

[26] Z. Huang, P. Du, D. Kosterev, and S. Yang, "Generator dynamic model validation and parameter calibration using phasor measurements at the point of connection," *IEEE Trans. Power Syst.*, vol. 28, no. 2, pp. 1939–1949, 2013, doi: 10.1109/TPWRS.2013.2251482.

[27] J. Zhao and L. Mili, "Robust unscented Kalman filter for power system dynamic state estimation with unknown noise statistics," *IEEE Trans. Smart Grid*, vol. 10, no. 2, pp. 1215–1224, Mar. 2019, doi: 10.1109/TSG.2017.2761452.

[28] J. Zhao and L. Mili, "A Robust Generalized-Maximum Likelihood Unscented Kalman Filter for Power System Dynamic State Estimation," *IEEE J. Sel. Top. Signal Process.*, vol. 12, no. 4, pp. 578–592, 2018, doi: 10.1109/JSTSP.2018.2827261.

[29] J. Zhao and L. Mili, "Power System Robust Decentralized Dynamic State Estimation Based on Multiple Hypothesis Testing," *IEEE Trans. Power Syst.*, vol. 33, no. 4, pp. 4553–4562, Jul. 2018, doi: 10.1109/TPWRS.2017.2785344.

[30] J. H. Chow, Ed., *Power System Coherency and Model Reduction*, vol. 94. New York, NY: Springer New York, 2013.

[31] J. Zhao, L. Mili, and F. Milano, "Robust Frequency Divider for Power System Online Monitoring and Control," *IEEE Trans. Power Syst.*, vol. 33, no. 4, pp. 4414–4423, 2018, doi: 10.1109/TPWRS.2017.2785348.

[32] J. Zhao, Y. Tang, and V. Terzija, "Robust Online Estimation of Power System Center of Inertia Frequency," *IEEE Trans. Power Syst.*, vol. 34, no. 1, pp. 821–825, 2019, doi: 10.1109/TPWRS.2018.2879782.

[33] A. Rouhani and A. Abur, "A robust dynamic state estimator against exciter failures," in *2016 North American Power Symposium (NAPS)*, 2016, pp. 1–6, doi: 10.1109/NAPS.2016.7747998.

[34] G. Anagnostou, F. Boem, S. Kuenzel, B. C. Pal, and T. Parisini, "Observer-Based Anomaly Detection of Synchronous Generators for Power Systems Monitoring," *IEEE Trans. Power Syst.*, vol. 33, no. 4, pp. 4228–4237, 2018, doi: 10.1109/TPWRS.2017.2771278.

[35] Dan Simon, *Optimal State Estimation: Kalman, H Infinity, and Nonlinear Approaches*. Wiley, 2006.

[36] N. Zhou, D. Meng, Z. Huang, and G. Welch, "Dynamic State Estimation of a Synchronous Machine Using PMU Data: A Comparative Study," *IEEE Trans. Smart Grid*, vol. 6, no. 1, pp. 450–460, 2015, doi: 10.1109/TSG.2014.2345698.

[37] J. G. Proakis and D. K. Manolakis, *Digital Signal Processing: Principles, Algorithms and Applications*, 4th ed. Pearson, 2007.

[38] M. Hassanzadeh, C. Y. Evrenosoğlu, and L. Mili, "A Short-Term Nodal Voltage Phasor Forecasting Method Using Temporal and Spatial Correlation," *IEEE Trans. Power Syst.*, vol. 31, no. 5, pp. 3881–3890, 2016, doi: 10.1109/TPWRS.2015.2487419.

[39] A. M. Leite da Silva, M. B. Do Coutto Filho, and J. F. de Queiroz, "STATE FORECASTING IN ELECTRIC POWER SYSTEMS.," *IEE Proc. C Gener. Transm. Distrib.*, vol. 130, no. 5, pp. 237–244, 1983, doi: 10.1049/ip-c.1983.0046.

[40] A. M. L. da Silva, M. B. Do Coutto Filho, and J. M. C. Cantera, "An Efficient Dynamic State Estimation Algorithm Including Bad Data Processing," *IEEE Trans. Power Syst.*, vol. 2, no. 4, pp. 1050–1058, 1987, doi: 10.1109/TPWRS.1987.4335300.

[41] P. Rousseaux, D. Mallieu, T. Van Cutsem, and M. Ribbens-Pavella, "Dynamic state prediction and hierarchical filtering for power system state estimation," *Automatica*, vol. 24, no. 5, pp. 595–618, Sep. 1988, doi: 10.1016/0005-1098(88)90108-2.

[42] K. R. Shih and S. J. Huang, "Application of a robust algorithm for dynamic state estimation of a power system," *IEEE Trans. Power Syst.*, vol. 17, no. 1, pp. 141–147, Feb. 2002, doi: 10.1109/59.982205.

[43] J. Zhao, G. Zhang, Z. Y. Dong, and M. La Scala, "Robust Forecasting Aided Power System State Estimation Considering State Correlations," *IEEE Trans. Smart Grid*, vol. 9, no. 4, pp. 2658–2666, Jul. 2018, doi: 10.1109/TSG.2016.2615473.

[44] N. R. Shivakumar and A. Jain, "A review of power system dynamic state estimation techniques," 2008, doi: 10.1109/ICPST.2008.4745312.

[45] M. B. D. C. Filho and J. C. S. de Souza, "Forecasting-Aided State Estimation—Part I: Panorama," *IEEE Trans. Power Syst.*, vol. 24, no. 4, pp. 1667–1677, 2009, doi: 10.1109/TPWRS.2009.2030295.

[46] A. S. Debs and R. E. Larson, "A Dynamic Estimator for Tracking the State of a Power System," *IEEE Trans. Power Appar. Syst.*, vol. PAS-89, no. 7, pp. 1670–1678, 1970, doi: 10.1109/TPAS.1970.292822.

[47] K. Nishiya, J. Hasegawa, and T. Koike, "DYNAMIC STATE ESTIMATION INCLUDING ANOMALY DETECTION AND IDENTIFICATION FOR POWER SYSTEMS.," *IEE Proc. C Gener. Transm. Distrib.*, vol. 129, no. 5, pp. 192–198, 1982, doi: 10.1049/ip-c.1982.0032.

[48] N. G. Bretas, "An iterative dynamic state estimation and bad data processing," *Int. J. Electr. Power Energy Syst.*, vol. 11, no. 1, pp. 70–74, Jan. 1989, doi: 10.1016/0142-0615(89)90010-0.

[49] A. Bahgat, M. M. F. Sakr, and A. R. El-Shafei, "Two level dynamic state estimator for electric power systems based on nonlinear transformation," *IEE Proc. C Gener. Transm. Distrib.*, vol. 136–C, no. 1, pp. 15–23, 1989, doi: 10.1049/ip-c.1989.0003.

[50] X. Bian, X. R. Li, H. Chen, D. Gan, and J. Qiu, "Joint Estimation of State and Parameter With Synchrophasors—Part I: State Tracking," *IEEE Trans. Power Syst.*, vol. 26, no. 3, pp. 1196–1208, 2011, doi: 10.1109/TPWRS.2010.2098422.

[51] M. Göl and A. Abur, "LAV Based Robust State Estimation for Systems Measured by PMUs," *IEEE Trans. Smart Grid*, vol. 5, no. 4, pp. 1808–1814, 2014, doi: 10.1109/TSG.2014.2302213.

[52] L. Zhang, A. Bose, A. Jampala, V. Madani, and J. Giri, "Design, Testing, and Implementation of a Linear State Estimator in a Real Power System," *IEEE Trans. Smart Grid*, vol. 8, no. 4, pp. 1782–1789, 2017, doi: 10.1109/TSG.2015.2508283.

[53] C. Xu and A. Abur, "A fast and robust linear state estimator for very large scale interconnected power grids," *IEEE Trans. Smart Grid*, vol. 9, no. 5, pp. 4975–4982, Sep. 2018, doi: 10.1109/TSG.2017.2676348.

[54] J. Qi, K. Sun, and W. Kang, "Optimal PMU Placement for Power System Dynamic State Estimation by Using Empirical Observability Gramian," *IEEE Trans. Power Syst.*, vol. 30, no. 4, pp. 2041–2054, 2015, doi: 10.1109/TPWRS.2014.2356797.

[55] K. Sun, J. Qi, and W. Kang, "Power system observability and dynamic state estimation for stability monitoring using synchrophasor measurements," *Control*

Eng. Pract., vol. 53, pp. 160–172, 2016, doi: https://doi.org/10.1016/j.conengprac.2016.01.013.

[56] A. Rouhani and A. Abur, "Observability Analysis for Dynamic State Estimation of Synchronous Machines," *IEEE Trans. Power Syst.*, vol. 32, no. 4, pp. 3168–3175, 2017, doi: 10.1109/TPWRS.2016.2614879.

[57] S. Diop and M. Filess, "On nonlinear observability," in *First European Control Conference*, 1991, pp. 152–157.

[58] G. Wang, C.-C. Liu, N. Bhatt, E. Farantatos, and M. Patel, "Observability of nonlinear power system dynamics using synchrophasor data," *Int. Trans. Electr. Energy Syst.*, vol. 26, no. 5, pp. 952–967, May 2016, doi: https://doi.org/10.1002/etep.2116.

[59] S. Lall, J. E. Marsden, and S. Glavaški, "Empirical model reduction of controlled nonlinear systems," *IFAC Proc. Vol.*, vol. 32, no. 2, pp. 2598–2603, 1999, doi: https://doi.org/10.1016/S1474-6670(17)56442-3.

[60] S. Lall, J. E. Marsden, and S. Glavaški, "A subspace approach to balanced truncation for model reduction of nonlinear control systems," *Int. J. Robust Nonlinear Control*, vol. 12, no. 6, pp. 519–535, May 2002, doi: https://doi.org/10.1002/rnc.657.

[61] J. Qi, K. Sun, and W. Kang, "Adaptive Optimal PMU Placement Based on Empirical Observability Gramian**This work was supported in part by U.S. Department of Energy, Office of Electricity Delivery and Energy Reliability under contract DE-AC02-06CHff357, the CURENT engineering research center, and Naval Research Laboratory and Defense Advanced Research Projects Agency.," *IFAC-PapersOnLine*, vol. 49, no. 18, pp. 482–487, 2016, doi: https://doi.org/10.1016/j.ifacol.2016.10.211.

[62] M. S. Arulampalam, S. Maskell, N. Gordon, and T. Clapp, "A tutorial on particle filters for online nonlinear/non-Gaussian Bayesian tracking," *IEEE Trans. Signal Process.*, vol. 50, no. 2, pp. 174–188, 2002, doi: 10.1109/78.978374.

[63] Z. Huang, K. Schneider, and J. Nieplocha, "Feasibility studies of applying Kalman Filter techniques to power system dynamic state estimation," in *2007 International Power Engineering Conference (IPEC 2007)*, 2007, pp. 376–382.

[64] E. Farantatos, G. K. Stefopoulos, G. J. Cokkinides, and A. P. Meliopoulos, "PMU-based dynamic state estimation for electric power systems," in *2009 IEEE Power & Energy Society General Meeting*, 2009, pp. 1–8, doi: 10.1109/PES.2009.5275407.

[65] S. Meliopoulos, G. Cokkinides, R. Huang, E. Farantatos, S. Choi, and Y. Lee, "Wide area dynamic monitoring and stability controls," in *2010 IREP Symposium Bulk Power System Dynamics and Control - VIII (IREP)*, 2010, pp. 1–8, doi: 10.1109/IREP.2010.5563253.

[66] L. Fan and Y. Wehbe, "Extended Kalman filtering based real-time dynamic state and parameter estimation using PMU data," *Electr. Power Syst. Res.*, vol. 103, pp. 168–177, 2013, doi: https://doi.org/10.1016/j.epsr.2013.05.016.

[67] E. Ghahremani and I. Kamwa, "Dynamic State Estimation in Power System by Applying the Extended Kalman Filter With Unknown Inputs to Phasor Measurements," *IEEE Trans. Power Syst.*, vol. 26, no. 4, pp. 2556–2566, 2011, doi: 10.1109/TPWRS.2011.2145396.

[68] E. Ghahremani and I. Kamwa, "Local and Wide-Area PMU-Based Decentralized Dynamic State Estimation in Multi-Machine Power Systems," *IEEE Trans. Power Syst.*, vol. 31, no. 1, pp. 547–562, 2016, doi: 10.1109/TPWRS.2015.2400633.

[69] S. J. Julier and J. K. Uhlmann, "Unscented filtering and nonlinear estimation," *Proc. IEEE*, vol. 92, no. 3, pp. 401–422, 2004, doi: 10.1109/JPROC.2003.823141.

[70] G. Evensen, "The Ensemble Kalman Filter: theoretical formulation and practical implementation," *Ocean Dyn.*, vol. 53, no. 4, pp. 343–367, 2003, doi: 10.1007/s10236-003-0036-9.

[71] E. Ghahremani and I. Kamwa, "Online State Estimation of a Synchronous Generator Using Unscented Kalman Filter From Phasor Measurements Units," *IEEE Trans. Energy Convers.*, vol. 26, no. 4, pp. 1099–1108, 2011, doi: 10.1109/TEC.2011.2168225.

[72] S. Wang, W. Gao, and A. P. S. Meliopoulos, "An alternative method for power system dynamic state estimation based on unscented transform," *IEEE Trans. Power Syst.*, vol. 27, no. 2, pp. 942–950, May 2012, doi: 10.1109/TPWRS.2011.2175255.

[73] J. Qi, K. Sun, J. Wang, and H. Liu, "Dynamic State Estimation for Multi-Machine Power System by Unscented Kalman Filter With Enhanced Numerical Stability," *IEEE Trans. Smart Grid*, vol. 9, no. 2, pp. 1184–1196, 2018, doi: 10.1109/TSG.2016.2580584.

[74] A. K. Singh and B. C. Pal, "Decentralized Dynamic State Estimation in Power Systems Using Unscented Transformation," *IEEE Trans. Power Syst.*, vol. 29, no. 2, pp. 794–804, 2014, doi: 10.1109/TPWRS.2013.2281323.

[75] G. Anagnostou and B. C. Pal, "Derivative-Free Kalman Filtering Based Approaches to Dynamic State Estimation for Power Systems With Unknown Inputs," *IEEE Trans. Power Syst.*, vol. 33, no. 1, pp. 116–130, 2018, doi: 10.1109/TPWRS.2017.2663107.

[76] A. K. Singh and B. C. Pal, "Decentralized Robust Dynamic State Estimation in Power Systems Using Instrument Transformers," *IEEE Trans. Signal Process.*, vol. 66, no. 6, pp. 1541–1550, 2018, doi: 10.1109/TSP.2017.2788424.

[77] J. Zhao, "Power System Dynamic State Estimation Considering Measurement Correlations," *IEEE Trans. Energy Convers.*, vol. 32, no. 4, pp. 1630–1632, 2017, doi: 10.1109/TEC.2017.2742405.

[78] Y. Li, Z. Huang, N. Zhou, B. Lee, R. Diao, and P. Du, "Application of ensemble Kalman filter in power system state tracking and sensitivity analysis," in *PES T&D 2012*, 2012, pp. 1–8, doi: 10.1109/TDC.2012.6281499.

[79] W. S. Rosenthal, A. M. Tartakovsky, and Z. Huang, "Ensemble Kalman Filter for Dynamic State Estimation of Power Grids Stochastically Driven by Time-Correlated Mechanical Input Power," *IEEE Trans. Power Syst.*, vol. 33, no. 4, pp. 3701–3710, 2018, doi: 10.1109/TPWRS.2017.2764492.

[80] B. Uzunoğlu and M. A. Ülker, "Maximum Likelihood Ensemble Filter State Estimation for Power Systems," *IEEE Trans. Instrum. Meas.*, vol. 67, no. 9, pp. 2097–2106, 2018, doi: 10.1109/TIM.2018.2814066.

[81] N. Zhou, D. Meng, and S. Lu, "Estimation of the Dynamic States of Synchronous Machines Using an Extended Particle Filter," *IEEE Trans. Power Syst.*, vol. 28, no. 4, pp. 4152–4161, 2013, doi: 10.1109/TPWRS.2013.2262236.

[82] K. Emami, T. Fernando, H. H. Iu, H. Trinh, and K. P. Wong, "Particle Filter Approach to Dynamic State Estimation of Generators in Power Systems," *IEEE Trans. Power Syst.*, vol. 30, no. 5, pp. 2665–2675, 2015, doi: 10.1109/TPWRS.2014.2366196.

[83] Y. Cui and R. Kavasseri, "A particle filter for dynamic state estimation in multi-machine systems with detailed models," in *2016 IEEE Power and Energy Society*

General Meeting (PESGM), 2016, p. 1, doi: 10.1109/PESGM.2016.7741845.

[84] S. Wang, J. Zhao, Z. Huang, and R. Diao, "Assessing Gaussian Assumption of PMU Measurement Error Using Field Data," *IEEE Trans. Power Deliv.*, vol. 33, no. 6, pp. 3233–3236, 2018, doi: 10.1109/TPWRD.2017.2762927.

[85] A. F. Taha, J. Qi, J. Wang, and J. H. Panchal, "Risk Mitigation for Dynamic State Estimation Against Cyber Attacks and Unknown Inputs," *IEEE Trans. Smart Grid*, vol. 9, no. 2, pp. 886–899, 2018, doi: 10.1109/TSG.2016.2570546.

[86] A. Rouhani and A. Abur, "Linear Phasor Estimator Assisted Dynamic State Estimation," *IEEE Trans. Smart Grid*, vol. 9, no. 1, pp. 211–219, 2018, doi: 10.1109/TSG.2016.2548244.

[87] M. Netto, J. Zhao, and L. Mili, "A robust extended Kalman filter for power system dynamic state estimation using PMU measurements," in *IEEE Power and Energy Society General Meeting*, Nov. 2016, vol. 2016-November, doi: 10.1109/PESGM.2016.7741374.

[88] J. Zhao, M. Netto, and L. Mili, "A Robust Iterated Extended Kalman Filter for Power System Dynamic State Estimation," *IEEE Trans. Power Syst.*, vol. 32, no. 4, pp. 3205–3216, 2017, doi: 10.1109/TPWRS.2016.2628344.

[89] J. Zhao and L. Mili, "Robust Unscented Kalman Filter for Power System Dynamic State Estimation With Unknown Noise Statistics," *IEEE Trans. Smart Grid*, vol. 10, no. 2, pp. 1215–1224, 2019, doi: 10.1109/TSG.2017.2761452.

[90] J. Zhao, "Dynamic State Estimation With Model Uncertainties Using H-infinity Extended Kalman Filter," *IEEE Trans. Power Syst.*, vol. 33, no. 1, pp. 1099–1100, Mar. 2017, doi: 10.1109/tpwrs.2017.2688131.

[91] J. Zhao and L. Mili, "A Decentralized H-Infinity Unscented Kalman Filter for Dynamic State Estimation Against Uncertainties," *IEEE Trans. Smart Grid*, vol. 10, no. 5, pp. 4870–4880, 2019, doi: 10.1109/TSG.2018.2870327.

[92] Simon Haykin, *Kalman Filtering and Neural Networks*. Wiley, 2004.

[93] M. A. M. Ariff, B. C. Pal, and A. K. Singh, "Estimating Dynamic Model Parameters for Adaptive Protection and Control in Power System," *IEEE Trans. Power Syst.*, vol. 30, no. 2, pp. 829–839, 2015, doi: 10.1109/TPWRS.2014.2331317.

[94] G. Valverde, E. Kyriakides, G. T. Heydt, and V. Terzija, "Nonlinear Estimation of Synchronous Machine Parameters Using Operating Data," *IEEE Trans. Energy Convers.*, vol. 26, no. 3, pp. 831–839, 2011, doi: 10.1109/TEC.2011.2141136.

[95] M. Huang, W. Li, and W. Yan, "Estimating parameters of synchronous generators using square-root unscented Kalman filter," *Electr. Power Syst. Res.*, vol. 80, no. 9, pp. 1137–1144, Sep. 2010, doi: 10.1016/j.epsr.2010.03.007.

[96] A. Rouhani and A. Abur, "Constrained Iterated Unscented Kalman Filter for Dynamic State and Parameter Estimation," *IEEE Trans. Power Syst.*, vol. 33, no. 3, pp. 2404–2414, May 2018, doi: 10.1109/TPWRS.2017.2764005.

[97] A. Rouhani and A. Abur, "Real-Time Dynamic Parameter Estimation for an Exponential Dynamic Load Model," *IEEE Trans. Smart Grid*, vol. 7, no. 3, pp. 1530–1536, May 2016, doi: 10.1109/TSG.2015.2449904.

[98] P. Regulski and V. Terzija, "Estimation of Frequency and Fundamental Power Components Using an Unscented Kalman Filter," *IEEE Trans. Instrum. Meas.*, vol. 61, no. 4, pp. 952–962, 2012, doi: 10.1109/TIM.2011.2179342.

[99] Z. Huang, P. Du, D. Kosterev, and B. Yang, "Application of extended Kalman filter techniques for dynamic model parameter calibration," in *2009 IEEE Power & Energy Society General Meeting*, 2009, pp. 1–8, doi:

10.1109/PES.2009.5275423.

[100] R. Huang *et al.*, "Calibrating Parameters of Power System Stability Models Using Advanced Ensemble Kalman Filter," *IEEE Trans. Power Syst.*, vol. 33, no. 3, pp. 2895–2905, May 2018, doi: 10.1109/TPWRS.2017.2760163.

[101] K. P. Schneider, Z. Huang, B. Yang, M. Hauer, and Y. Nieplocha, "Dynamic state estimation utilizing high performance computing methods," in *2009 IEEE/PES Power Systems Conference and Exposition*, 2009, pp. 1–6, doi: 10.1109/PSCE.2009.4839961.

[102] A. Paul, I. Kamwa, and G. Joos, "Centralized dynamic state estimation using a federation of extended kalman filters with intermittent PMU data from generator terminals," *IEEE Trans. Power Syst.*, vol. 33, no. 6, pp. 6109–6119, Nov. 2018, doi: 10.1109/TPWRS.2018.2834365.

[103] I. Kamwa, B. Baraboi, and R. Wamkeue, "Sensorless ANN-Based Speed Estimation of Synchronous Generators: Improved Performance through Physically Motivated Pre-filters," in *The 2006 IEEE International Joint Conference on Neural Network Proceedings*, 2006, pp. 1710–1718, doi: 10.1109/IJCNN.2006.246641.

[104] A. Del Angel, P. Geurts, D. Ernst, M. Glavic, and L. Wehenkel, "Estimation of rotor angles of synchronous machines using artificial neural networks and local PMU-based quantities," *Neurocomputing*, vol. 70, no. 16, pp. 2668–2678, 2007, doi: https://doi.org/10.1016/j.neucom.2006.12.017.

[105] M. Netto and L. Mili, "A Robust Data-Driven Koopman Kalman Filter for Power Systems Dynamic State Estimation," *IEEE Trans. Power Syst.*, vol. 33, no. 6, pp. 7228–7237, 2018, doi: 10.1109/TPWRS.2018.2846744.

[106] A. Abur, "Dynamic-State Estimation," in *Smart Grid Handbook*, Chichester, UK: John Wiley & Sons, Ltd, 2016, pp. 1–14.

[107] B. Kroposki *et al.*, "Achieving a 100% Renewable Grid: Operating Electric Power Systems with Extremely High Levels of Variable Renewable Energy," *IEEE Power Energy Mag.*, vol. 15, no. 2, pp. 61–73, Mar. 2017, doi: 10.1109/MPE.2016.2637122.

[108] P. W. Sauer, M. A. Pai, and J. H. Chow, *Power System Dynamics and Stability: With Synchrophasor Measurement and Power System Toolbox*. Wiley-IEEE Press, 2017.

[109] J. Zhao *et al.*, "Power System Dynamic State Estimation: Motivations, Definitions, Methodologies, and Future Work," *IEEE Trans. Power Syst.*, vol. 34, no. 4, 2019, doi: 10.1109/TPWRS.2019.2894769.

[110] W. L. Miller and J. B. Lewis, "Dynamic State Estimation in Power Systems," *IEEE Transactions on Automatic Control*, vol. 16, no. 6. pp. 841–846, 1971, doi: 10.1109/TAC.1971.1099844.

[111] E. Y. Song, K. B. Lee, G. J. Fitzpatrick, and Y. Zhang, "Interoperability test for IEC 61850-9-2 standard-based merging units," Oct. 2017, doi: 10.1109/ISGT.2017.8086084.

[112] J. Zhao and L. Mili, "A Theoretical Framework of Robust H-Infinity Unscented Kalman Filter and Its Application to Power System Dynamic State Estimation," *IEEE Trans. Signal Process.*, vol. 67, no. 10, pp. 2734–2746, May 2019, doi: 10.1109/TSP.2019.2908910.

[113] L. Wang and K. Morison, "Implementation of online security assessment," *IEEE Power and Energy Magazine*, vol. 4, no. 5. pp. 46–59, 2006, doi: 10.1109/MPAE.2006.1687817.

[114] Z. Huang, R. Diao, S. Jin, and Y. Chen, "Predictive dynamic security assessment

through advanced computing," in *IEEE Power and Energy Society General Meeting*, Oct. 2014, vol. 2014-October, no. October, doi: 10.1109/PESGM.2014.6938850.

[115] "IEEE Recommended Practice for Excitation System Models for Power System Stability Studies," *IEEE Std 421.5-2016 (Revision IEEE Std 421.5-2005*, pp. 1–207, 2016.

[116] H. Su, R. Mutukutti, and D. Apps, "Impacts of variable quadrature reactance on power system stabilizer performance," 2013, doi: 10.1109/PESMG.2013.6672446.

[117] A. K. Singh and B. C. Pal, "Rate of Change of Frequency Estimation for Power Systems Using Interpolated DFT and Kalman Filter," *IEEE Trans. Power Syst.*, vol. 34, no. 4, pp. 2509–2517, Jul. 2019, doi: 10.1109/TPWRS.2018.2881151.

[118] N. Zhou, S. Wang, J. Zhao, and Z. Huang, "Application of Detectability Analysis for Power System Dynamic State Estimation," *IEEE Trans. Power Syst.*, vol. 35, no. 4, pp. 3274–3277, Jul. 2020, doi: 10.1109/TPWRS.2020.2987472.

[119] J. Zhang, G. Welch, G. Bishop, and Z. Huang, "Optimal PMU placement evaluation for power system dynamic state estimation," 2010, doi: 10.1109/ISGTEUROPE.2010.5639006.

[120] J. Zhao, L. Mili, and R. C. Pires, "Statistical and numerical robust state estimator for heavily loaded power systems," *IEEE Trans. Power Syst.*, vol. 33, no. 6, pp. 6904–6914, Nov. 2018, doi: 10.1109/TPWRS.2018.2849325.

[121] J. Chen, Y. Liao, and B. Gou, "Study of WLS state estimation convergence characteristics under topology errors," 2013, doi: 10.1109/SECON.2013.6567383.

[122] M. Boutayeb, H. Rafaralahy, and M. Darouach, "Convergence analysis of the extended Kalman filter used as an observer for nonlinear deterministic discrete-time systems," *IEEE Trans. Automat. Contr.*, vol. 42, no. 4, pp. 581–586, 1997, doi: 10.1109/9.566674.

[123] A. Daid, E. Busvelle, and M. Aidene, "On the convergence of the unscented Kalman filter," *Eur. J. Control*, vol. 57, pp. 125–134, Jan. 2021, doi: 10.1016/j.ejcon.2020.05.003.

[124] J. Mandel, L. Cobb, and J. D. Beezley, "On the convergence of the ensemble Kalman filter," *Appl. Math.*, vol. 56, no. 6, pp. 533–541, Dec. 2011, doi: 10.1007/s10492-011-0031-2.

[125] S. Wei, M. Yang, J. Qi, J. Wang, S. Ma, and X. Han, "Model-Free MLE Estimation for Online Rotor Angle Stability Assessment with PMU Data," *IEEE Trans. Power Syst.*, vol. 33, no. 3, pp. 2463–2476, May 2018, doi: 10.1109/TPWRS.2017.2761598.

[126] S. Akhlaghi, S. Raheem, and N. Zhou, "Model Validation Lessons Learned through Implementing NERC MOD-033-1," in *IEEE Power and Energy Society General Meeting*, Aug. 2020, vol. 2020-August, doi: 10.1109/PESGM41954.2020.9281444.

[127] M. A. Gonzalez-Cagigal, J. A. Rosendo-Macias, and A. Gomez-Exposito, "Parameter estimation of fully regulated synchronous generators using Unscented Kalman Filters," *Electr. Power Syst. Res.*, vol. 168, pp. 210–217, Mar. 2019, doi: 10.1016/j.epsr.2018.11.018.

[128] P. Bhui, N. Senroy, A. K. Singh, and B. C. Pal, "Estimation of Inherent Governor Dead-Band and Regulation Using Unscented Kalman Filter," *IEEE Trans. Power Syst.*, vol. 33, no. 4, pp. 3546–3558, Jul. 2018, doi: 10.1109/TPWRS.2017.2765692.

[129] Y. Zhang, E. Muljadi, D. Kosterev, and M. Singh, "Wind Power Plant Model

Validation Using Synchrophasor Measurements at the Point of Interconnection," *IEEE Trans. Sustain. Energy*, vol. 6, no. 3, pp. 984–992, Jul. 2015, doi: 10.1109/TSTE.2014.2343794.

[130] R. Fan, Z. Huang, S. Wang, R. Diao, and D. Meng, "Dynamic state estimation and parameter calibration of a DFIG using the ensemble Kalman filter," in *IEEE Power and Energy Society General Meeting*, Sep. 2015, vol. 2015-September, doi: 10.1109/PESGM.2015.7285990.

[131] S. K. Joo, C. C. Liu, L. E. Jones, and J. W. Choe, "Coherency and aggregation techniques incorporating rotor and voltage dynamics," *IEEE Trans. Power Syst.*, vol. 19, no. 2, pp. 1068–1075, May 2004, doi: 10.1109/TPWRS.2004.825825.

[132] M. R. Aghamohammadi and S. M. Tabandeh, "A new approach for online coherency identification in power systems based on correlation characteristics of generators rotor oscillations," *Int. J. Electr. Power Energy Syst.*, vol. 83, pp. 470–484, Dec. 2016, doi: 10.1016/j.ijepes.2016.04.019.

[133] A. Chakrabortty, J. H. Chow, and A. Salazar, "A measurement-based framework for dynamic equivalencing of large power systems using wide-area phasor measurements," *IEEE Trans. Smart Grid*, vol. 2, no. 1, pp. 68–81, 2011, doi: 10.1109/TSG.2010.2093586.

[134] S. Maslennikov *et al.*, "A test cases library for methods locating the sources of sustained oscillations," in *IEEE Power and Energy Society General Meeting*, Nov. 2016, vol. 2016-November, doi: 10.1109/PESGM.2016.7741772.

[135] F. Milano and Á. Ortega, "Frequency Divider," *IEEE Trans. Power Syst.*, vol. 32, no. 2, pp. 1493–1501, Mar. 2017, doi: 10.1109/TPWRS.2016.2569563.

[136] J. Zhao, L. Mili, and A. Gómez-Expósito, "Constrained Robust Unscented Kalman Filter for Generalized Dynamic State Estimation," *IEEE Trans. Power Syst.*, vol. 34, no. 5, pp. 3637–3646, Sep. 2019, doi: 10.1109/TPWRS.2019.2909000.

[137] Y. Chakhchoukh, H. Lei, and B. K. Johnson, "Diagnosis of Outliers and Cyber Attacks in Dynamic PMU-Based Power State Estimation," *IEEE Trans. Power Syst.*, vol. 35, no. 2, pp. 1188–1197, Mar. 2020, doi: 10.1109/TPWRS.2019.2939192.

[138] Q. Yang, T. Bi, and J. Wu, "WAMS implementation in China and the challenges for bulk power system protection," 2007, doi: 10.1109/PES.2007.385835.

[139] G. Anagnostou and B. C. Pal, "Impact of overexcitation limiters on the power system stability margin under stressed conditions," *IEEE Trans. Power Syst.*, vol. 31, no. 3, pp. 2327–2337, May 2016, doi: 10.1109/TPWRS.2015.2440559.

[140] J. Zhao *et al.*, "Correlation-Aided Robust Decentralized Dynamic State Estimation of Power Systems with Unknown Control Inputs," *IEEE Trans. Power Syst.*, vol. 35, no. 3, pp. 2443–2451, May 2020, doi: 10.1109/TPWRS.2019.2953256.

[141] P. Marchi, P. G. Estevez, F. Messina, and C. G. Galarza, "Loss of Excitation Detection in Synchronous Generators Based on Dynamic State Estimation," *IEEE Trans. Energy Convers.*, vol. 35, no. 3, pp. 1606–1616, Sep. 2020, doi: 10.1109/TEC.2020.2985529.

[142] M. Diaz-Aguiló and F. León, "Adaptive soil model for real-time thermal rating of underground power cables," *IET Sci. Meas. Technol.*, vol. 9, no. 6, pp. 654–660, Sep. 2015, doi: 10.1049/iet-smt.2014.0269.

[143] A. Gomez-Exposito *et al.*, "City-Friendly Smart Network Technologies and Infrastructures: The Spanish Experience," *Proceedings of the IEEE*, vol. 106, no. 4. Institute of Electrical and Electronics Engineers Inc., pp. 626–660, Apr. 01, 2018, doi: 10.1109/JPROC.2018.2793461.

[144] I. L. Ortega Rivera, V. Vittal, G. T. Heydt, C. R. Fuerte-Esquivel, and C. Angeles-Camacho, "A dynamic state estimator based control for power system damping," *IEEE Trans. Power Syst.*, vol. 33, no. 6, pp. 6839–6848, Nov. 2018, doi: 10.1109/TPWRS.2018.2825301.

[145] A. Paul, I. Kamwa, and G. Joos, "PMU Signals Responses-Based RAS for Instability Mitigation through On-The Fly Identification and Shedding of the Run-Away Generators," *IEEE Trans. Power Syst.*, vol. 35, no. 3, pp. 1707–1717, May 2020, doi: 10.1109/TPWRS.2019.2926243.

[146] M. Glavic and T. Van Cutsem, "Wide-area detection of voltage instability from synchronized phasor measurements. Part I: Principle," *IEEE Trans. Power Syst.*, vol. 24, no. 3, pp. 1408–1416, 2009, doi: 10.1109/TPWRS.2009.2023271.

[147] N. Hatziargyriou (Chair), "Stability definitions and characterization of dynamic behavior in systems with high penetration of power electronic interfaced technologies," IEEE Technical Report PES-TR77, 2020.

[148] S. Swain and B. Subudhi, "Grid synchronization of a PV system with power quality disturbances using unscented Kalman filtering," *IEEE Trans. Sustain. Energy*, vol. 10, no. 3, pp. 1240–1247, Jul. 2019, doi: 10.1109/TSTE.2018.2864822.

[149] S. Yu, K. Emami, T. Fernando, H. H. C. Iu, and K. P. Wong, "State Estimation of Doubly Fed Induction Generator Wind Turbine in Complex Power Systems," *IEEE Trans. Power Syst.*, vol. 31, no. 6, pp. 4935–4944, Nov. 2016, doi: 10.1109/TPWRS.2015.2507620.

[150] S. Yu, T. Fernando, H. H. C. Iu, and K. Emami, "Realization of State-Estimation-Based DFIG Wind Turbine Control Design in Hybrid Power Systems Using Stochastic Filtering Approaches," *IEEE Trans. Ind. Informatics*, vol. 12, no. 3, pp. 1084–1092, Jun. 2016, doi: 10.1109/TII.2016.2549940.

[151] S. S. Yu, J. Guo, T. K. Chau, T. Fernando, H. H. C. Iu, and H. Trinh, "An Unscented Particle Filtering Approach to Decentralized Dynamic State Estimation for DFIG Wind Turbines in Multi-Area Power Systems," *IEEE Trans. Power Syst.*, vol. 35, no. 4, pp. 2670–2682, Jul. 2020, doi: 10.1109/TPWRS.2020.2966443.

[152] G. Anagnostou, L. P. Kunjumuhammed, and B. C. Pal, "Dynamic State Estimation for Wind Turbine Models with Unknown Wind Velocity," *IEEE Trans. Power Syst.*, vol. 34, no. 5, pp. 3879–3890, Sep. 2019, doi: 10.1109/TPWRS.2019.2909160.

[153] M. A. Gonzalez-Cagigal, J. A. Rosendo-Macias, and A. Gomez-Exposito, "Parameter estimation of wind turbines with PMSM using cubature Kalman filters," IEEE Trans. Power Syst., vol. 35, no. 3, pp. 1796–1804, May 2020.

[154] "1,200 MW Fault Induced Solar Photovoltaic Resource Interruption Disturbance Report: Southern California 8/16/2016 Event," North American Electric Reliability Corporation (NERC) Technical Report, 2017.

[155] J. Zhao, et al., "Roles of dynamic state estimation in power system modeling, monitoring and operation," IEEE Trans. Power Syst., 2020.

[156] N. Hatziargyriou et al., "Definition and classification of power system stability revisited & extended," IEEE Trans. Power Syst., 2020.

[157] V. Telukunta, J. Pradhan, A. Agrawal, M. Singh and S. G. Srivani, "Protection challenges under bulk penetration of renewable energy resources in power systems: A review", CSEE Journal Power Energy Syst., vol. 3, no. 4, pp. 365-379, Dec. 2017.

[158] Protection System Misoperation Task Force, "Misoperations report", NERC Planning Committee, Atlanta, GA, USA, 2014.

[159] IEC Std 61850, “Communication Networks and Systems in Substations”, 2003.
[160] Z. Huang, H. Krishnaswami, G. Yuan, and R. Huang, “Ubiquitous power electronics in future power systems”, IEEE Electrification Magzine, September 2020.
[161] V. Venkatasubramanian, H. Schattler, and J. Zaborszky, “Fast time-varying phasor analysis in the balanced three-phase large electric power system," IEEE Trans. on Automatic Control, vol. 40, no. 11, pp. 1975-1982, Nov. 1995.
[162] S. R. Sanders, J. M. Noworolski, X. Z. Liu, G. C. Verghese, “Generalized averaging method for power conversion circuits,” IEEE Trans. on Power Elec., vol. 6, no. 3, pp. 251-259, April 1991.
[163] H. K. Khalil, Nonlinear Systems, 3rd ed., Prentice-Hall, 2002.
[164] M. Korda and I. Mezić, “Linear predictors for nonlinear dynamical systems: Koopman operator meets model predictive control,” Automatica, vol. 93, pp. 149–160, Jul. 2018.
[165] M. Nicolai, L. Lorenz-Meyer, A. Bobtsov, R. Ortega, N. Nikolaev, and J. Chiffer, “PMU-based decentralized mixed algebraic and dynamic state observation in multi-machine power systems”, IET Gener. Transm. Distrib., accepted.
[166] J. Qi, A.F. Taha, J. Wang, "Comparing Kalman filters and observers for power system dynamic state estimation with model uncertainty and malicious cyber-attacks," IEEE Access, vol. 6, pp. 77155-77168, 2018.
[167] S. Nugroho, A.F. Taha, J. Qi, "Robust dynamic state estimation of synchronous machines with asymptotic state estimation error performance guarantees," IEEE Trans. Power Syst., vol. 35, no. 3, pp. 1923-1935, 2020.
[168] S. Stefani, H. Savant, Design of Feedback Systems, Oxford University Press, New York, 2002
[169] J. A. de la O Serna, "Dynamic phasor estimates for power system oscillations," IEEE Trans. Instrumentation and Measurement, vol. 56, no. 5, pp. 1648-1657, Oct. 2007.
[170] A.F. Taha, M. Bazrafshan, S. A. Nugroho, N. Gatsis, J. Qi, “Robust control for renewable-integrated power networks considering input bound constraints and worst-case uncertainty measure," IEEE Trans. Contr. Network Syst., 2019
[171] A.M. Ersdal, L. Imsland, K. Uhlen, “Model predictive load frequency control," IEEE Trans. Power Syst., vol. 31, no. 1, pp. 777-785, Jan. 2016.
[172] W. Yao, L. Jiang, J. Wen, Q. H. Wu, S. Cheng, “Wide-area damping controller of FACTS devices for inter-area oscillations considering communication time delays," IEEE Trans. Power Syst., vol. 29, no. 1, pp. 318-329, Jan. 2014.
[173] M.A. Pai, P.W. Sauer, Power System Dynamics and Stability, Prentice Hall, New Jersey, USA, 1998.
[174] S. Liu, X. Li, D. Chen, “Wide-area-signals-based nonlinear excitation control in multi-machine power systems", IEEJ Trans. Elec. Electron. Eng., vol. 14, pp. 366-375, 2019.
[175] H. Liu, J. Su, J. Qi, N. Wang, C. Li, “Decentralized voltage and power control of multi-machine power systems with global asymptotic stability," IEEE Access, vol. 7, pp. 14273-14282, 2019.
[176] A. S. Mir, S. Bhasin, N. Senroy, “Decentralized nonlinear adaptive optimal control scheme for enhancement of power system stability,” IEEE Trans. Power. Syst, vol. 35, no. 2, pp. 1400-1410, 2020.
[177] H. Bevrani, Robust Power System Frequency Control. New York, NY, USA:

Springer, 2009.
[178] C. Nichita, D. Luca, B. Dakyo and E. Ceanga, “Large band simu-lation of the wind speed for real time wind turbine simulators,” IEEE Trans. Energy Convers., vol. 17, no. 4, pp. 523-529, Dec. 2002.
[179] A. S. Mir and N. Senroy, "Self-tuning neural predictive control scheme for ultra-battery to emulate a virtual synchronous machine in autonomous power systems," IEEE Trans. Neural Netw. Learn. Syst., vol. 31, no. 1, pp. 136-147, Jan. 2020.
[180] K. Emami, T. Fernando, H. H. Iu, B. D. Nener, K. P. Wong, “Application of unscented transform in frequency control of a complex power system using noisy PMU data” IEEE Trans. Ind. Informat., vol. 12, no. 2, pp. 853-863, 2016.
[181] H. Trinh, T. Fernando, H. H. C. Iu, K. P. Wong, “Quasi-decentralized functional observers for the LFC of interconnected power systems”, IEEE Trans. Power Syst., vol. 28, no. 3, pp. 3513-3514, 2013.
[182] H. Bevrani, P. R. Daneshmand, P. Babahajyani, Y. Mitani and T. Hiyama, “Intelligent LFC concerning high penetration of wind power: synthesis and real-time application,” IEEE Trans. Sustain. Energy, vol. 5, no. 2, pp. 655-662, April 2014.
[183] X. Yang, H. He and X. Zhong, “Adaptive dynamic programming for robust regulation and its application to power systems,” IEEE Trans. Ind. Electron., vol. 65, no. 7, pp. 5722-5732, July 2018.
[184] B. A. Alcaide-Moreno, C. R. Fuerte-Esquivel, M. Glavic, T. Van Cutsem, "Electric power network state tracking from multirate measurements," IEEE Trans. Instrumentation and Measurement, vol. 67, no. 1, pp. 33-44, 2018.
[185] G. K. Morison, B. Gao, P. Kundur, "Voltage stability analysis using static and dynamic approaches," IEEE Trans. Power Syst., vol. 8, no. 3, pp. 1159-1171, 1993.
[186] M. Glavic, T. Van Cutsem, “Some reflections on model predictive control of transmission voltages,” 38th North American Power Symposium, Carbondale, IL, USA, 2006.
[187] B. Otomega, M. Glavic, T. Van Cutsem, "A two-level emergency control scheme against power system voltage instability," Control Engineering Practice, vol. 30, pp. 93-104, 2014.
[188] S. Yu, T. Fernando, K. Emami and H. H.-C. Iu, “Dynamic state estimation-based control strategy for DFIG wind turbine connected to complex power systems," IEEE Trans. Power Syst., vol. 32, no. 2, pp. 1272-1281, 2016.
[189] A. S. Mir and N. Senroy, “DFIG damping controller design using robust CKF based adaptive dynamic programming,” IEEE Trans. Sustain. Energy, vol. 11, no. 2, pp. 839-850, Apr. 2020.
[190] S. Yu, G. Zhang, T. Fernando and H. H.-C. Iu, “A DSE-based SMC method of sensorless DFIG wind turbines connected to power grids for energy extraction and power quality enhancement," IEEE Access, no. 6, pp. 76596-76605, 2018.
[191] S. Yu, L. Zhang, H. H. Lu, T. Fernando, K. P. Wong, “A DSE-based power system frequency restoration strategy for PV-integrated power systems considering solar irradiance variations," IEEE Trans. Industrial Informatics, vol. 13, no. 5, pp. 2511-2518, 2017.
[192] “Wind Energy Systems Subsynchronous Oscillations: Events and Modeling," IEEE PES Wind SSO Taskforce, Technical Report, PES-TR80, 2020.
[193] A. P. Meliopoulos, V. Vittal, M. Saeedifard, and R. Data, "Stability, protection and control of systems with high penetration of converter interfaced generation", PSERC Publication 16-03, March 2016.

[194] Y. Liu, A. P. Meliopoulos, L. Sun, and S. Choi, “Protection and control of microgrids using dynamic state estimation”, Protection Control Modern Power Syst., vol. 3, no. 31, pp. 1-13, Oct. 2018.

[195] R. Grondin A. Heniche, et al., "Loss of synchronism detection a strategic function for power system protection", Proc. 2006 CIGRE Session 41 B5-205.

[196] North American Electric Reliability Corporation, “State of Reliability 2016”, May 2016.

[197] Y. Liu, A. P. Meliopoulos, L. Sun and R. Fan, “Dynamic state estimation based protection on mutually coupled transmission lines," CSEE Journal Power Energy Syst., vol. 2, no. 4, pp. 6-14, Dec. 2016.

[198] R. Fan, Y. Liu, A. P. Meliopoulos, L. Sun, Z. Tan and R. Huang, “Comparison of transformer legacy protective functions and a dynamic state estimation-based approach”, Electric Power Syst. Research, 2020.

[199] V. Terzija, G. Preston, V. Stanojević, N. I. Elkalashy, and M. Popov, "Synchronized measurements-based algorithm for short transmission line fault analysis", IEEE Trans Smart Grid, vol. 6, no. 17, pp. 2639-2648, Nov. 2015.

[200] Y. Liu, A. P. Meliopoulos, Z. Tan, L. Sun and R. Fan, “Dynamic state estimation-based fault locating on transmission lines”, IET Gener. Transm. Distrib., vol. 11, no. 17, pp. 4184-4192, Nov. 2017.

[201] B. Wang, Y. Liu, D. Lu, K. Yue and R. Fan, “Transmission line fault location in MMC-HVDC grids based on dynamic state estimation and gradient descent”, IEEE Trans. Power Del., 2020.

[202] M. B. Djuric, Z. M. Radojevic, and V. V. Terzija. “Time domain solution of fault distance estimation and arcing faults detection on overhead lines,” IEEE Trans. Power Del., vol 14, no. 1, pp. 60-67, Feb. 1999.

[203] H. F. Albinali and A. P. Meliopoulos, “Resilient protection system through centralized substation protection," IEEE Trans. Power Del., vol. 33, no. 3, pp. 1418-1427, June 2018.

[204] A. P. Deshpande, S. C. Patwardhan, S. S. Narasimhan, “Intelligent state estimation for fault tolerant nonlinear predictive control,” Journal of Process Control, vol. 19, pp. 187-204, 2009.

[205] T. K. Chau, S.S. Yu, T. Fernando, H. H.C. Iu, Michael Small, and Mark Reynolds. "An adaptive-phasor approach to PMU measurement rectification for LFOD enhancement." IEEE Trans. on Power Syst. 34, no. 5 (2019): 3941-3950.

[206] S.S. Yu, T. K. Chau, T. Fernando, and H. H.C. Iu. "An enhanced adaptive phasor power oscillation damping approach with latency compensation for modern power systems." IEEE Trans. on Power Syst. 33, no. 4 (2017): 4285-4296.

[207] P. Kundur, N. J. Balu, and M. G. Lauby, Power System Stability Control, vol. 7. New York, NY, USA: McGraw-Hill, 1994.

[208] N. R. Chaudhuri, Ray, S., Majumder, R., & Chaudhuri, B. (2009). A new approach to continuous latency compensation with adaptive phasor power oscillation damping controller (POD). IEEE Trans. on Power Syst., 25(2), 939-946.

9. APPENDIX

IEEE PES Webinar Session on DSE Questions and Answers

Session 1- Dynamic State and Parameter Estimation for Power System Monitoring, Modeling and Operation

1. You showed that the dynamic state estimation can estimate voltage and phase angle along with the angle and speed of a generator. If that is the case can we say that if we have a dynamic state estimator in a power system, we don't need a static estimator?

Answer: dynamic state estimation (DSE) allows us to estimate the system's true dynamic variables and with them, the system algebraic variables can be calculated as well in theory. However, there are currently practical aspects in terms of measurement redundancy, dynamic observability, and computational performance that can limit DSE applications. We believe these issues will be resolved given time. But in the interim, our vision is that DSE and static state estimation (SSE) will co-exist in the control center, providing complementary information and supporting different applications. For example, if there are large disturbances, only the results of the dynamic state estimator should be trusted.

2. Do you have the information on where those PMUs are installed? The reason I am asking how to estimate frequency response at the balancing authority level?

Answer: For PMU locations, there has been extensive research on optimal placement as well as practical guidelines such as that issued by NERC for PMU placement. Note that according to the NERC PMU placement guideline, the generator is the preferred location to have PMUs. Mathematically, the key is to have adequate observability. DSE can be implemented in a centralized or decentralized manner. Decentralized implementation is performed for each generator. If a generator terminal bus is not equipped with a PMU but the local system is fully observable by PMUs, a PMU-based linear state estimator for that local system should be performed first. Then, the estimated measurements at the generator terminal buses can be obtained and the decentralized DSE is executed. For centralized implementation, the whole system needs to be observable with a minimum number of PMUs. For balancing authority level applications, the local decentralized DSE results should be sent to the control center while the centralized dynamic state estimation naturally provides that information. As rotor speeds are part of DSE results, they naturally provide frequency response estimation.

3. Does PMU require calibration? If yes - how frequently?

Answer: Yes. One advantage of DSE is that the data quality issues of PMUs can be detected. If the continuous data quality issue occurs, it indicates the instrumental errors of PMUs and calibration need to be done. It is worth noting that PMU calibration requirements are “almost” the same as those of “protection devices”. In fact, some PMU vendors combine these two functions in the same hardware box. This means that a class

M PMU requires a careful calibration of the A2D inputs the guarantee that the theoretical accuracy (observed during PMU certification) is met in the field.

4. As in the slides, the time scale of DSE is around 1/30 (s) ~ half cycle of 60Hz. Could the current communication infrastructure and processing time handle this fast? Could you give some comments about the role of communication infrastructure in DSE?

Answer: Yes, and as a matter of fact, many PMU networks are going beyond the speed of 30 samples per second (1/30 second). We did field measurement at Hydro-Quebec to confirm this. With dedicated optical fiber-based communication, the delay is less than 8ms and the PMU reporting can be sustained. In our opinion, modern PMUs can achieve 240 Hz reporting rate over private networks. For public networks, you may check Verizon network performance here: https://www.verizon.com/about/our-company/network-performance.

5. Could you provide some comments on load dynamic models? As my knowledge, the dynamic models of power lines and generation units are quite clear but not the loads since they comprise from many components and may change anytime.

Answer: Mathematically, dynamic load models are also a set of differential-algebraic equations and can be handled using the same DSE algorithms as generator models, provided that appropriate measurements are available. But it is worth pointing out that since load models are always an aggregate "synthetic" or "equivalent" model mapped to complex, actually distributed loads, they contain higher uncertainties than generator models, and the dynamic states of load models have little or no physical meaning in contrast to the internal states of synchronous generators. According to the answer to Question 2, if decentralized DSE is implemented, the dynamic load models have no effects since DSE is executed for the local generators only if the dynamic states in load models are not of interest. For centralized DSE, the dynamic load models can be integrated into the overall DSE formulation. Effective approaches in handling the uncertainties in dynamic load models need to be further developed.

6. What are the capabilities of DSE overs traditional SE to predict and detect bad data injected by cyber-attack that use false data injection?

Answer: One of the advantages of DSE over the traditional static SE is that we have the predicted state information from the dynamic model. This can be used to help identify the consistency between model outputs and the received measurements, i.e., benefiting the detection of false data injection attacks. But one needs to be careful in distinguishing between physical power system failures and cyberattacks in PMU data channels. Research along this line has been reported in the literature.

7. Dynamic State Estimation is mostly related to the advent of PMUs in the power grid. What is the future for the SCADA measurements in this context? Will they be neglected, or will they aid in somehow the dynamic estimators (and vice-versa)?

Answer: Please refer to the answer to Question 1. In summary, DSE and SSE will co-exist for a long period. But with a lower cost of PMU leading to PMU everywhere, we

can imagine that even SSE can be based on PMU only, without SCADA. DSE and SSE will then use the same information, even if not for the same purpose.

8. For system monitoring with DSE, how much more volume of information does system operators need to process in addition to those in today's control center?

Answer: This depends on the applications. Please refer to the reference listed below to see the requirements for processing DSE information for different applications. It is worth noting that for decentralized applications, the system operators may not need to process them as DSE is done locally with very fast speed. For centralized applications, as the system dynamics are involving very fast, advanced signal processing and machine learning techniques may be needed.

J. B. Zhao, M. Netto, Z. Huang, S. Yu, A. Exposito, S. Wang, I. Kamwa, S. Akhlaghi, L. Mili, V. Terzija, A. P. Sakis Meliopoulos, B. Pal, A. K. Singh, A. Abur, T. Bi, A. Rouhani, "Roles of Dynamic State Estimation in Power System Modeling, Monitoring and Operation," IEEE Trans. Power Systems, 2021.

9. We are working on an application to directly assess inter-area power oscillations in the Mexican interconnected power system through a state estimator. We estimate the nodal frequencies during the estimation process, from which we detect inter-area power oscillations and which power plants are involved in the phenomenon. Do you know if there are works on this topic? Is it possible to develop instability indexes to detect this kind of phenomenon from the DSE directly?

Answer: Thanks for your discussions. We are not sure if you derive frequency oscillation patterns from SSE results. It is hard to justify using conventional SSE for monitoring inter-area oscillations. SCADA measurements for SSE estimates of bus phase angle are sampled every 2-4 seconds: https://www.naspi.org/sites/default/files/reference_documents/NASPI_CRSTT_VideoSummary.pdf . Such sampling rates are not adequate to capture the oscillation dynamics, and it is unrealistic to study inter-area oscillations without PMU data at a sub-second sampling rate. Regarding the last question, see Dr. Innocent's presentation and references. DSE is a nice framework for generating a wide range of contingency severity indices that can be used for detecting transient or inter-area instability using machine learning or multi-variable fuzzy decision rules. If it is only for inter-area oscillation detection, there has also been significant work reported in the literature for estimating oscillation modes (i.e. eigenvalues) directly from PMU data, without SSE or DSE.

10. Thanks for the presentation. I have a question about the real model. What kind of real model is used, the model from simulation software or the realistic operating system? Thanks

Answer: For practical applications, we are using the actual generator dynamic models as well as the field PMU measurements to test and validated the developed power plant model validation and calibration tools, the DSE, DSE-based protection, etc. For simulations, our model is the same used in PSS/E by control-room engineers to perform dynamic security assessments. We have the same simplifying assumptions and the same dynamic parameters. However, saturation is not represented in current implementations, which may be a point requiring further attention.

11. Prof. Exposito do you think multiarea methods could be extended for dynamic estimators in order to deal with such large scale?

Answer: Yes, indeed. In fact, it is advisable to resort to distributed (multi-area) implementations of DSE, considering that solving a whole large-scale system is a challenging computational problem. In this context, though, the "area" notion may be of a different nature than in multi-area static SE, where usually each area represents a TSO/ISO.

12. Can DSE be used to tune PSS?

Answer: DSE can be used for online detection of any need for PSS re-tuning. Tuning PSS is a well-established process that can be effectively performed without DSE. This has been done for years. However, by providing the “true” patterns of “rotor speed and angle”, the DSE allows a more accurate/reliable means for monitoring oscillation damping in the control room. Of course, if PSS dynamic model is embedded in the DSE equations, it is even possible to detect the failure in the PSS component from DSE results. But in general, using DSE for PSS tuning is an overkill solution.

Session 2- Dynamic State and Parameter Estimation for Power System Control and Protection

1. I have question as: " As mentioned the actual system states is rotor angles and speeds (of generators) not bus voltage phasors? Is this statement remains valid in weak grids or in the distribution network or microgrids where the load changes could be more significant than stiff girds as transmission systems? "

Answer: Yes. For the transmission systems fed exclusively by synchronous generators, the rotor angle and speeds of generators are the true systems dynamic state variables. From the dynamic system theory, true dynamic states are those state variables in the differential terms of the system equations. These state variables could include governor/voltage control variables, inverter control variables, load dynamic states, etc. in addition to rotor angle and speed, depending on the system conditions and the equations.

2. Has DSE been implemented in any actual power system anywhere in the world? What are the challenges to implement in practical application?

Answer: Yes. For offline applications, such as power plant model validation and calibration, the developed DSE tools by PNNL have been integrated with several commercial software, i.e., PSSE/PSLF, etc. For online applications, Hydro-Quebec team has tested the technologies in their lab and Canada. DSE-based tools have also been tested in China. The DSE-based protection technologies by Sakis’s team have been successfully tested at NYPA, Southern Company, etc. Though these are good examples, there is still further work to be done for practical implementations and applications.

3. Professor Kamwa, how do you make sure, in data for training the machine learning you cover all the operating states?

Answer: This is an interesting question which points to one of the major pitfalls of machine learning approaches. There are techniques for sampling the space of feasible operations to minimize blind spots. This is called scenario-based sampling or Monte-Carlo sampling. If the sampled operating space is incomplete, we can use incremental learning, whereby the training space is kept growing by adding newly discovered operating points, not previously included in the database. But no approach is perfect, it remains an art requiring experience and judgment. Building a good database should be the most important (and exclusive) contribution of power system engineers to the learning task since machine learning algorithms are already provided by the AI community. Rather than focusing on a single system, we can also broaden the question: is it possible to find a generic classifier (physics-inspired), which works on all systems (test systems, actual systems)? This problem is challenging but if it has a solution we will not need to care anymore about the correct sampling of "operating points".

4. What is or should be the response time for the instability detector? am I hearing that response time is 200ms?

Answer: It is well-known in the industry that a RAS should act within 10 to 15 cycles after fault clearing (or the last consequential disturbance like a line outage) for their actions to be effective in preventing instability. Therefore, instability should be detected 3 cycles ahead of RAS corrective action to account for the time lag in action implementation (breakers, communications). Most of the algorithms developed by Dr. Kamwa and his students assume decision windows of 6 to 12 cycles. Below 6, it is often difficult to reach 100% reliability in response-based decision making while a more than 12 cycles time-response results in a useless detector.

5. My question goes to Dr Kamwa on the number and location of PMUs. What if there is not sufficient PMUs in the system or not deployed at the terminal of the generator, how effective and accurate is the proposed DSE and thus stability indicator? Thank you.

Answer: The DSE is fully decentralized, which means that in my scheme we have a single DSE per generator (or one PMU for a large power plant with similar generators). Therefore, the number doesn't matter. It will only limit the footprint you can observe. If you have a small amount of PMUs you would observe a limited number of critical plants. If you have PMUs at all plants, you will observe the full dynamics of the system.

6. Innocent, how your proposed system will work with a grid with increased penetration of inverter-based resources?

Answer: I have not studied this issue carefully enough to answer your question. But if the system is synchronous generators dominated as today, the DSE as I see it will remain relevant and feasible. With power electronic-dominated systems, we will need a new formulation to account for virtual synchronous generators with their PLL states included. Yet another research opportunity I guess.

7. Do you see the need or scope for more advanced (complex) DSE solution methodologies (e.g. GM-UKF, etc.) for protection applications using sample values? Or is the conventional WLS-NR method is sufficient to deal with measurement and model uncertainties?

Answer: Yes. The estimation-based protection has been implemented with three alternate state estimation algorithms (user selected): (a) unconstraint weighted least squares approach, (b) constraint optimization approach (handling virtual measurements as constraints) and (c) extended Kalman filter. More methods will be welcome. More specifically, it should be emphasized that the estimation-based protection requires a validated dynamical model of the protection zone as well as the instrumentation channel. This is done via dynamic state estimation to fine-tune the parameters of the model and instrument transformers accordingly. Some of these issues can be addressed via software, i.e. state estimation methods that are tolerant to large statistical errors and model inconsistencies. Specifically, measurements are always subject to noise that may be non-Gaussian, data quality and cybersecurity issues. In these cases, advanced robust DSE solutions can be used for critical applications, such as protection. WLS is sensitive to model uncertainties and data quality issues. To deal with model uncertainties, advanced H-infinity filters can be good candidates. We suggest you look at the following TF paper about how to deal with model uncertainties and data quality issues. Keep in mind that whatever method is selected for estimation-based protection, the method must be real-time, i.e. the computations of the dynamic state estimation must be completed before the next set of data arrives in real-time.

J. B. Zhao, A. Exposito, M. Netto, L. Mili, A. Abur, V. Terzija, I. Kamwa, B. Pal, A. K. Singh, J. Qi, Z. Huang, A. P. Sakis Meliopoulos, "Power System Dynamic State Estimation: Motivations, Definitions, Methodologies and Future Work," IEEE Trans. Power Systems, vol. 34, no. 4, pp. 3188-3198, 2019.